



Search for flavour-changing neutral-current couplings between the top quark and the photon with the ATLAS detector at $\sqrt{s} = 13$ TeV



The ATLAS Collaboration*

ARTICLE INFO

Article history:

Received 6 May 2022

Received in revised form 19 July 2022

Accepted 9 August 2022

Available online 18 August 2022

Editor: M. Doser

Dataset link: <https://hepdata.cedar.ac.uk>

ABSTRACT

This letter documents a search for flavour-changing neutral currents (FCNCs), which are strongly suppressed in the Standard Model, in events with a photon and a top quark with the ATLAS detector. The analysis uses data collected in pp collisions at $\sqrt{s} = 13$ TeV during Run 2 of the LHC, corresponding to an integrated luminosity of 139 fb^{-1} . Both FCNC top-quark production and decay are considered. The final state consists of a charged lepton, missing transverse momentum, a b -tagged jet, one high-momentum photon and possibly additional jets. A multiclass deep neural network is used to classify events either as signal in one of the two categories, FCNC production or decay, or as background. No significant excess of events over the background prediction is observed and 95% CL upper limits are placed on the strength of left- and right-handed FCNC interactions. The 95% CL bounds on the branching fractions for the FCNC top-quark decays, estimated (expected) from both top-quark production and decay, are $\mathcal{B}(t \rightarrow u\gamma) < 0.85 (0.88^{+0.37}_{-0.25}) \times 10^{-5}$ and $\mathcal{B}(t \rightarrow c\gamma) < 4.2 (3.40^{+1.35}_{-0.95}) \times 10^{-5}$ for a left-handed $tq\gamma$ coupling, and $\mathcal{B}(t \rightarrow u\gamma) < 1.2 (1.20^{+0.50}_{-0.33}) \times 10^{-5}$ and $\mathcal{B}(t \rightarrow c\gamma) < 4.5 (3.70^{+1.47}_{-1.03}) \times 10^{-5}$ for a right-handed coupling.

© 2022 The Author(s). Published by Elsevier B.V. This is an open access article under the CC BY license (<http://creativecommons.org/licenses/by/4.0/>). Funded by SCOAP³.

1. Introduction

Flavour-changing neutral currents (FCNCs) are forbidden at tree level in the Standard Model (SM) and strongly suppressed at higher orders via the GIM mechanism [1], but several extensions to the SM include additional sources of FCNCs. In particular, some of these models predict the branching fractions (BRs) of top-quark decays via FCNCs to be orders of magnitude larger [2] than those predicted by the SM, which are of the order of 10^{-14} [2]. Examples are R-parity-violating supersymmetric models [3–6] and models with two Higgs doublets [7,8], which allow FCNC processes involving top quarks to have measurable rates.

This letter presents a search for FCNCs in processes with a top quark (t) and a photon (γ) based on the full dataset of $\sqrt{s} = 13$ TeV proton–proton collisions collected by the ATLAS experiment [9] during Run 2 of the LHC. The analysis is optimised to search for the production of a single top quark in association with a photon as well as to search for the decay of a top quark into an up (u) or charm (c) quark in association with a photon in the case of pair-produced top quarks ($t\bar{t}$). Tree-level Feynman diagrams for these processes are shown in Fig. 1, where in both cases, exactly one top quark decays via the SM-favoured tWb coupling.

FCNC contributions to the production ($q \rightarrow t\gamma$, $q = u, c$, Fig. 1 left), and decay ($t \rightarrow q\gamma$, Fig. 1 right), modes can be parameterised in terms of effective coupling parameters [10,11]. Following the notation of Refs. [12,13], the relevant dimension-six operators are $O_{uB}^{(ij)}$ and $O_{uW}^{(ij)}$, where $i \neq j$ are indices for the quark generation. In general, left-handed (LH) and right-handed (RH) couplings could exist, resulting in different helicities for the top quark in the production mode, which leads to different kinematic properties for the final-state particles from the weak decay of the top quark.

The CMS Collaboration has searched for the production mode using data taken at $\sqrt{s} = 8$ TeV [14]. The ATLAS Collaboration also performed an analysis that was optimised for the production mode using 81 fb^{-1} of data at $\sqrt{s} = 13$ TeV [15], resulting in the strongest upper limits to date. The limits on the LH (RH) effective coupling parameters were translated into BR upper limits of 2.8×10^{-5} (6.1×10^{-5}) for $t \rightarrow u\gamma$ and 22×10^{-5} (18×10^{-5}) for $t \rightarrow c\gamma$. The search presented in this letter supersedes the one in Ref. [15], uses the full 139 fb^{-1} Run 2 dataset at $\sqrt{s} = 13$ TeV and is optimised for both the decay and production modes by training a neural-network (NN) classifier to separate the signal in decay and production modes from the SM background.

2. The ATLAS detector

ATLAS [9,16,17] is a multipurpose particle detector designed with a forward-backward symmetric cylindrical geometry and

* E-mail address: atlas.publications@cern.ch.

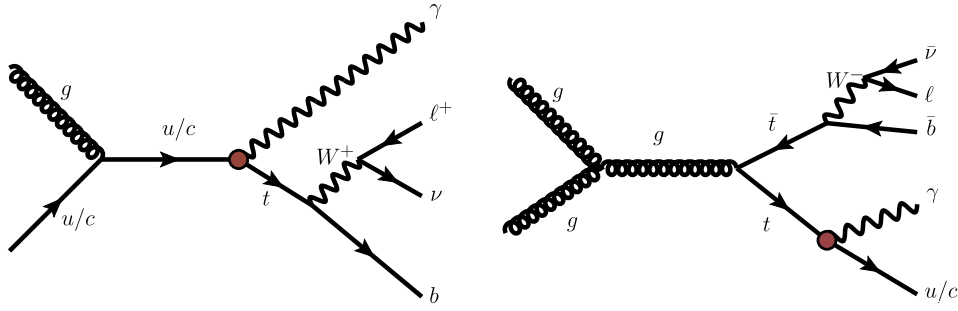


Fig. 1. Tree-level Feynman diagrams for top-quark production (left) and decay (right) via FCNCs. The $t\gamma$ vertex, which is not present in the SM, is highlighted.

nearly full 4π coverage in solid angle.¹ It consists of an inner tracking detector (ID) surrounded by a thin superconducting solenoid providing a 2 T axial magnetic field, electromagnetic and hadronic calorimeters, and a muon spectrometer (MS). The ID covers the pseudorapidity range $|\eta| < 2.5$ and is composed of silicon pixel, silicon microstrip, and transition radiation tracking (TRT) detectors. Lead/liquid-argon (LAr) sampling calorimeters provide electromagnetic (EM) energy measurements with high granularity. Hadronic calorimetry is provided by the steel/scintillator-tile calorimeter covering the central pseudorapidity range ($|\eta| < 1.7$). The endcap and forward regions are instrumented with LAr calorimeters for both the EM and hadronic energy measurements up to $|\eta| = 4.9$. The MS surrounds the calorimeters and is based on three large air-core toroidal superconducting magnets with eight coils each. The field integral of the toroids ranges between 2.0 and 6.0 Tm across most of the detector. The MS includes a system of precision tracking chambers and fast detectors for triggering. A two-level trigger system is used to select events. The first-level trigger is implemented in hardware and uses a subset of the detector information to keep the accepted event rate below 100 kHz [18]. This is followed by a software-based trigger that reduces the accepted event rate to 1 kHz on average. An extensive software suite [19] is used in the reconstruction and analysis of real and simulated data, in detector operations, and in the trigger and data acquisition systems of the experiment.

3. Analysis strategy

A signal region (SR) is defined by selecting events that contain one high-momentum photon and the decay products of a semileptonically decaying top quark, i.e. an electron or muon, a b -tagged jet and missing transverse momentum. Additional jets may be present in the final state, as one such jet is expected at leading order for signal in the decay mode and additional jets may result from initial- or final-state radiation in both signal modes. The main backgrounds stem from events with prompt photons (mostly $t\bar{t}\gamma$ events in the lepton+jets channel and $W\gamma$ +jets events), from events with an electron that is misidentified as a photon (referred to as $e \rightarrow \gamma$ fakes, mostly in dileptonic $t\bar{t}$ events), and from events with hadrons that are misidentified as photons (referred to as $h \rightarrow \gamma$ fakes, mostly in semileptonic $t\bar{t}$ events). Backgrounds with prompt photons are modelled by Monte Carlo (MC) simulations, and control regions (CRs) are defined for the $t\bar{t}\gamma$ and the $W\gamma$ +jets processes. The $t\bar{t}\gamma$ CR is based on the presence of additional jets, especially an additional b -tagged jet. The $W\gamma$ +jets

CR is constructed by requiring that the b -tagged jet fulfils only a looser b -tagging requirement and not the tight b -tagging requirement that is used in the SR. The contributions from $e \rightarrow \gamma$ and $h \rightarrow \gamma$ fakes are modelled by MC simulations but are corrected with data-driven scale factors (SFs). In the SR, signal and background events are distinguished using a NN with three output nodes, one for each signal mode and one for the SM background. The three nodes are combined into a one-dimensional discriminant to separate the total signal from the background. The signal contribution is then estimated with a binned profile likelihood fit to this discriminant, with systematic uncertainties modelled as nuisance parameters. Separate NNs are trained for the $t\gamma$ and $t\bar{t}\gamma$ couplings because the signal processes differ in their kinematic properties, due to differences between the up- and charm-quark parton distribution functions (PDFs), and also in their b -tagging probabilities. The different b -tagging properties stem from the jets initiated by the c -quark from the FCNC top-quark decay in the case of the $t\gamma$ coupling.

4. Data and simulation

The proton-proton (pp) collision data analysed for this search were recorded with the ATLAS detector from 2015 to 2018 at a centre-of-mass energy of $\sqrt{s} = 13$ TeV. Events were selected using single-lepton triggers [18,20,21] and are required to have at least one reconstructed primary vertex that has at least three associated tracks with transverse momenta greater than 500 MeV. After the application of data-quality requirements [22], the data sample corresponds to an integrated luminosity of 139 fb^{-1} , as determined by using the LUCID-2 detector [23] for the primary luminosity measurements.

Monte Carlo simulated events samples are used in the analysis to optimise the event selection, to train the NN and to predict contributions from various SM processes. The effect of multiple interactions in the same and neighbouring bunch crossings (pile-up) was modelled by overlaying the simulated hard-scattering event with inelastic pp events generated by PYTHIA8.186 [24] using the NNPDF2.3LO set of PDFs [25] and parameter values set according to the A3 tune [26]. After the event generation, the ATLAS detector response was simulated [27] by using the GEANT4 toolkit [28] with either the full simulation of the ATLAS detector or the fast-simulation package [29]. In all processes, the top-quark mass was set to 172.5 GeV. For all samples of simulated events, except those generated using SHERPA, the decays of bottom and charm hadrons were performed by EvtGEN [30].

The signal in the production mode ($pp \rightarrow t\gamma \rightarrow b\bar{b}\nu\gamma$) and in the decay mode ($pp \rightarrow t\bar{t} \rightarrow b\bar{b}\nu\bar{\gamma}\gamma$) was simulated with the MADGRAPH5_AMC@NLO 2.4.3 generator [31] with the UFO model TopFCNC [11,32] at next-to-leading order (NLO) in QCD, using the NNPDF3.0NLO PDF set [33]. The scale of new physics was set to $\Lambda = 1$ TeV. The charged leptons, ℓ , include electrons, muons and tau leptons. Interference effects between the production and decay FCNC processes can be neglected [34]. For SM decays of the

¹ ATLAS uses a right-handed coordinate system with its origin at the nominal interaction point (IP) in the centre of the detector and the z -axis along the beam pipe. The x -axis points from the IP to the centre of the LHC ring, and the y -axis points upwards. Cylindrical coordinates (r, ϕ) are used in the transverse plane, ϕ being the azimuthal angle around the z -axis. The pseudorapidity is defined in terms of the polar angle θ as $\eta = -\ln \tan(\theta/2)$. Angular distance is measured in units of $\Delta R \equiv \sqrt{(\Delta\eta)^2 + (\Delta\phi)^2}$.

top quark, the spin correlation was preserved using MADSPIN [35]. The parton showering and hadronisation were simulated using PYTHIA 8.212 [36] with the A14 tune [37] and the NNPDF2.3LO PDF set. In the production mode, four samples were generated with different couplings set to non-zero values: $t\gamma$ LH, $t\gamma$ RH, $t\gamma$ LH, and $t\gamma$ RH. In the decay mode, only samples with $t\gamma$ LH coupling and $t\gamma$ LH coupling have been simulated since the kinematic properties of the LH and RH couplings were found to be very similar. Correspondingly, only the LH coupling for the $t\gamma$ coupling in the decay is considered. The production and decay processes contribute similarly for the $t\gamma$ coupling, while for the $t\gamma$ coupling the decay is the dominant process. For given values of the Wilson coefficients, the cross-section for the production process is calculated with MADGRAPH5_AMC@NLO at NLO using the TopFCNC model. Then, for given values of the Wilson coefficients, the $t\gamma$ BR is calculated by the LO relation between the BR and the Wilson coefficients as given in Ref. [11]. The following effective cross-sections, calculated as total cross-section times branching fractions assuming $\mathcal{B}(t \rightarrow q\gamma)$ of 10^{-3} , are used for the production processes: 417 fb for the $t\gamma$ LH coupling, 416 fb for the $t\gamma$ RH coupling, 59.5 fb for both the $t\gamma$ LH coupling and the $t\gamma$ RH coupling. For the decay processes, the effective cross-section is 542 fb for both $t\gamma$ and $t\gamma$ couplings.

Two dedicated MC samples are used to model $t\bar{t}\gamma$ events. In the first sample, photon radiation in $t\bar{t}$ production was generated at NLO precision in QCD. In the second sample, photons in the decay were generated at LO precision in QCD while removing the overlap with the former sample. Events in both samples were modelled using the MADGRAPH5_AMC@NLO 2.7.3 [38] generator with the NNPDF2.3LO PDF set. The events were interfaced with PYTHIA 8.240 [36], which used the A14 tune and the NNPDF2.3LO PDF set. To combine the two samples, a K -factor is applied to scale the predicted cross-section of the decay sample, while no K -factor is applied to the production sample. The nominal value of the K -factor for the decay sample is chosen so that the inclusive cross-section agrees with the theoretical cross-section calculation at NLO in QCD in Ref. [39], resulting in a K -factor of 1.67 for the decay sample.

The production of $t\bar{t}$ events was modelled using the POWHEG Box v2 [40–43] generator at NLO with the NNPDF3.0NLO PDF set and the h_{damp} parameter² set to 1.5 times the top-quark mass [44]. The events were interfaced to PYTHIA 8.230 [36] to model the parton shower, hadronisation, and underlying event, with parameters set according to the A14 tune and using the NNPDF2.3LO set of PDFs. The $t\bar{t}$ sample is normalised to the cross-section prediction at next-to-next-to-leading order (NNLO) in QCD including the resummation of next-to-next-to-leading logarithmic (NNLL) soft-gluon terms calculated using TOP++ 2.0 [45–51].

Simulated events for the SM $tq\gamma$ process, with photon radiation in the production of the top quark, were generated at NLO in the four-flavour scheme using the MADGRAPH5_AMC@NLO 2.6.2 event generator interfaced with PYTHIA 8.240 for parton showering. Contributions with photon radiation from top-quark decay products were modelled by using the SM single-top-quark t -channel sample described below. The top quark was decayed using MADSPIN.

The single-top-quark samples are split into three processes: s -channel, t -channel and tW -channel. These samples were modelled using the POWHEG Box v2 [52] generator at NLO in QCD using the four-flavour (five-flavour) scheme for the t -channel (s -channel and tW -channel) and the corresponding NNPDF3.0NLO set of PDFs. In

the case of the tW -channel, the diagram removal scheme [53] was used. To avoid an overlap with the SM $tq\gamma$ sample, t -channel events with a prompt photon were only selected when the photon is radiated from the top-quark decay products. The events were interfaced with PYTHIA 8.230, which used the A14 tune and the NNPDF2.3LO set of PDFs.

The production of $V\gamma$ +jets ($V = W, Z$) final states was simulated with the SHERPA 2.2.8 [54] generator. Matrix elements (MEs) at NLO QCD accuracy for up to one additional parton and at LO accuracy for up to three additional parton emissions were matched and merged with the SHERPA parton shower based on Catani-Seymour dipole factorisation [55,56] using the MEPS@NLO prescription [57–60]. The virtual QCD corrections for MEs at NLO accuracy were provided by the OPENLOOPS library [61–64]. Samples were generated using the NNPDF3.0NLO set of PDFs, along with the dedicated set of tuned parton-shower parameters developed by the SHERPA authors.

The production of V +jets events was simulated with the SHERPA 2.2.1 [54] generator using NLO MEs for up to two partons, and LO MEs for up to four partons, calculated with the Comix [55] and OPENLOOPS libraries. The MEPS@NLO prescription was used to match the MEs with the SHERPA parton shower, which used the set of tuned parameters developed by the SHERPA authors. The NNPDF3.0NLO set of PDFs was used and the samples are normalised to a NNLO prediction [65].

Samples of diboson final states (VV) were simulated with the SHERPA 2.2.1 or 2.2.2 [54] generator depending on the process, including off-shell effects and Higgs boson contributions where appropriate. Fully leptonic final states and semileptonic final states, where one boson decays leptonically and the other hadronically, were generated using MEs at NLO accuracy in QCD for up to one additional parton and at LO accuracy for up to three additional parton emissions. The NNPDF3.0NLO set of PDFs was used, along with the dedicated set of tuned parton-shower parameters developed by the SHERPA authors.

An overlap removal scheme was applied to remove double-counting of events stemming from photon radiation in samples in which a photon was not explicitly required in the final state, similarly to Ref. [66]. This procedure was applied to the $t\bar{t}$, W +jets, Z +jets and single-top t -channel samples, to avoid overlaps with the $t\bar{t}\gamma$, $W\gamma$ +jets, $Z\gamma$ +jets and SM $tq\gamma$ samples, respectively.

5. Object and event selection

Electron candidates are reconstructed from clusters of energy deposits in the electromagnetic calorimeter matched to charged-particle tracks in the ID. The candidates must satisfy the *TightLH* likelihood-based identification criteria [67,68] with $p_T > 27$ GeV and $|\eta| < 2.47$, with the region $1.37 < |\eta| < 1.52$ excluded. Additionally, electron candidates must meet two impact-parameter selection criteria: $|z_0 \sin \theta| < 0.5$ mm, where z_0 is the z coordinate of the transverse impact point, and $|d_0/\sigma(d_0)| < 5$ for the transverse impact-parameter significance. Muon candidates are reconstructed from tracks in the MS matched to tracks in the ID. The candidates are required to meet *Medium* identification criteria [69] with $p_T > 27$ GeV and $|\eta| < 2.5$. Additionally, muon candidates must satisfy $|z_0 \sin \theta| < 0.5$ mm and $|d_0/\sigma(d_0)| < 3$. Isolated electrons and muons are selected by requiring both the amount of energy deposited nearby in the calorimeters and the scalar sum of the transverse momenta of nearby tracks in the ID to be small.

Photon candidates are reconstructed from clusters of energy deposits in the electromagnetic calorimeter that have either no matched ID track or one or two matched ID tracks which are compatible with electron or positron tracks from a photon conversion [68]. Based on the number of ID tracks matched to the electromagnetic cluster, photons are separated into different cat-

² The h_{damp} parameter is a resummation damping factor and one of the parameters that controls the matching of POWHEG matrix elements to the parton shower and thus effectively regulates the high- p_T radiation against which the $t\bar{t}$ system recoils.

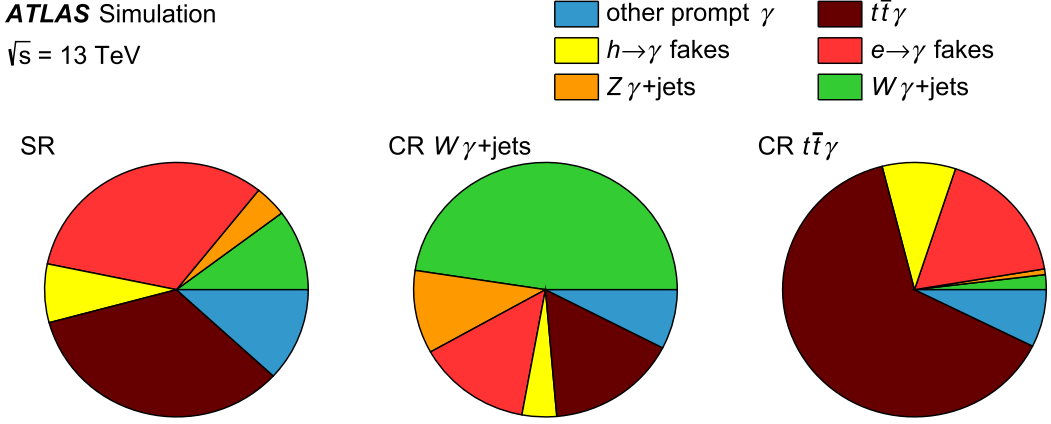


Fig. 2. Expected background composition of the SR (left), $W\gamma + \text{jets}$ CR (middle) and $t\bar{t}\gamma$ CR (right).

egories. If one or two tracks are matched, the photon is labelled as converted; if zero tracks are matched, the photon is labelled as unconverted. Photon candidates are required to have $p_T > 20$ GeV and be within $|\eta| < 2.37$, with the region at $1.37 < |\eta| < 1.52$ excluded. The candidates are required to meet the *Tight* identification criteria [67,68]. Photons must be isolated from nearby energy deposits in the calorimeter and from nearby tracks in the ID. The sum of the energy deposited (p_T of the tracks) within $\Delta R = 0.4$ ($\Delta R = 0.2$) of the photon direction is required to be smaller than $0.022 \times p_T^\gamma + 2.45$ GeV ($0.05 \times p_T^\gamma$), excluding the photon energy deposition (tracks associated with the photon) [68].

Jet candidates are reconstructed from particle-flow objects [70], using the anti- k_t [71] jet algorithm with radius parameter $R = 0.4$ implemented in FastJet [72]. Jets are calibrated by applying a jet energy scale derived from 13 TeV data and simulation [73]. After the calibration, jet candidates are required to have $p_T > 25$ GeV and $|\eta| < 2.5$. To suppress jets originating from pile-up collisions, a cut on the jet-vertex tagger (JVT) [74] discriminant as defined in the *JVTight* working point (WP) is applied for jets with p_T below 120 GeV. Jets containing b -hadrons are identified (b -tagged) using a deep neural network. This neural network, DL1r [75,76], combines inputs from the impact parameters of tracks and the displaced vertices reconstructed in the ID. The inputs of the DL1r neural network also include discriminating variables constructed by a recurrent neural network, which exploits the spatial and kinematic correlations between tracks originating from the same b -hadron. The outputs of the neural network represent the probabilities of the jet to originate from a light-flavour quark or gluon, a c -quark and a b -quark, which are then combined into a single discriminant.

The missing transverse momentum vector \vec{p}_T^{miss} , with magnitude E_T^{miss} , is defined as the negative sum of the transverse momenta of the reconstructed and calibrated physical objects and a soft term built from all tracks that are associated with the primary vertex but not with these objects [77].

To avoid double-counting of detector signatures, objects are removed in the following order³: electrons sharing a track with a muon; jets within $\Delta R = 0.2$ of an electron; electrons within $\Delta R = 0.4$ of a jet; jets within $\Delta R = 0.4$ of a muon if they have at most two associated tracks; muons within $\Delta R = 0.4$ of a jet; photons within $\Delta R = 0.4$ of an electron or muon; jets within $\Delta R = 0.4$ of a photon.

SFs are used to correct the efficiencies in simulation in order to match the efficiencies measured in data for the electron [68,78–80] and muon [80] trigger, reconstruction, identification, and isolation

Table 1

Summary of the analysis region definitions. While the requirements on photons, leptons and E_T^{miss} are shared, the regions differ in their jet and b -tagged jet requirements. The latter ensure orthogonality. All jets that pass the 60% b -tagging WP automatically pass the looser b -tagging WPs. A hyphen indicates that no criterion has to be fulfilled.

Object	SR	CR $t\bar{t}\gamma$	CR $W\gamma + \text{jets}$
Photon ($p_T > 20$ GeV)		= 1	
Lepton ($p_T > 27$ GeV)		= 1	
E_T^{miss}		> 30 GeV	
Jets ($p_T > 25$ GeV)	≥ 1	≥ 4	≥ 1
b -tagged jets (60% WP)	= 1	–	= 0
b -tagged jets (70% WP)	= 1	≥ 1	= 0
b -tagged jets (77% WP)	= 1	≥ 2	= 1
$m(e, \gamma)$	–	–	notin [80, 100] GeV

criteria, as well as for the photon identification [68] and isolation requirements. SFs are also applied for the JVT requirement [81] and for the b -tagging efficiencies for jets that originate from the hadronisation of b -quarks [75], c -quarks [82], and u -, d -, s -quarks or gluons [83].

The selected events have exactly one electron or muon, exactly one photon, at least one jet and $E_T^{\text{miss}} > 30$ GeV. The lepton must be matched, with $\Delta R < 0.15$, to the lepton reconstructed by the trigger. Events meeting these criteria are further separated into three orthogonal regions: the SR, the $t\bar{t}\gamma$ CR and the $W\gamma + \text{jets}$ CR. In the SR, exactly one b -tagged jet identified with the 60% efficiency WP is required while vetoing events with additional jets that pass the 77% WP, to ensure orthogonality to the CRs. Events in the $t\bar{t}\gamma$ CR are required to have at least four jets with at least two b -tagged jets identified at the 77% WP, and at least one of these must also be b -tagged at the 70% WP. In order to select a $W\gamma + \text{jets}$ event sample with jets originating from light-flavour and heavy-flavour quarks in proportions similar to those in events satisfying the SR criteria, events in the $W\gamma + \text{jets}$ CR are required to have exactly one b -tagged jet identified at the 77% WP, with no jet passing the 70% WP. Additionally, events with an electron-photon pair invariant mass of 80–100 GeV are excluded from the $W\gamma + \text{jets}$ CR to suppress $Z + \text{jets}$ events with $e \rightarrow \gamma$ fakes. Table 1 summarises the selection criteria for the individual analysis regions. The selection efficiency of the signal events in the SR is about 8% for the FCNC production mode and about 6.5% for the FCNC decay mode for the $t\bar{t}\gamma$ LH coupling. The composition of the SM backgrounds after the selection is presented in Fig. 2. Around 60% (35%) of the jets in the signal region originate from the hadronisation of b -quarks (c -quarks), while around 10% (75%) of the jets in the $W\gamma + \text{jets}$ CR originate from the hadronisation of b -quarks (c -quarks). The residual differences between the kinematics of jets originating from the

³ For the overlap removal, ΔR is defined as $\Delta R \equiv \sqrt{(\Delta y)^2 + (\Delta \phi)^2}$, where y is the rapidity of the object.

hadronisation of b - and c -quarks were found to be negligible. Setting the FCNC couplings to the 95% CL limits measured in Ref. [15], the signal contamination in the CRs is less than 0.3% (1%) for the $t\bar{t}\gamma$ CR ($W\gamma$ +jets CR).

6. Data-driven estimate of misidentified photons

6.1. Electrons misidentified as photons

Electrons can be misidentified as photons, for example, if the electron track is not reconstructed or if the track is not matched to the energy clusters in the electromagnetic calorimeter. These misidentified photons are referred to in the following as $e \rightarrow \gamma$ fakes. The probability for an electron to be misidentified as a photon, $f_{e \rightarrow \gamma}$, is measured from data and simulation following the methodology used previously [15,84]. The ratio of the probabilities measured in data and simulation is then applied to correct the simulation.

Two regions are defined in order to measure $f_{e \rightarrow \gamma}$. The $Z \rightarrow e\gamma$ region is defined by requiring exactly one electron and one photon with an electron-photon invariant mass in the range 70–110 GeV. The $Z \rightarrow ee$ region is defined by requiring exactly two electrons with opposite electric charge, no photons, and a dielectron invariant mass in the range 70–110 GeV. Both regions are required to have $E_T^{\text{miss}} < 30$ GeV, and a veto on the presence of b -tagged jets is applied. In both regions, electrons and muons need to fulfil the same criteria as described in Chapter 5. Templates from MC simulation for the invariant mass of the dielectron (electron–photon) pair are estimated from a binned-likelihood fit in the $Z \rightarrow ee$ ($Z \rightarrow e\gamma$) region. The templates also include the SM backgrounds originating from $W\gamma$ +jets and $Z\gamma$ +jets events. For the $Z \rightarrow e\gamma$ region, third-order Bernstein polynomials are used to create templates for the remaining SM backgrounds. The ratio of the integrals of the aforementioned fitted signal templates is calculated in order to estimate $2f_{e \rightarrow \gamma}$, where the factor of two accounts for the two electrons in $Z \rightarrow ee$ events that may be misidentified as a photon. The $f_{e \rightarrow \gamma}$ probabilities are measured independently in six bins in photon $|\eta|$ and separately for the different reconstruction types for converted photons, defined by the number of hits in the silicon detectors and in the TRT. The measured $f_{e \rightarrow \gamma}$ probabilities range from about 3% for the central photons up to 12% for the forward photons, with an inclusive probability of about 5%.

The following systematic uncertainties in the estimated $f_{e \rightarrow \gamma}$ probabilities are assessed: removing the third-order Bernstein polynomial functions used to describe the background contributions from the fits, removing the MC templates for $W\gamma$ +jets and $Z\gamma$ +jets from the fits, varying the fit range from 70–110 GeV to 80–100 GeV, increasing and decreasing the photon energy by 1%, and considering modelling uncertainties of the Z +jets events, as the Z +jets process is the only process that contributes significantly. SFs are defined by the ratios of the measured and simulated values of $f_{e \rightarrow \gamma}$, and range from about 0.8 for the forward photons to 2.5 for the central photons for one of the reconstruction types for the converted photons. The total uncertainties differ between the η bins and the reconstruction types and vary from about 1.5% to about 30%, dominated by systematic uncertainties arising from the removal of the Bernstein polynomials and from the Z +jets modelling uncertainties in most bins. The validity of the measured $f_{e \rightarrow \gamma}$ SFs was cross-checked using a selection similar to the $Z \rightarrow e\gamma$ region but requiring at least one b -tagged jet to be present. Good agreement between the corrected prediction and the data was observed. The main processes contributing to the analysis regions via $e \rightarrow \gamma$ fakes are $t\bar{t}$ with about 65% and Z +jets with about 25%.

6.2. Hadrons misidentified as photons

A jet can be misreconstructed as a photon, e.g. when a hadron inside the jet decays into two photons that are reconstructed as a single one. The number of events with misidentified hadrons is estimated from data. SFs, defined as the ratio of the numbers of misidentified hadrons in data and in simulation, are applied to the simulation to correct the normalisation of the events with misidentified hadrons. The shapes of the distributions for these processes are estimated from the MC simulation with their uncertainties.

Three hadron fake regions (HFR) are defined by the same criteria as the SR but with modified photon identification and isolation requirements following the same prescription as in Ref. [15]. Assuming no correlation between the identification and isolation variables used to define the hadron fake regions, the contribution of this background in the SR can be estimated using the ABCD method (see e.g. Ref. [85]) as

$$N(\text{SR}_{h \rightarrow \gamma}^{\text{pass\&pass, data}}) = \frac{N(\text{HFR}^{\text{pass\&fail, data}}) \cdot N(\text{HFR}^{\text{fail\&pass, data}})}{N(\text{HFR}^{\text{fail\&fail, data}})},$$

where $N(\text{HFR}^{\text{pass\&fail, data}})$ represents the number of $h \rightarrow \gamma$ events estimated from data after subtracting contributions from other sources in the HFR where events pass the identification requirements and fail the isolation requirements, as defined in Ref. [15], and $N(\text{HFR}^{\text{fail\&pass, data}})$ and $N(\text{HFR}^{\text{fail\&fail, data}})$ are defined analogously. Since the identification and isolation variables are not fully uncorrelated, the estimate is corrected for the non-zero correlation as estimated from MC simulations. The correction factor for the correlations ranges from about 0.9 to about 1.15 depending on the photon p_T and η bin. The data-driven SFs are then calculated as $\text{SF}(h \rightarrow \gamma) = N(\text{SR}_{h \rightarrow \gamma}^{\text{pass\&pass, data, corr}})/N(\text{SR}_{h \rightarrow \gamma}^{\text{pass\&pass, MC, corr}})$, where $N(\text{SR}_{h \rightarrow \gamma}^{\text{pass\&pass, MC, corr}})$ represents the number of events the MC simulation predicts in the SR after the correction for the non-zero correlations of the identification and isolation variables. The SFs are estimated independently in six photon $|\eta|$ bins and two photon p_T bins, and separately for converted and unconverted photons.

The following sources of systematic uncertainty are considered for the estimation of the SFs: the finite number of events in the data and MC simulated samples, variations of the $e \rightarrow \gamma$ SFs used to subtract the $e \rightarrow \gamma$ background in the different regions by one standard deviation, variations of the correlation between identification and isolation variables, estimated as the maximum correlation seen in the simulation across all p_T and η bins, and variations in the prompt-photon subtraction in the non-tight regions by considering normalisation uncertainties for the individual processes and modelling uncertainties of the $t\bar{t}$ and $t\bar{t}\gamma$ processes.

The measured data-driven SFs range from about 0.6 for high- p_T central unconverted photons to up to 2.2 for high- p_T forward unconverted photons. The total uncertainties in the SFs vary between about 45% to 65%, where in most of the bins the dominant uncertainty arises from the assumptions about the correlation of the photon identification and isolation variables. The main processes contributing to the analysis regions via $h \rightarrow \gamma$ fakes are $t\bar{t}$ with about 80% and single top with about 10%.

7. Neural network for discrimination between signal and background

The signal is distinguished from the sum of the background processes by a fully connected feed-forward NN with backpropagation, implemented in KERAS [86] with the TENSORFLOW [87] back end. Separate NNs are trained for FCNC processes with a $t\gamma\gamma$ or a $t\gamma\gamma$ vertex, reflecting the differences stemming mainly from the

different PDFs involved in the production mode. Differences between the LH and RH couplings were found to mostly impact the acceptance of the event selection. The following acceptances were found for the FCNC production modes: 8.2% for the $t\gamma\gamma$ LH coupling, 6.7% for the $t\gamma\gamma$ RH coupling, 9.3% for the $t\gamma\gamma$ LH coupling and 7.5% for the $t\gamma\gamma$ RH coupling. For the decay modes, the acceptances are 6.6% for the $t\gamma\gamma$ coupling and 5.8% for the $t\gamma\gamma$ coupling. However, no significant impact on the discrimination power of the network was found originating from the difference of the LH and RH couplings. Thus, the LH and RH couplings are not separated in the network.

An optimised set of 37 variables is used as the input to the NN: these were selected by removing the input variables with negligible impact on the separation power of the final discriminant. The input variables include the p_T and η of the charged leptons, photons, b -tagged jets and the two leading non- b -tagged jets, E_T^{miss} and the photon conversion status. High-level variables, such as invariant masses and angular distances between the objects, jet multiplicities and the b -tagging information, are also included. All variables are transformed using scikit-learn's [88] StandardScaler.

The NN consists of six hidden layers with 512, 256, 128, 64, 32, 16 nodes, respectively. The network architecture was optimised, using the expected limit without considering systematic uncertainties, to provide the best separation of the simulated FCNC signals and SM background. The output of the NN consists of three nodes representing the three classes: the FCNC production signal, the FCNC decay signal and the SM background. The softmax function, $f_i(x) = \exp(x_i) / \sum_{j=1}^3 \exp(x_j)$, in three dimensions for the i -th class is used for the activation of the output nodes. Consequently, the target vector of the NN in the training is $(1, 0, 0)^\top$ for FCNC production mode events, $(0, 1, 0)^\top$ for the decay mode, and $(0, 0, 1)^\top$ for all background processes. The NN is trained with the ADAM optimiser [89]. The output of the multiclass discriminator is illustrated in Fig. 3, showing good separation between the three output classes. The strongest separation is achieved between the FCNC production class and the SM background class.

From the three-dimensional NN output, a one-dimensional discriminant, \mathcal{D} , is formed using

$$\mathcal{D} = \ln \frac{a \cdot y_{\text{prod}} + (1 - a) \cdot y_{\text{dec}}}{y_{\text{bkg}}},$$

where $y_{\text{prod}(\text{dec})}$ represents the NN output for the FCNC production (decay) class and y_{bkg} represents the NN output for the SM background class. The discriminant \mathcal{D} is inspired by the log-likelihood ratio, with an optimisable parameter $a \in (0, 1)$ that changes the relative contribution of the NN outputs for the signal modes to the discriminant. The discriminant is in the range $(-\infty, +\infty)$. The optimal value of the parameter a was found to be 0.3 for the $t\gamma\gamma$ NN, and 0.2 for the $t\gamma\gamma$ NN, reflecting the smaller contribution of the production mode in the case of charm-quark-initiated FCNC $t\gamma\gamma$ production. The multiclass NN was found to outperform a simpler binary NN that discriminates only between the FCNC signal and the SM background. The expected upper limit on the signal was found to be up to 30% lower in the case of the multiclass neural network.

8. Systematic uncertainties

Systematic effects may change the expected numbers of events from the signal and background processes and the shape of the fitted discriminants in the SR and the CRs. These effects are evaluated by varying each source of systematic uncertainty by $\pm 1\sigma$ and considering the resulting deviation from the nominal expectation as the uncertainty.

Uncertainties due to the theoretical cross-sections are evaluated by varying the cross-section by $\pm 5.6\%$ for $t\bar{t}$ production [25],

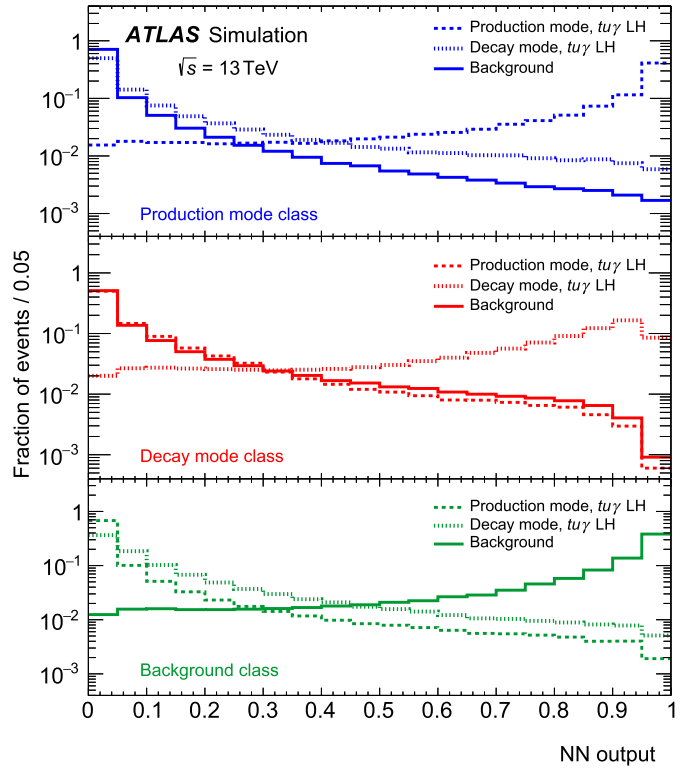


Fig. 3. The classifier output of the multiclass NN for the $t\gamma\gamma$ LH coupling. The output of the FCNC production mode class is shown in blue (top), the output of the FCNC decay mode class is shown in red (middle) and the output of the SM background class is shown in green (bottom). For each output class, the distribution of the three processes is shown: FCNC production mode with the dashed line, FCNC decay mode with the dotted line and SM background with the solid line. The vertical axis represents the fraction of events predicted by the simulation.

[51,90–92], by $^{+4.0\%}_{-3.4\%} (^{+5.0\%}_{-4.5\%})$ for t -channel single-(anti-)top production [93], by $^{+3.6\%}_{-3.1\%} (^{+4.8\%}_{-4.3\%})$ for s -channel single-(anti-)top production [94], by $\pm 5.3\%$ for tW production [95], by $\pm 5\%$ for W -jets and Z -jets production [96], by $\pm 30\%$ for $Z\gamma$ -jets production, by $\pm 50\%$ for the SM $tq\gamma$ process, and by $\pm 6\%$ for diboson production [97]. No cross-section uncertainty is considered for $t\bar{t}\gamma$ and $W\gamma$ -jets production, because their normalisations are determined in the fit.

Uncertainties due to the modelling of the signal are estimated by considering independent variations of the renormalisation and factorisation scales by factors of 2 and 0.5, but normalising the signal to the nominal cross-section. Additionally, an uncertainty due to the choice of parton shower generator is estimated by considering the change when using an alternative MC sample that uses the HERWIG 7.2.1 [98,99] prediction with the H7UE set of tuned parameters [99] and the MMHT2014LO PDF set [100] instead of the PYTHIA 8.212 generator. Uncertainties due to the PDFs are estimated by using the NNPDF set of replicas.

For the background processes, uncertainties due to the renormalisation and factorisation scales and from the PDFs are estimated separately for each process, following the same procedure as for the signal. An additional uncertainty due to the chosen h_{damp} parameter value for the $t\bar{t}$ process is estimated by doubling it to three times the top-quark mass. For the $t\bar{t}\gamma$, $t\bar{t}$ and single-top processes, an uncertainty is estimated from an independent variation of the A14 tune to its Var3c up and down variants [101]. For the $t\bar{t}$ and single-top processes, an uncertainty due to the final-state radiation modelling is estimated from an independent variation of the renormalisation scale for emissions from the parton shower by factors of 2.0 and 0.5. In addition, a variation of

the K -factor for decay-sample $t\bar{t}\gamma$ events from 1.67 to 1.97 is considered in order to account for uncertainties in the extrapolation to the search phase-space. The variation is motivated by the dedicated calculation yielding the inclusive NLO K -factor of 1.30 used in Ref. [66] assuming no K -factor for the production sample. This uncertainty is decorrelated between the regions to account for the phase-space dependence of the inclusive K -factor. The uncertainty due to the choice of parton shower generator is estimated by comparing the nominal predictions with an alternative set using MADGRAPH5_AMC@NLO interfaced with HERWIG for the $t\bar{t}\gamma$ and SM $tq\gamma$ processes, and POWHEG Box v2 interfaced with HERWIG for the $t\bar{t}$ and single-top processes. The parton shower uncertainty for the $t\bar{t}\gamma$ and $t\bar{t}$ processes is fully decorrelated between the individual analysis regions to relax the constraints from these uncertainties by taking into account possible phase-space differences. The impact on the $t\bar{t}$ process is further split between $e \rightarrow \gamma$ and $h \rightarrow \gamma$ fakes. Additionally, for the $t\bar{t}\gamma$ CR, the impact of the parton shower modelling of $t\bar{t} h \rightarrow \gamma$ fakes is split into distribution normalisation and residual uncertainties where the normalisation difference is removed. Furthermore, an uncertainty due to the choice of generator is considered for the $t\bar{t}$ and single-top processes by comparing the nominal prediction with a prediction from MADGRAPH5_AMC@NLO interfaced with PYTHIA8. Finally, for the tW single-top process, an uncertainty due to the overlap with the $t\bar{t}$ process is estimated by replacing the diagram removal scheme with the diagram subtraction scheme [53].

An uncertainty of 1.7% in the integrated luminosity is considered [102] for all processes. The uncertainty due to pile-up is determined by varying the average number of interactions per bunch-crossing by 3% in the simulation. The uncertainties due to the SFs for electrons and hadrons that are misidentified as photons are determined as described in Section 6.

For the triggering, reconstruction, identification, and calibration of the objects, systematic uncertainties are evaluated for the following: electron and muon trigger, reconstruction, identification and isolation SFs [68,78,80]; photon identification [68,103] and isolation SFs; electron- and photon-energy and muon-momentum calibration and resolution [68,80]; jet energy scale [104] and jet energy resolution [105]; JVT SF [81]; b -tagging SFs [75,82,83]; E_T^{miss} soft term [77].

The uncertainty originating from the limited number of simulated MC events is implemented via the Barlow–Beeston approach [106]. Two uncertainties for each bin of the fitted distributions are considered, one for the uncertainty originating from the SM backgrounds and one for the combined production and decay FCNC signal.

9. Results

The normalisations of the signal contribution and the two contributions from $t\bar{t}\gamma$ and $W\gamma$ +jets production are obtained from a simultaneous binned profile-likelihood fit to the NN discriminant distribution in the SR and the photon p_T distribution in the $t\bar{t}\gamma$ and $W\gamma$ +jets CRs, with systematic uncertainties included as nuisance parameters. Fig. 4 shows the corresponding post-fit distribution of the NN discriminant for the $t\gamma$ signal. The signal is scaled to 10 times the observed upper limit on the BR for the $t \rightarrow u\gamma$ LH coupling, corresponding to a BR of 8.5×10^{-5} . The qualitative features of these distributions are similar for the $t\gamma$ NN.

The data and SM predictions agree within uncertainties and no significant FCNC contributions are observed. From the 95% confidence level (CL) upper limits on the signal contribution, derived using the CL_s method [107], the corresponding limits on the effective coupling parameters are calculated [108]. From these, limits on the BRs are also derived. The background contributions from

Table 2

The 95% CL limits on the effective coupling constants, BRs and production cross-sections. The expected limits with their uncertainties, representing one standard deviation, as well as observed limits are shown. The scale of new physics is set to $\Lambda = 1$ TeV.

Observable	Coupling	Expected	Observed
$ C_{uW}^{(13)*} + C_{ub}^{(13)*} $	$t \rightarrow u\gamma$ LH	$0.104^{+0.020}_{-0.016}$	0.103
$ C_{uW}^{(31)} + C_{ub}^{(31)} $	$t \rightarrow u\gamma$ RH	$0.122^{+0.023}_{-0.018}$	0.123
$ C_{uW}^{(23)*} + C_{ub}^{(23)*} $	$t \rightarrow c\gamma$ LH	$0.205^{+0.037}_{-0.031}$	0.227
$ C_{uW}^{(32)} + C_{ub}^{(32)} $	$t \rightarrow c\gamma$ RH	$0.214^{+0.039}_{-0.032}$	0.235
BR ($t \rightarrow q\gamma$)	$t \rightarrow u\gamma$ LH	$0.88^{+0.37}_{-0.25}$	0.85
BR ($t \rightarrow q\gamma$)	$t \rightarrow u\gamma$ RH	$1.20^{+0.50}_{-0.32}$	1.22
BR ($t \rightarrow q\gamma$)	$t \rightarrow c\gamma$ LH	$3.40^{+1.35}_{-0.95}$	4.16
BR ($t \rightarrow q\gamma$)	$t \rightarrow c\gamma$ RH	$3.70^{+1.47}_{-1.03}$	4.46
$\sigma(pp \rightarrow t\gamma)$ [fb]	$t \rightarrow u\gamma$ LH	$11.2^{+4.7}_{-3.1}$	10.9
$\sigma(pp \rightarrow t\gamma)$ [fb]	$t \rightarrow u\gamma$ RH	$15.3^{+6.4}_{-4.3}$	15.6
$\sigma(pp \rightarrow t\gamma)$ [fb]	$t \rightarrow c\gamma$ LH	$6.2^{+2.5}_{-1.7}$	7.6
$\sigma(pp \rightarrow t\gamma)$ [fb]	$t \rightarrow c\gamma$ RH	$6.8^{+2.7}_{-1.9}$	8.2

$t\bar{t}\gamma$ and $W\gamma$ +jets production are scaled by normalisation factors estimated to be 1.00 ± 0.10 and 1.15 ± 0.15 , respectively, from the fit for the $t\gamma$ LH coupling. The normalisation values determined in the fit for the $t\gamma$ LH coupling are 0.97 ± 0.10 for the $t\bar{t}\gamma$ contribution and 1.16 ± 0.15 for $W\gamma$ +jets. The normalisation values are similar for the fits with the RH FCNC couplings. The K-factors for the $t\bar{t}\gamma$ decay-sample are fitted to the values of about 1.57 for the SR, about 1.61 for the $t\bar{t}\gamma$ CR and about 1.73 for the $W\gamma$ +jets CR. The smallest post-fit uncertainty on the K-factor is seen in the $t\bar{t}\gamma$ CR, where the uncertainty is found to be about 0.24. The observed and expected 95% CL limits on the effective coupling strengths, the BRs and the production cross-sections are presented in Table 2 as well as in Fig. 5. The fitted normalisations of the FCNC $t\gamma$ signal are larger than zero, although consistent with zero within one standard deviation. Thus, the observed 95% CL limits for the $t\gamma$ couplings are larger than the expected 95% CL limits. The dominant source of uncertainty in the signal contribution for the $t\gamma$ couplings is the statistical uncertainty. All systematic uncertainties worsen the limit by only about 20%. For the $t\gamma$ couplings, the effect of the systematic uncertainties is larger, worsening the limit by about 40%, but the statistical uncertainties also play an important role. The different importance of the systematic uncertainties on the observed limits between $t\gamma$ and $t\bar{t}\gamma$ couplings result in a difference in the improvement in the limits compared to the previous results [15] for the two couplings. The sources of systematic uncertainty with the largest impact on the estimated signal contribution depend on the coupling studied. For the $t\gamma$ couplings, the dominant systematic uncertainties arise from the cross-section uncertainty of the SM $tq\gamma$ process, the uncertainty in the electron-photon energy scale and the decay K -factor uncertainty in the $t\bar{t}\gamma$ process. For the $t\gamma$ couplings, the dominant systematic uncertainties originate from the cross-section uncertainty of the SM $tq\gamma$ process, the uncertainty in the hadron-to-photon SFs and the limited number of simulated events for the SM backgrounds. No nuisance parameters are significantly pulled or constrained. The difference in the improvement for the $t\gamma$ and $t\bar{t}\gamma$ coupling with respect to the previously published result [15] stems mainly from the different relative contribution of the production and decay modes between the couplings. The efficiency for the decay mode with higher jet multiplicity is particularly increased compared to the previous result, increasing the improvement for the $t\gamma$ coupling limits.

10. Conclusion

A search for flavour-changing neutral currents (FCNCs) in events with one top quark and a photon is presented using 139 fb^{-1} of

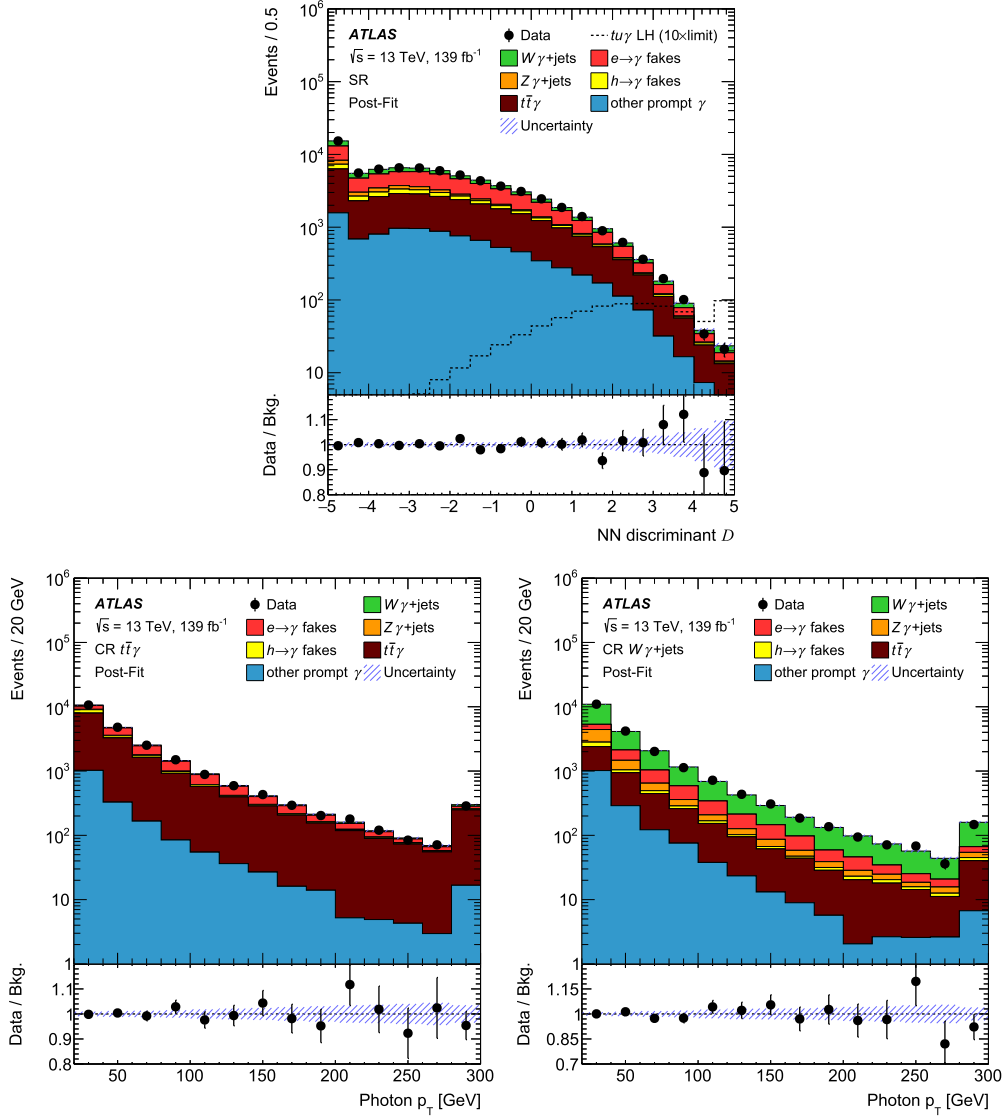


Fig. 4. Post-fit distributions of a background-only fit to the NN discriminant in the SR for the $t\gamma$ coupling (top) and the photon p_T distribution in the $t\bar{t}\gamma$ (bottom left) and $W\gamma$ +jet CRs (bottom right). The last bin of the distributions contains the overflow and in the case of the SR, the first bin also contains the underflow. In addition, in the SR, the expected $t\gamma$ LH signal is overlaid for an expected number of events corresponding to the observed 95% CL limit scaled by a factor of ten, representing BR for the $t \rightarrow u\gamma$ LH coupling of 8.5×10^{-5} . The lower panels show the ratios of the data ('Data') to the background prediction ('Bkg.'). The uncertainty band includes both the statistical and systematic uncertainties in the background prediction. Correlations among uncertainties were taken into account as determined in the fit.

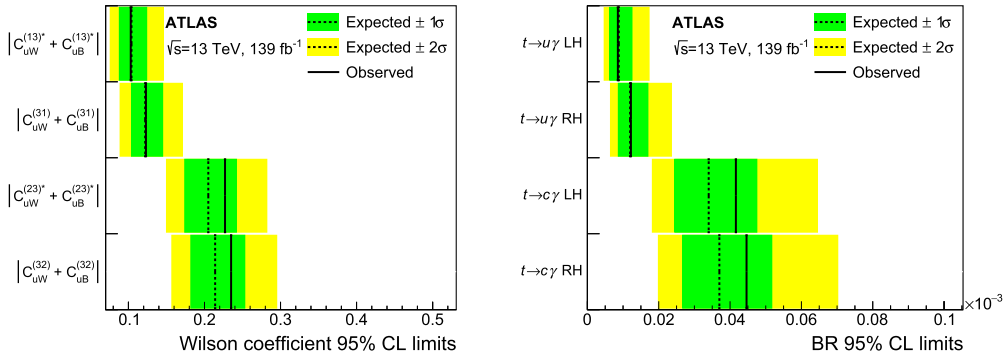


Fig. 5. The 95% CL upper limits on the effective coupling constants (left) and BRs (right). The expected (observed) limits are shown with the dotted (solid) lines. The green (yellow) bands represent one (two) standard deviations for the limits. The scale of new physics is set to $\Lambda = 1$ TeV.

$\sqrt{s} = 13$ TeV pp collision data collected with the ATLAS detector at the LHC. Events with a photon, an electron or muon, exactly one b -tagged jet, missing transverse momentum and possibly additional

jets are selected. The contribution from events with electrons or hadrons that are misidentified as photons is estimated from simulation with data-driven corrections, and the two main background

processes with a prompt photon are estimated with control regions. Multiclass neural networks are used to distinguish events with FCNCs in the production process, events with FCNCs in the decay process, and background events. The outputs are combined into a one-dimensional discriminant to search for the FCNC signal. The data are consistent with the background-only hypothesis. Limits are set on the strength of effective operators that introduce a left- or right-handed flavour-changing $tq\gamma$ coupling with an up-type quark q . The 95% CL bounds on the corresponding branching fractions for the FCNC top-quark decays are $\mathcal{B}(t \rightarrow u\gamma) < 0.85 \times 10^{-5}$ and $\mathcal{B}(t \rightarrow c\gamma) < 4.2 \times 10^{-5}$ for a left-handed $tq\gamma$ coupling, and $\mathcal{B}(t \rightarrow u\gamma) < 1.2 \times 10^{-5}$ and $\mathcal{B}(t \rightarrow c\gamma) < 4.5 \times 10^{-5}$ for a right-handed coupling. The obtained limits are the most stringent to date and improve on the previous ATLAS limits by factors of 3.3 to 5.4. The improvements in the limits originate mainly from considering events with more than one jet, the optimisation of the signal separation and the increased integrated luminosity.

Declaration of competing interest

The authors declare that they have no known competing financial interests or personal relationships that could have appeared to influence the work reported in this paper.

Data availability

The data for this manuscript are not available. The values in the plots and tables associated to this article are stored in HEPDATA (<https://hepdata.cedar.ac.uk>).

Acknowledgements

We thank CERN for the very successful operation of the LHC, as well as the support staff from our institutions without whom ATLAS could not be operated efficiently.

We acknowledge the support of ANPCyT, Argentina; YerPhI, Armenia; ARC, Australia; BMWFW and FWF, Austria; ANAS, Azerbaijan; CNPq and FAPESP, Brazil; NSERC, NRC and CFI, Canada; CERN; ANID, Chile; CAS, MOST and NSFC, China; Minciencias, Colombia; MEYS CR, Czech Republic; DNRF and DNSRC, Denmark; IN2P3-CNRS and CEA-DRF/IRFU, France; SRNSFC, Georgia; BMBF, HGF and MPG, Germany; GSRI, Greece; RGC and Hong Kong SAR, China; ISF and Benoziyo Center, Israel; INFN, Italy; MEXT and JSPS, Japan; CNRST, Morocco; NWO, Netherlands; RCN, Norway; MEiN, Poland; FCT, Portugal; MNE/IFA, Romania; MESTD, Serbia; MSSR, Slovakia; ARRS and MIZŠ, Slovenia; DSI/NRF, South Africa; MICINN, Spain; SRC and Wallenberg Foundation, Sweden; SERI, SNSF and Canton of Bern and Geneva, Switzerland; MOST, Taiwan; TENMAK, Türkiye; STFC, United Kingdom; DOE and NSF, United States of America. In addition, individual groups and members have received support from BCKDF, Canarie, Compute Canada and CRC, Canada; PRIMUS 21/SCI/017 and UNCE SCI/013, Czech Republic; COST, ERC, ERDF, Horizon 2020 and Marie Skłodowska-Curie Actions, European Union; Investissements d'Avenir Labex, Investissements d'Avenir Idex and ANR, France; DFG and AvH Foundation, Germany; Herakleitos, Thales and Aristeia programmes co-financed by EU-ESF and the Greek NSRF, Greece; BSF-NSF and MINERVA, Israel; Norwegian Financial Mechanism 2014-2021, Norway; NCN and NAWA, Poland; La Caixa Banking Foundation, CERCA Programme Generalitat de Catalunya and PROMETEO and GenT Programmes Generalitat Valenciana, Spain; Göran Gustafssons Stiftelse, Sweden; The Royal Society and Leverhulme Trust, United Kingdom.

The crucial computing support from all WLCG partners is acknowledged gratefully, in particular from CERN, the ATLAS Tier-1 facilities at TRIUMF (Canada), NDGF (Denmark, Norway, Sweden),

CC-IN2P3 (France), KIT/GridKA (Germany), INFN-CNAF (Italy), NL-T1 (Netherlands), PIC (Spain), ASGC (Taiwan), RAL (UK) and BNL (USA), the Tier-2 facilities worldwide and large non-WLCG resource providers. Major contributors of computing resources are listed in Ref. [109].

References

- [1] S.L. Glashow, J. Iliopoulos, L. Maiani, Weak interactions with lepton-hadron symmetry, *Phys. Rev. D* 2 (1970) 1285.
- [2] J.A. Aguilar-Saavedra, Top flavor-changing neutral interactions: theoretical expectations and experimental detection, *Acta Phys. Pol. B* 35 (2004) 2695, arXiv:hep-ph/0409342.
- [3] J.M. Yang, B.-L. Young, X. Zhang, Flavor-changing top quark decays in R-parity-violating supersymmetric models, *Phys. Rev. D* 58 (1998) 055001, arXiv:hep-ph/9705341.
- [4] D. Delépine, S. Khalil, Top flavour violating decays in general supersymmetric models, *Phys. Lett. B* 599 (2004) 62, arXiv:hep-ph/0406264.
- [5] J.J. Cao, et al., Supersymmetry-induced flavor-changing neutral-current top-quark processes at the CERN Large Hadron Collider, *Phys. Rev. D* 75 (2007) 075021, arXiv:hep-ph/0702264.
- [6] J.-L. Yang, T.-F. Feng, H.-B. Zhang, G.-Z. Ning, X.-Y. Yang, Top quark decays with flavor violation in the B-LSSM, *Eur. Phys. J. C* 78 (2018) 438, arXiv:1806.01476 [hep-ph].
- [7] D. Atwood, L. Reina, A. Soni, Phenomenology of two Higgs doublet models with flavor-changing neutral currents, *Phys. Rev. D* 55 (1997) 3156, arXiv:hep-ph/9609279.
- [8] S. Béjar, J. Guasch, J. Solà, Loop induced flavor changing neutral decays of the top quark in a general two-Higgs-doublet model, *Nucl. Phys. B* 600 (2001) 21, arXiv:hep-ph/0011091.
- [9] ATLAS Collaboration, The ATLAS experiment at the CERN large hadron collider, *J. Instrum.* 3 (2008) S08003.
- [10] J.A. Aguilar-Saavedra, A minimal set of top anomalous couplings, *Nucl. Phys. B* 812 (2009) 181, arXiv:0811.3842 [hep-ph].
- [11] G. Durieux, F. Maltoni, C. Zhang, Global approach to top-quark flavor-changing interactions, *Phys. Rev. D* 91 (2015) 074017, arXiv:1412.7166 [hep-ph].
- [12] B. Grzadkowski, M. Iskrzyński, M. Misiak, J. Rosiek, Dimension-six terms in the standard model Lagrangian, *J. High Energy Phys.* 10 (2010) 085, arXiv:1008.4884 [hep-ph].
- [13] J.A. Aguilar-Saavedra, et al., Interpreting top-quark LHC measurements in the standard-model effective field theory, arXiv:1802.07237 [hep-ph].
- [14] CMS Collaboration, Search for anomalous single top quark production in association with a photon in pp collisions at $\sqrt{s} = 8$ TeV, *J. High Energy Phys.* 04 (2016) 035, arXiv:1511.03951 [hep-ex].
- [15] ATLAS Collaboration, Search for flavour-changing neutral currents in processes with one top quark and a photon using 81 fb^{-1} of pp collisions at $\sqrt{s} = 13\text{ TeV}$ with the ATLAS experiment, *Phys. Lett. B* 800 (2020) 135082, arXiv:1908.08461 [hep-ex].
- [16] B. Abbott, et al., Production and integration of the ATLAS Insertable B-Layer, *J. Instrum.* 13 (2018) T05008, arXiv:1803.00844 [physics.ins-det].
- [17] ATLAS Collaboration, ATLAS insertable B-layer technical design report addendum, CERN-LHCC-2012-009, Addendum to CERN-LHCC-2010-013, ATLAS-TDR-019, <https://cds.cern.ch/record/1451888>, 2012.
- [18] ATLAS Collaboration, Performance of the ATLAS trigger system in 2015, *Eur. Phys. J. C* 77 (2017) 317, arXiv:1611.09661 [hep-ex].
- [19] ATLAS Collaboration, The ATLAS Collaboration Software and Firmware, ATL-SOFT-PUB-2021-001, <https://cds.cern.ch/record/2767187>, 2021.
- [20] ATLAS Collaboration, Performance of electron and photon triggers in ATLAS during LHC Run 2, *Eur. Phys. J. C* 80 (2020) 47, arXiv:1909.00761 [hep-ex].
- [21] ATLAS Collaboration, Performance of the ATLAS muon triggers in Run 2, *J. Instrum.* 15 (2020) P09015, arXiv:2004.13447 [hep-ex].
- [22] ATLAS Collaboration, ATLAS data quality operations and performance for 2015–2018 data-taking, *J. Instrum.* 15 (2020) P04003, arXiv:1911.04632 [physics.ins-det].
- [23] G. Avoni, et al., The new LUCID-2 detector for luminosity measurement and monitoring in ATLAS, *J. Instrum.* 13 (2018) P07017.
- [24] T. Sjöstrand, S. Mrenna, P. Skands, A brief introduction to PYTHIA 8.1, *Comput. Phys. Commun.* 178 (2008) 852, arXiv:0710.3820 [hep-ph].
- [25] R.D. Ball, et al., Parton distributions with LHC data, *Nucl. Phys. B* 867 (2013) 244, arXiv:1207.1303 [hep-ph].
- [26] ATLAS Collaboration, The Pythia 8 A3 tune description of ATLAS minimum bias and inelastic measurements incorporating the Donnachie-Landshoff diffractive model, ATL-PHYS-PUB-2016-017, <https://cds.cern.ch/record/2206965>, 2016.
- [27] ATLAS Collaboration, The ATLAS simulation infrastructure, *Eur. Phys. J. C* 70 (2010) 823, arXiv:1005.4568 [physics.ins-det].
- [28] GEANT4 Collaboration, S. Agostinelli, et al., GEANT4 – a simulation toolkit, *Nucl. Instrum. Methods Phys. Res., Sect. A, Accel. Spectrom. Detect. Assoc. Equip.* 506 (2003) 250.

- [29] ATLAS Collaboration, The simulation principle and performance of the ATLAS fast calorimeter simulation FastCaloSim, ATL-PHYS-PUB-2010-013, <https://cds.cern.ch/record/1300517>, 2010.
- [30] D.J. Lange, The EvtGen particle decay simulation package, Nucl. Instrum. Methods Phys. Res., Sect. A, Accel. Spectrom. Detect. Assoc. Equip. 462 (2001) 152.
- [31] S. Mrenna, P. Skands, Automated parton-shower variations in PYTHIA 8, Phys. Rev. D 94 (2016) 074005, arXiv:1605.08352 [hep-ph].
- [32] C. Degrande, F. Maltoni, J. Wang, C. Zhang, Automatic computations at next-to-leading order in QCD for top-quark flavor-changing neutral processes, Phys. Rev. D 91 (2015) 034024, arXiv:1412.5594 [hep-ph].
- [33] R.D. Ball, et al., Parton distributions for the LHC run II, J. High Energy Phys. 04 (2015) 040, arXiv:1410.8849 [hep-ph].
- [34] M. Barros, et al., Study of interference effects in the search for flavour-changing neutral current interactions involving the top quark and a photon or a Z boson at the LHC, Eur. Phys. J. Plus 135 (2020) 339, arXiv:1909.08443 [hep-ph].
- [35] P. Artoisenet, R. Frederix, O. Mattelaer, R. Rietkerk, Automatic spin-entangled decays of heavy resonances in Monte Carlo simulations, J. High Energy Phys. 03 (2013) 015, arXiv:1212.3460 [hep-ph].
- [36] T. Sjöstrand, et al., An introduction to PYTHIA 8.2, Comput. Phys. Commun. 191 (2015) 159, arXiv:1410.3012 [hep-ph].
- [37] ATLAS Collaboration, ATLAS Pythia 8 tunes to 7 TeV data, ATL-PHYS-PUB-2014-021, <https://cds.cern.ch/record/1966419>, 2014.
- [38] J. Alwall, et al., The automated computation of tree-level and next-to-leading order differential cross sections, and their matching to parton shower simulations, J. High Energy Phys. 07 (2014) 079, arXiv:1405.0301 [hep-ph].
- [39] K. Melnikov, M. Schulze, A. Scharf, QCD corrections to top quark pair production in association with a photon at hadron colliders, Phys. Rev. D 83 (2011) 074013, arXiv:1102.1967 [hep-ph].
- [40] S. Frixione, G. Ridolfi, P. Nason, A positive-weight next-to-leading-order Monte Carlo for heavy flavour hadroproduction, J. High Energy Phys. 09 (2007) 126, arXiv:0707.3088 [hep-ph].
- [41] P. Nason, A new method for combining NLO QCD with shower Monte Carlo algorithms, J. High Energy Phys. 11 (2004) 040, arXiv:hep-ph/0409146.
- [42] S. Frixione, P. Nason, C. Oleari, Matching NLO QCD computations with parton shower simulations: the POWHEG method, J. High Energy Phys. 11 (2007) 070, arXiv:0709.2092 [hep-ph].
- [43] S. Alioli, P. Nason, C. Oleari, E. Re, A general framework for implementing NLO calculations in shower Monte Carlo programs: the POWHEG BOX, J. High Energy Phys. 06 (2010) 043, arXiv:1002.2581 [hep-ph].
- [44] ATLAS Collaboration, Studies on top-quark Monte Carlo modelling for Top2016, ATL-PHYS-PUB-2016-020, <https://cds.cern.ch/record/2216168>, 2016.
- [45] M. Beneke, P. Falgari, S. Klein, C. Schwinn, Hadronic top-quark pair production with NNLL threshold resummation, Nucl. Phys. B 855 (2012) 695, arXiv:1109.1536 [hep-ph].
- [46] M. Cacciari, M. Czakon, M. Mangano, A. Mitov, P. Nason, Top-pair production at hadron colliders with next-to-next-to-leading logarithmic soft-gluon resummation, Phys. Lett. B 710 (2012) 612, arXiv:1111.5869 [hep-ph].
- [47] P. Bärnreuther, M. Czakon, A. Mitov, Percent-level-precision physics at the Tevatron: next-to-next-to-leading order QCD corrections to $q\bar{q} \rightarrow t\bar{t} + X$, Phys. Rev. Lett. 109 (2012) 132001, arXiv:1204.5201 [hep-ph].
- [48] M. Czakon, A. Mitov, NNLO corrections to top-pair production at hadron colliders: the all-fermionic scattering channels, J. High Energy Phys. 12 (2012) 054, arXiv:1207.0236 [hep-ph].
- [49] M. Czakon, A. Mitov, NNLO corrections to top pair production at hadron colliders: the quark-gluon reaction, J. High Energy Phys. 01 (2013) 080, arXiv:1210.6832 [hep-ph].
- [50] M. Czakon, P. Fiedler, A. Mitov, Total top-quark pair-production cross section at hadron colliders through $O(\alpha_s^4)$, Phys. Rev. Lett. 110 (2013) 252004, arXiv:1303.6254 [hep-ph].
- [51] M. Czakon, A. Mitov, Top++: a program for the calculation of the top-pair cross-section at hadron colliders, Comput. Phys. Commun. 185 (2014) 2930, arXiv:1112.5675 [hep-ph].
- [52] R. Frederix, E. Re, P. Torrielli, Single-top t -channel hadroproduction in the four-flavour scheme with POWHEG and aMC@NLO, J. High Energy Phys. 09 (2012) 130, arXiv:1207.5391 [hep-ph].
- [53] S. Frixione, E. Laenen, P. Motylinski, C. White, B.R. Webber, Single-top hadroproduction in association with a W boson, J. High Energy Phys. 07 (2008) 029, arXiv:0805.3067 [hep-ph].
- [54] E. Bothmann, et al., Event generation with Sherpa 2.2, SciPost Phys. 7 (2019) 034, arXiv:1905.09127 [hep-ph].
- [55] T. Gleisberg, S. Höche, Comix, a new matrix element generator, J. High Energy Phys. 12 (2008) 039, arXiv:0808.3674 [hep-ph].
- [56] S. Schumann, F. Krauss, A parton shower algorithm based on Catani–Seymour dipole factorisation, J. High Energy Phys. 03 (2008) 038, arXiv:0709.1027 [hep-ph].
- [57] S. Höche, F. Krauss, M. Schönher, F. Siegert, A critical appraisal of NLO+PS matching methods, J. High Energy Phys. 09 (2012) 049, arXiv:1111.1220 [hep-ph].
- [58] S. Höche, F. Krauss, M. Schönher, F. Siegert, QCD matrix elements + parton showers. The NLO case, J. High Energy Phys. 04 (2013) 027, arXiv:1207.5030 [hep-ph].
- [59] S. Catani, F. Krauss, B.R. Webber, R. Kuhn, QCD matrix elements + parton showers, J. High Energy Phys. 11 (2001) 063, arXiv:hep-ph/0109231.
- [60] S. Höche, F. Krauss, S. Schumann, F. Siegert, QCD matrix elements and truncated showers, J. High Energy Phys. 05 (2009) 053, arXiv:0903.1219 [hep-ph].
- [61] F. Buccioni, et al., OpenLoops 2, Eur. Phys. J. C 79 (2019) 866, arXiv:1907.13071 [hep-ph].
- [62] F. Cascioli, P. Maierhöfer, S. Pozzorini, Scattering amplitudes with open loops, Phys. Rev. Lett. 108 (2012) 111601, arXiv:1111.5206 [hep-ph].
- [63] F. Buccioni, S. Pozzorini, M. Zoller, On-the-fly reduction of open loops, Eur. Phys. J. C 78 (2018) 70, arXiv:1710.11452 [hep-ph].
- [64] A. Denner, S. Dittmaier, L. Hofer, COLLIER: a fortran-based complex one-loop library in extended regularizations, Comput. Phys. Commun. 212 (2017) 220, arXiv:1604.06792 [hep-ph].
- [65] C. Anastasiou, L. Dixon, K. Melnikov, F. Petriello, High-precision QCD at hadron colliders: electroweak gauge boson rapidity distributions at next-to-next-to-leading order, Phys. Rev. D 69 (2004) 094008, arXiv:hep-ph/0312266.
- [66] ATLAS Collaboration, Measurements of inclusive and differential fiducial cross-sections of $t\bar{t}\gamma$ production in leptonic final states at $\sqrt{s} = 13$ TeV in ATLAS, Eur. Phys. J. C 79 (2019) 382, arXiv:1812.01697 [hep-ex].
- [67] ATLAS Collaboration, Electron and photon reconstruction and performance in ATLAS using a dynamical, topological cell clustering-based approach, ATL-PHYS-PUB-2017-022, <https://cds.cern.ch/record/2298955>, 2017.
- [68] ATLAS Collaboration, Electron and photon performance measurements with the ATLAS detector using the 2015–2017 LHC proton–proton collision data, J. Instrum. 14 (2019) P12006, arXiv:1908.00005 [hep-ex].
- [69] ATLAS Collaboration, Muon reconstruction and identification efficiency in ATLAS using the full Run 2 pp collision data set at $\sqrt{s} = 13$ TeV, Eur. Phys. J. C 81 (2021) 578, arXiv:2012.00578 [hep-ex].
- [70] ATLAS Collaboration, Jet reconstruction and performance using particle flow with the ATLAS detector, Eur. Phys. J. C 77 (2017) 466, arXiv:1703.10485 [hep-ex].
- [71] M. Cacciari, G.P. Salam, G. Soyez, The anti- k_t jet clustering algorithm, J. High Energy Phys. 04 (2008) 063, arXiv:0802.1189 [hep-ph].
- [72] M. Cacciari, G.P. Salam, G. Soyez, FastJet user manual, Eur. Phys. J. C 72 (2012) 1896, arXiv:1111.6097 [hep-ph].
- [73] ATLAS Collaboration, Jet energy scale and resolution measured in proton–proton collisions at $\sqrt{s} = 13$ TeV with the ATLAS detector, Eur. Phys. J. C 81 (2020) 689, arXiv:2007.02645 [hep-ex].
- [74] ATLAS Collaboration, Performance of pile-up mitigation techniques for jets in pp collisions at $\sqrt{s} = 8$ TeV using the ATLAS detector, Eur. Phys. J. C 76 (2016) 581, arXiv:1510.03823 [hep-ex].
- [75] ATLAS Collaboration, ATLAS b-jet identification performance and efficiency measurement with $t\bar{t}$ events in pp collisions at $\sqrt{s} = 13$ TeV, Eur. Phys. J. C 79 (2019) 970, arXiv:1907.05120 [hep-ex].
- [76] ATLAS Collaboration, Optimisation and performance studies of the ATLAS b-tagging algorithms for the 2017–18 LHC run, ATL-PHYS-PUB-2017-013, <https://cds.cern.ch/record/2273281>, 2017.
- [77] ATLAS Collaboration, Performance of missing transverse momentum reconstruction with the ATLAS detector using proton–proton collisions at $\sqrt{s} = 13$ TeV, Eur. Phys. J. C 78 (2018) 903, arXiv:1802.08168 [hep-ex].
- [78] ATLAS Collaboration, Electron reconstruction and identification in the ATLAS experiment using the 2015 and 2016 LHC proton–proton collision data at $\sqrt{s} = 13$ TeV, Eur. Phys. J. C 79 (2019) 639, arXiv:1902.04655 [hep-ex].
- [79] ATLAS Collaboration, Electron and photon energy calibration with the ATLAS detector using 2015–2016 LHC proton–proton collision data, J. Instrum. 14 (2019) P03017, arXiv:1812.03848 [hep-ex].
- [80] ATLAS Collaboration, Muon reconstruction performance of the ATLAS detector in proton–proton collision data at $\sqrt{s} = 13$ TeV, Eur. Phys. J. C 76 (2016) 292, arXiv:1603.05598 [hep-ex].
- [81] ATLAS Collaboration, Tagging and suppression of pileup jets with the ATLAS detector, ATLAS-CONF-2014-018, <https://cds.cern.ch/record/1700870>, 2014.
- [82] ATLAS Collaboration, Measurement of b-tagging efficiency of c-jets in $t\bar{t}$ events using a likelihood approach with the ATLAS detector, ATLAS-CONF-2018-001, <https://cds.cern.ch/record/2306649>, 2018.
- [83] ATLAS Collaboration, Calibration of light-flavour b-jet mistagging rates using ATLAS proton–proton collision data at $\sqrt{s} = 13$ TeV, ATLAS-CONF-2018-006, <https://cds.cern.ch/record/2314418>, 2018.
- [84] ATLAS Collaboration, Measurement of the photon identification efficiencies with the ATLAS detector using LHC Run 2 data collected in 2015 and 2016, Eur. Phys. J. C 79 (2019) 205, arXiv:1810.05087 [hep-ex].
- [85] CDF Collaboration, Measurement of $\sigma B(W \rightarrow e\nu)$ and $\sigma B(Z^0 \rightarrow e^+e^-)$ in $\bar{p}p$ collisions at $\sqrt{s} = 1800$ GeV, Phys. Rev. D 44 (1991) 29.
- [86] F. Chollet, et al., <https://keras.io>, 2015.
- [87] M. Abadi, et al., TensorFlow: large-scale machine learning on heterogeneous systems, <https://www.tensorflow.org>, 2015.
- [88] F. Pedregosa, et al., Scikit-learn: machine learning in Python, J. Mach. Learn. Res. 12 (2011) 2825, arXiv:1201.0490 [cs.LG], <http://jmlr.org/papers/v12/pedregosa11a.html>.

- [89] D.P. Kingma, J. Ba, Adam: a method for stochastic optimization, arXiv:1412.6980, 2014.
- [90] M. Botje, et al., The PDF4LHC working group interim recommendations, arXiv: 1101.0538 [hep-ph], 2011.
- [91] A.D. Martin, W.J. Stirling, R.S. Thorne, G. Watt, Uncertainties on α_S in global PDF analyses and implications for predicted hadronic cross sections, Eur. Phys. J. C 64 (2009) 653, arXiv:0905.3531 [hep-ph].
- [92] J. Gao, et al., CT10 next-to-next-to-leading order global analysis of QCD, Phys. Rev. D 89 (2014) 033009, arXiv:1302.6246 [hep-ph].
- [93] N. Kidonakis, Next-to-next-to-leading-order collinear and soft gluon corrections for t-channel single top quark production, Phys. Rev. D 83 (2011) 091503, arXiv:1103.2792 [hep-ph].
- [94] N. Kidonakis, Next-to-next-to-leading logarithm resummation for s-channel single top quark production, Phys. Rev. D 81 (2010) 054028, arXiv:1001.5034 [hep-ph].
- [95] N. Kidonakis, Two-loop soft anomalous dimensions for single top quark associated production with a W^- or H^- , Phys. Rev. D 82 (2010) 054018, arXiv:1005.4451 [hep-ph].
- [96] ATLAS Collaboration, Monte Carlo generators for the production of a W or Z/γ^* boson in association with jets at ATLAS in Run 2, ATL-PHYS-PUB-2016-003, <https://cds.cern.ch/record/2120133>, 2016.
- [97] ATLAS Collaboration, Multi-boson simulation for 13 TeV ATLAS analyses, ATL-PHYS-PUB-2016-002, <https://cds.cern.ch/record/2119986>, 2016.
- [98] M. Bähr, et al., Herwig++ physics and manual, Eur. Phys. J. C 58 (2008) 639, arXiv:0803.0883 [hep-ph].
- [99] J. Bellm, et al., Herwig 7.0/Herwig++ 3.0 release note, Eur. Phys. J. C 76 (2016) 196, arXiv:1512.01178 [hep-ph].
- [100] L. Harland-Lang, A. Martin, P. Motylinski, R. Thorne, Parton distributions in the LHC era: MMHT 2014 PDFs, Eur. Phys. J. C 75 (2015) 204, arXiv:1412.3989 [hep-ph].
- [101] ATLAS Collaboration, Studies on top-quark Monte Carlo modelling with Sherpa and MG5_aMC@NLO, ATL-PHYS-PUB-2017-007, <https://cds.cern.ch/record/2261938>, 2017.
- [102] ATLAS Collaboration, Luminosity determination in pp collisions at $\sqrt{s} = 13\text{TeV}$ using the ATLAS detector at the LHC, ATLAS-CONF-2019-021, <https://cds.cern.ch/record/2677054>, 2019.
- [103] ATLAS Collaboration, Photon identification in 2015 ATLAS data, ATL-PHYS-PUB-2016-014, <https://cds.cern.ch/record/2203125>, 2016.
- [104] ATLAS Collaboration, Jet energy scale measurements and their systematic uncertainties in proton-proton collisions at $\sqrt{s} = 13\text{TeV}$ with the ATLAS detector, Phys. Rev. D 96 (2017) 072002, arXiv:1703.09665 [hep-ex].
- [105] ATLAS Collaboration, Jet calibration and systematic uncertainties for jets reconstructed in the ATLAS detector at $\sqrt{s} = 13\text{TeV}$, ATL-PHYS-PUB-2015-015, <https://cds.cern.ch/record/2037613>, 2015.
- [106] R. Barlow, C. Beeston, Fitting using finite Monte Carlo samples, Comput. Phys. Commun. 77 (1993) 219.
- [107] A.L. Read, Presentation of search results: the CL_s technique, J. Phys. G 28 (2002) 2693.
- [108] G. Cowan, K. Cranmer, E. Gross, O. Vitells, Asymptotic formulae for likelihood-based tests of new physics, Eur. Phys. J. C 71 (2011) 1554, arXiv:1007.1727 [physics.data-an], Erratum: Eur. Phys. J. C 73 (2013) 2501.
- [109] ATLAS Collaboration, ATLAS Computing Acknowledgements, ATL-SOFT-PUB-2021-003.

The ATLAS Collaboration

G. Aad¹⁰¹, B. Abbott¹¹⁹, D.C. Abbott¹⁰², A. Abed Abud³⁶, K. Abeling⁵⁵, S.H. Abidi²⁹, A. Aboulhorma^{35e}, H. Abramowicz¹⁵⁰, H. Abreu¹⁴⁹, Y. Abulaiti¹¹⁶, A.C. Abusleme Hoffman^{136a}, B.S. Acharya^{68a,68b,o}, B. Achkar⁵⁵, L. Adam⁹⁹, C. Adam Bourdarios⁴, L. Adamczyk^{84a}, L. Adamek¹⁵⁴, S.V. Addepalli²⁶, J. Adelman¹¹⁴, A. Adiguzel^{21c}, S. Adorni⁵⁶, T. Adye¹³³, A.A. Affolder¹³⁵, Y. Afik³⁶, M.N. Agaras¹³, J. Agarwala^{72a,72b}, A. Aggarwal⁹⁹, C. Agheorghiesei^{27c}, J.A. Aguilar-Saavedra^{129f}, A. Ahmad³⁶, F. Ahmadov^{38,w}, W.S. Ahmed¹⁰³, X. Ai⁴⁸, G. Aielli^{75a,75b}, I. Aizenberg¹⁶⁸, M. Akbiyik⁹⁹, T.P.A. Åkesson⁹⁷, A.V. Akimov³⁷, K. Al Khoury⁴¹, G.L. Alberghi^{23b}, J. Albert¹⁶⁴, P. Albicocco⁵³, M.J. Alconada Verzini⁸⁹, S. Alderweireldt⁵², M. Alekса³⁶, I.N. Aleksandrov³⁸, C. Alexa^{27b}, T. Alexopoulos¹⁰, A. Alfonsi¹¹³, F. Alfonsi^{23b}, M. Alhroob¹¹⁹, B. Ali¹³¹, S. Ali¹⁴⁷, M. Aliev³⁷, G. Alimonti^{70a}, C. Allaire³⁶, B.M.M. Allbrooke¹⁴⁵, P.P. Allport²⁰, A. Aloisio^{71a,71b}, F. Alonso⁸⁹, C. Alpigiani¹³⁷, E. Alunno Camelia^{75a,75b}, M. Alvarez Estevez⁹⁸, M.G. Alviggi^{71a,71b}, Y. Amaral Coutinho^{81b}, A. Ambler¹⁰³, C. Amelung³⁶, C.G. Ames¹⁰⁸, D. Amidei¹⁰⁵, S.P. Amor Dos Santos^{129a}, S. Amoroso⁴⁸, K.R. Amos¹⁶², C.S. Amrouche⁵⁶, V. Ananiev¹²⁴, C. Anastopoulos¹³⁸, N. Andari¹³⁴, T. Andeen¹¹, J.K. Anders¹⁹, S.Y. Andrean^{47a,47b}, A. Andreazza^{70a,70b}, S. Angelidakis⁹, A. Angerami^{41,y}, A.V. Anisenkov³⁷, A. Annovi^{73a}, C. Antel⁵⁶, M.T. Anthony¹³⁸, E. Antipov¹²⁰, M. Antonelli⁵³, D.J.A. Antrim^{17a}, F. Anulli^{74a}, M. Aoki⁸², J.A. Aparisi Pozo¹⁶², M.A. Aparo¹⁴⁵, L. Aperio Bella⁴⁸, C. Appelt¹⁸, N. Aranzabal³⁶, V. Araujo Ferraz^{81a}, C. Arcangeletti⁵³, A.T.H. Arce⁵¹, E. Arena⁹¹, J.-F. Arguin¹⁰⁷, S. Argyropoulos⁵⁴, J.-H. Arling⁴⁸, A.J. Armbruster³⁶, O. Arnaez¹⁵⁴, H. Arnold¹¹³, Z.P. Arrubarrena Tame¹⁰⁸, G. Artoni^{74a,74b}, H. Asada¹¹⁰, K. Asai¹¹⁷, S. Asai¹⁵², N.A. Asbah⁶¹, E.M. Asimakopoulou¹⁶⁰, J. Assahsah^{35d}, K. Assamagan²⁹, R. Astalos^{28a}, R.J. Atkin^{33a}, M. Atkinson¹⁶¹, N.B. Atlay¹⁸, H. Atmani^{62b}, P.A. Atmasiddha¹⁰⁵, K. Augsten¹³¹, S. Auricchio^{71a,71b}, A.D. Auriol²⁰, V.A. Astrup¹⁷⁰, G. Avner¹⁴⁹, G. Avolio³⁶, K. Axiotis⁵⁶, M.K. Ayoub^{14c}, G. Azuelos^{107,ad}, D. Babal^{28a}, H. Bachacou¹³⁴, K. Bachas^{151,q}, A. Bachiu³⁴, F. Backman^{47a,47b}, A. Badea⁶¹, P. Bagnaia^{74a,74b}, M. Bahmani¹⁸, A.J. Bailey¹⁶², V.R. Bailey¹⁶¹, J.T. Baines¹³³, C. Bakalis¹⁰, O.K. Baker¹⁷¹, P.J. Bakker¹¹³, E. Bakos¹⁵, D. Bakshi Gupta⁸, S. Balaji¹⁴⁶, R. Balasubramanian¹¹³, E.M. Baldin³⁷, P. Balek¹³², E. Ballabene^{70a,70b}, F. Balli¹³⁴, L.M. Baltes^{63a}, W.K. Balunas³², J. Balz⁹⁹, E. Banas⁸⁵, M. Bandieramonte¹²⁸, A. Bandyopadhyay²⁴, S. Bansal²⁴, L. Barak¹⁵⁰, E.L. Barberio¹⁰⁴, D. Barberis^{57b,57a}, M. Barbero¹⁰¹, G. Barbour⁹⁵, K.N. Barends^{33a}, T. Barillari¹⁰⁹, M.-S. Barisits³⁶, J. Barkeloo¹²², T. Barklow¹⁴², R.M. Barnett^{17a}, P. Baron¹²¹, D.A. Baron Moreno¹⁰⁰, A. Baroncelli^{62a}, G. Barone²⁹, A.J. Barr¹²⁵, L. Barranco Navarro^{47a,47b}, F. Barreiro⁹⁸, J. Barreiro Guimarães da Costa^{14a}, U. Barron¹⁵⁰, S. Barsov³⁷, F. Bartels^{63a}, R. Bartoldus¹⁴², A.E. Barton⁹⁰, P. Bartos^{28a}, A. Basalaev⁴⁸,

- A. Basan ⁹⁹, M. Baselga ⁴⁹, I. Bashta ^{76a,76b}, A. Bassalat ^{66,z}, M.J. Basso ¹⁵⁴, C.R. Basson ¹⁰⁰, R.L. Bates ⁵⁹, S. Batlamous ^{35e}, J.R. Batley ³², B. Batool ¹⁴⁰, M. Battaglia ¹³⁵, M. Bauce ^{74a,74b}, P. Bauer ²⁴, A. Bayirli ^{21a}, J.B. Beacham ⁵¹, T. Beau ¹²⁶, P.H. Beauchemin ¹⁵⁷, F. Becherer ⁵⁴, P. Bechtle ²⁴, H.P. Beck ^{19,p}, K. Becker ¹⁶⁶, C. Becot ⁴⁸, A.J. Beddall ^{21d}, V.A. Bednyakov ³⁸, C.P. Bee ¹⁴⁴, L.J. Beemster ¹⁵, T.A. Beermann ³⁶, M. Begalli ^{81b}, M. Begel ²⁹, A. Behera ¹⁴⁴, J.K. Behr ⁴⁸, C. Beirao Da Cruz E Silva ³⁶, J.F. Beirer ^{55,36}, F. Beisiegel ²⁴, M. Belfkir ¹⁵⁸, G. Bella ¹⁵⁰, L. Bellagamba ^{23b}, A. Bellerive ³⁴, P. Bellos ²⁰, K. Beloborodov ³⁷, K. Belotskiy ³⁷, N.L. Belyaev ³⁷, D. Benchekroun ^{35a}, Y. Benhammou ¹⁵⁰, D.P. Benjamin ²⁹, M. Benoit ²⁹, J.R. Bensinger ²⁶, S. Bentvelsen ¹¹³, L. Beresford ³⁶, M. Beretta ⁵³, D. Berge ¹⁸, E. Bergeaas Kuutmann ¹⁶⁰, N. Berger ⁴, B. Bergmann ¹³¹, J. Beringer ^{17a}, S. Berlendis ⁷, G. Bernardi ⁵, C. Bernius ¹⁴², F.U. Bernlochner ²⁴, T. Berry ⁹⁴, P. Berta ¹³², A. Berthold ⁵⁰, I.A. Bertram ⁹⁰, O. Bessidskaia Bylund ¹⁷⁰, S. Bethke ¹⁰⁹, A. Betti ⁴⁴, A.J. Bevan ⁹³, S. Bhatta ¹⁴⁴, D.S. Bhattacharya ¹⁶⁵, P. Bhattacharai ²⁶, V.S. Bhopatkar ⁶, R. Bi ¹²⁸, R. Bi ^{29,ag}, R.M. Bianchi ¹²⁸, O. Biebel ¹⁰⁸, R. Bielski ¹²², N.V. Biesuz ^{73a,73b}, M. Biglietti ^{76a}, T.R.V. Billoud ¹³¹, M. Bindi ⁵⁵, A. Bingul ^{21b}, C. Bini ^{74a,74b}, S. Biondi ^{23b,23a}, A. Biondini ⁹¹, C.J. Birch-sykes ¹⁰⁰, G.A. Bird ^{20,133}, M. Birman ¹⁶⁸, T. Bisanz ³⁶, D. Biswas ^{169,k}, A. Bitadze ¹⁰⁰, K. Bjørke ¹²⁴, I. Bloch ⁴⁸, C. Blocker ²⁶, A. Blue ⁵⁹, U. Blumenschein ⁹³, J. Blumenthal ⁹⁹, G.J. Bobbink ¹¹³, V.S. Bobrovnikov ³⁷, M. Boehler ⁵⁴, D. Bogavac ¹³, A.G. Bogdanchikov ³⁷, C. Bohm ^{47a}, V. Boisvert ⁹⁴, P. Bokan ⁴⁸, T. Bold ^{84a}, M. Bomben ⁵, M. Bona ⁹³, M. Boonekamp ¹³⁴, C.D. Booth ⁹⁴, A.G. Borbély ⁵⁹, H.M. Borecka-Bielska ¹⁰⁷, L.S. Borgna ⁹⁵, G. Borissov ⁹⁰, D. Bortoletto ¹²⁵, D. Boscherini ^{23b}, M. Bosman ¹³, J.D. Bossio Sola ³⁶, K. Bouaouda ^{35a}, J. Boudreau ¹²⁸, E.V. Bouhova-Thacker ⁹⁰, D. Boumediene ⁴⁰, R. Bouquet ⁵, A. Boveia ¹¹⁸, J. Boyd ³⁶, D. Boye ²⁹, I.R. Boyko ³⁸, J. Bracinik ²⁰, N. Brahimi ^{62d,62c}, G. Brandt ¹⁷⁰, O. Brandt ³², F. Braren ⁴⁸, B. Brau ¹⁰², J.E. Brau ¹²², W.D. Breaden Madden ⁵⁹, K. Brendlinger ⁴⁸, R. Brener ¹⁶⁸, L. Brenner ³⁶, R. Brenner ¹⁶⁰, S. Bressler ¹⁶⁸, B. Brickwedde ⁹⁹, D. Britton ⁵⁹, D. Britzger ¹⁰⁹, I. Brock ²⁴, G. Brooijmans ⁴¹, W.K. Brooks ^{136f}, E. Brost ²⁹, P.A. Bruckman de Renstrom ⁸⁵, B. Brüers ⁴⁸, D. Bruncko ^{28b,*}, A. Bruni ^{23b}, G. Bruni ^{23b}, M. Bruschi ^{23b}, N. Bruscino ^{74a,74b}, L. Bryngemark ¹⁴², T. Buanes ¹⁶, Q. Buat ¹³⁷, P. Buchholz ¹⁴⁰, A.G. Buckley ⁵⁹, I.A. Budagov ^{38,*}, M.K. Bugge ¹²⁴, O. Bulekov ³⁷, B.A. Bullard ⁶¹, S. Burdin ⁹¹, C.D. Burgard ⁴⁸, A.M. Burger ⁴⁰, B. Burghgrave ⁸, J.T.P. Burr ³², C.D. Burton ¹¹, J.C. Burzynski ¹⁴¹, E.L. Busch ⁴¹, V. Büscher ⁹⁹, P.J. Bussey ⁵⁹, J.M. Butler ²⁵, C.M. Buttar ⁵⁹, J.M. Butterworth ⁹⁵, W. Buttinger ¹³³, C.J. Buxo Vazquez ¹⁰⁶, A.R. Buzykaev ³⁷, G. Cabras ^{23b}, S. Cabrera Urbán ¹⁶², D. Caforio ⁵⁸, H. Cai ¹²⁸, Y. Cai ^{14a,14d}, V.M.M. Cairo ³⁶, O. Cakir ^{3a}, N. Calace ³⁶, P. Calafiura ^{17a}, G. Calderini ¹²⁶, P. Calfayan ⁶⁷, G. Callea ⁵⁹, L.P. Caloba ^{81b}, D. Calvet ⁴⁰, S. Calvet ⁴⁰, T.P. Calvet ¹⁰¹, M. Calvetti ^{73a,73b}, R. Camacho Toro ¹²⁶, S. Camarda ³⁶, D. Camarero Munoz ⁹⁸, P. Camarri ^{75a,75b}, M.T. Camerlingo ^{76a,76b}, D. Cameron ¹²⁴, C. Camincher ¹⁶⁴, M. Campanelli ⁹⁵, A. Camplani ⁴², V. Canale ^{71a,71b}, A. Canesse ¹⁰³, M. Cano Bret ⁷⁹, J. Cantero ¹⁶², Y. Cao ¹⁶¹, F. Capocasa ²⁶, M. Capua ^{43b,43a}, A. Carbone ^{70a,70b}, R. Cardarelli ^{75a}, J.C.J. Cardenas ⁸, F. Cardillo ¹⁶², T. Carli ³⁶, G. Carlino ^{71a}, B.T. Carlson ^{128,r}, E.M. Carlson ^{164,155a}, L. Carminati ^{70a,70b}, M. Carnesale ^{74a,74b}, S. Caron ¹¹², E. Carquin ^{136f}, S. Carrá ⁴⁸, G. Carratta ^{23b,23a}, J.W.S. Carter ¹⁵⁴, T.M. Carter ⁵², M.P. Casado ^{13,h}, A.F. Casha ¹⁵⁴, E.G. Castiglia ¹⁷¹, F.L. Castillo ^{63a}, L. Castillo Garcia ¹³, V. Castillo Gimenez ¹⁶², N.F. Castro ^{129a,129e}, A. Catinaccio ³⁶, J.R. Catmore ¹²⁴, V. Cavaliere ²⁹, N. Cavalli ^{23b,23a}, V. Cavasinni ^{73a,73b}, E. Celebi ^{21a}, F. Celli ¹²⁵, M.S. Centonze ^{69a,69b}, K. Cerny ¹²¹, A.S. Cerqueira ^{81a}, A. Cerri ¹⁴⁵, L. Cerrito ^{75a,75b}, F. Cerutti ^{17a}, A. Cervelli ^{23b}, S.A. Cetin ^{21d}, Z. Chadi ^{35a}, D. Chakraborty ¹¹⁴, M. Chala ^{129f}, J. Chan ¹⁶⁹, W.S. Chan ¹¹³, W.Y. Chan ¹⁵², J.D. Chapman ³², B. Chargeishvili ^{148b}, D.G. Charlton ²⁰, T.P. Charman ⁹³, M. Chatterjee ¹⁹, S. Chekanov ⁶, S.V. Chekulaev ^{155a}, G.A. Chelkov ^{38,a}, A. Chen ¹⁰⁵, B. Chen ¹⁵⁰, B. Chen ¹⁶⁴, C. Chen ^{62a}, H. Chen ^{14c}, H. Chen ²⁹, J. Chen ^{62c}, J. Chen ²⁶, S. Chen ¹⁵², S.J. Chen ^{14c}, X. Chen ^{62c}, X. Chen ^{14b,ac}, Y. Chen ^{62a}, C.L. Cheng ¹⁶⁹, H.C. Cheng ^{64a}, A. Cheplakov ³⁸, E. Cheremushkina ⁴⁸, E. Cherepanova ³⁸, R. Cherkaoui El Moursli ^{35e}, E. Cheu ⁷, K. Cheung ⁶⁵, L. Chevalier ¹³⁴, V. Chiarella ⁵³, G. Chiarella ^{73a}, G. Chiodini ^{69a}, A.S. Chisholm ²⁰, A. Chitan ^{27b}, Y.H. Chiu ¹⁶⁴, M.V. Chizhov ³⁸, K. Choi ¹¹, A.R. Chomont ^{74a,74b}, Y. Chou ¹⁰², E.Y.S. Chow ¹¹³, T. Chowdhury ^{33g}, L.D. Christopher ^{33g}, K.L. Chu ^{64a}, M.C. Chu ^{64a}, X. Chu ^{14a,14d}, J. Chudoba ¹³⁰, J.J. Chwastowski ⁸⁵, D. Cieri ¹⁰⁹, K.M. Ciesla ⁸⁵, V. Cindro ⁹², A. Ciocio ^{17a}, F. Cirotto ^{71a,71b}, Z.H. Citron ^{168,l}, M. Citterio ^{70a}, D.A. Ciubotaru ^{27b}, B.M. Ciungu ¹⁵⁴, A. Clark ⁵⁶, P.J. Clark ⁵², J.M. Clavijo Columbie ⁴⁸, S.E. Clawson ¹⁰⁰, C. Clement ^{47a,47b}, J. Clercx ⁴⁸, L. Clissa ^{23b,23a}, Y. Coadou ¹⁰¹, M. Cobal ^{68a,68c}, A. Coccaro ^{57b}, R.F. Coelho Barrue ^{129a}, R. Coelho Lopes De Sa ¹⁰², S. Coelli ^{70a}, H. Cohen ¹⁵⁰, A.E.C. Coimbra ¹⁴⁹, B. Cole ⁴¹, J. Collot ⁶⁰, P. Conde Muiño ^{129a,129g}, S.H. Connell ^{33c}, I.A. Connally ⁵⁹,

- E.I. Conroy ¹²⁵, F. Conventi ^{71a,ae}, H.G. Cooke ²⁰, A.M. Cooper-Sarkar ¹²⁵, F. Cormier ¹⁶³, L.D. Corpe ³⁶, M. Corradi ^{74a,74b}, E.E. Corrigan ⁹⁷, F. Corriveau ^{103,v}, A. Cortes-Gonzalez ¹⁸, M.J. Costa ¹⁶², F. Costanza ⁴, D. Costanzo ¹³⁸, B.M. Cote ¹¹⁸, G. Cowan ⁹⁴, J.W. Cowley ³², K. Cranmer ¹¹⁶, S. Crépé-Renaudin ⁶⁰, F. Crescioli ¹²⁶, M. Cristinziani ¹⁴⁰, M. Cristoforetti ^{77a,77b,c}, V. Croft ¹⁵⁷, G. Crosetti ^{43b,43a}, A. Cueto ³⁶, T. Cuhadar Donszelmann ¹⁵⁹, H. Cui ^{14a,14d}, Z. Cui ⁷, A.R. Cukierman ¹⁴², W.R. Cunningham ⁵⁹, F. Curcio ^{43b,43a}, P. Czodrowski ³⁶, M.M. Czurylo ^{63b}, M.J. Da Cunha Sargedas De Sousa ^{62a}, J.V. Da Fonseca Pinto ^{81b}, C. Da Via ¹⁰⁰, W. Dabrowski ^{84a}, T. Dado ⁴⁹, S. Dahbi ^{33g}, T. Dai ¹⁰⁵, C. Dallapiccola ¹⁰², M. Dam ⁴², G. D'amen ²⁹, V. D'Amico ^{76a,76b}, J. Damp ⁹⁹, J.R. Dandoy ¹²⁷, M.F. Daneri ³⁰, M. Danner ¹⁴¹, V. Dao ³⁶, G. Darbo ^{57b}, S. Darmora ⁶, S.J. Das ²⁹, A. Dattagupta ¹²², S. D'Auria ^{70a,70b}, C. David ^{155b}, T. Davidek ¹³², D.R. Davis ⁵¹, B. Davis-Purcell ³⁴, I. Dawson ⁹³, K. De ⁸, R. De Asmundis ^{71a}, M. De Beurs ¹¹³, S. De Castro ^{23b,23a}, N. De Groot ¹¹², P. de Jong ¹¹³, H. De la Torre ¹⁰⁶, A. De Maria ^{14c}, A. De Salvo ^{74a}, U. De Sanctis ^{75a,75b}, M. De Santis ^{75a,75b}, A. De Santo ¹⁴⁵, J.B. De Vivie De Regie ⁶⁰, D.V. Dedovich ³⁸, J. Degens ¹¹³, A.M. Deiana ⁴⁴, F. Del Corso ^{23b,23a}, J. Del Peso ⁹⁸, F. Del Rio ^{63a}, F. Deliot ¹³⁴, C.M. Delitzsch ⁴⁹, M. Della Pietra ^{71a,71b}, D. Della Volpe ⁵⁶, A. Dell'Acqua ³⁶, L. Dell'Asta ^{70a,70b}, M. Delmastro ⁴, P.A. Delsart ⁶⁰, S. Demers ¹⁷¹, M. Demichev ³⁸, S.P. Denisov ³⁷, L. D'Eramo ¹¹⁴, D. Derendarz ⁸⁵, F. Derue ¹²⁶, P. Dervan ⁹¹, K. Desch ²⁴, K. Dette ¹⁵⁴, C. Deutsch ²⁴, P.O. Deviveiros ³⁶, F.A. Di Bello ^{74a,74b}, A. Di Ciacio ^{75a,75b}, L. Di Ciacio ⁴, A. Di Domenico ^{74a,74b}, C. Di Donato ^{71a,71b}, A. Di Girolamo ³⁶, G. Di Gregorio ^{73a,73b}, A. Di Luca ^{77a,77b}, B. Di Micco ^{76a,76b}, R. Di Nardo ^{76a,76b}, C. Diaconu ¹⁰¹, F.A. Dias ¹¹³, T. Dias Do Vale ¹⁴¹, M.A. Diaz ^{136a,136b}, F.G. Diaz Capriles ²⁴, M. Didenko ¹⁶², E.B. Diehl ¹⁰⁵, L. Diehl ⁵⁴, S. Díez Cornell ⁴⁸, C. Diez Pardos ¹⁴⁰, C. Dimitriadi ^{24,160}, A. Dimitrieva ^{17a}, W. Ding ^{14b}, J. Dingfelder ²⁴, I-M. Dinu ^{27b}, S.J. Dittmeier ^{63b}, F. Dittus ³⁶, F. Djama ¹⁰¹, T. Djobera ^{148b}, J.I. Djuvsland ¹⁶, D. Dodsworth ²⁶, C. Doglioni ^{100,97}, J. Dolejsi ¹³², Z. Dolezal ¹³², M. Donadelli ^{81c}, B. Dong ^{62c}, J. Donini ⁴⁰, A. D'Onofrio ^{14c}, M. D'Onofrio ⁹¹, J. Dopke ¹³³, A. Doria ^{71a}, M.T. Dova ⁸⁹, A.T. Doyle ⁵⁹, M.A. Draguet ¹²⁵, E. Drechsler ¹⁴¹, E. Dreyer ¹⁶⁸, I. Drivas-koulouris ¹⁰, A.S. Drobac ¹⁵⁷, D. Du ^{62a}, T.A. du Pree ¹¹³, F. Dubinin ³⁷, M. Dubovsky ^{28a}, E. Duchovni ¹⁶⁸, G. Duckeck ¹⁰⁸, O.A. Ducu ^{36,27b}, D. Duda ¹⁰⁹, A. Dudarev ³⁶, M. D'uffizi ¹⁰⁰, L. Duflot ⁶⁶, M. Dührssen ³⁶, C. Dülsen ¹⁷⁰, A.E. Dumitriu ^{27b}, M. Dunford ^{63a}, S. Dungs ⁴⁹, K. Dunne ^{47a,47b}, A. Duperrin ¹⁰¹, H. Duran Yildiz ^{3a}, M. Düren ⁵⁸, A. Durglishvili ^{148b}, B.L. Dwyer ¹¹⁴, G.I. Dyckes ^{17a}, M. Dyndal ^{84a}, S. Dysch ¹⁰⁰, B.S. Dziedzic ⁸⁵, B. Eckerova ^{28a}, M.G. Eggleston ⁵¹, E. Egidio Purcino De Souza ^{81b}, L.F. Ehrke ⁵⁶, G. Eigen ¹⁶, K. Einsweiler ^{17a}, T. Ekelof ¹⁶⁰, P.A. Ekman ⁹⁷, Y. El Ghazali ^{35b}, H. El Jarrari ^{35e,147}, A. El Moussaoui ¹⁶⁰, V. Ellajosyula ¹⁶⁰, M. Ellert ¹⁶⁰, F. Ellinghaus ¹⁷⁰, A.A. Elliot ⁹³, N. Ellis ³⁶, J. Elmsheuser ²⁹, M. Elsing ³⁶, D. Emeliyanov ¹³³, A. Emerman ⁴¹, Y. Enari ¹⁵², I. Ene ^{17a}, S. Epari ¹³, J. Erdmann ^{49,ai}, A. Ereditato ¹⁹, P.A. Erland ⁸⁵, M. Errenst ¹⁷⁰, M. Escalier ⁶⁶, C. Escobar ¹⁶², E. Etzion ¹⁵⁰, G. Evans ^{129a}, H. Evans ⁶⁷, M.O. Evans ¹⁴⁵, A. Ezhilov ³⁷, S. Ezzarqtouni ^{35a}, F. Fabbri ⁵⁹, L. Fabbri ^{23b,23a}, G. Facini ⁹⁵, V. Fadeyev ¹³⁵, R.M. Fakhrutdinov ³⁷, S. Falciano ^{74a}, P.J. Falke ²⁴, S. Falke ³⁶, J. Faltova ¹³², Y. Fan ^{14a}, Y. Fang ^{14a,14d}, G. Fanourakis ⁴⁶, M. Fanti ^{70a,70b}, M. Faraj ^{68a,68b}, A. Farbin ⁸, A. Farilla ^{76a}, T. Farooque ¹⁰⁶, S.M. Farrington ⁵², F. Fassi ^{35e}, D. Fassouliotis ⁹, M. Facci Giannelli ^{75a,75b}, W.J. Fawcett ³², L. Fayard ⁶⁶, O.L. Fedin ^{37,a}, G. Fedotov ³⁷, M. Feickert ¹⁶¹, L. Feligioni ¹⁰¹, A. Fell ¹³⁸, D.E. Fellers ¹²², C. Feng ^{62b}, M. Feng ^{14b}, M.J. Fenton ¹⁵⁹, A.B. Fenyuk ³⁷, L. Ferencz ⁴⁸, S.W. Ferguson ⁴⁵, J. Ferrando ⁴⁸, A. Ferrari ¹⁶⁰, P. Ferrari ¹¹³, R. Ferrari ^{72a}, D. Ferrere ⁵⁶, C. Ferretti ¹⁰⁵, F. Fiedler ⁹⁹, A. Filipčič ⁹², E.K. Filmer ¹, F. Filthaut ¹¹², M.C.N. Fiolhais ^{129a,129c,b}, L. Fiorini ¹⁶², F. Fischer ¹⁴⁰, W.C. Fisher ¹⁰⁶, T. Fitschen ^{20,66}, I. Fleck ¹⁴⁰, P. Fleischmann ¹⁰⁵, T. Flick ¹⁷⁰, L. Flores ¹²⁷, M. Flores ^{33d}, L.R. Flores Castillo ^{64a}, F.M. Follega ^{77a,77b}, N. Fomin ¹⁶, J.H. Foo ¹⁵⁴, B.C. Forland ⁶⁷, A. Formica ¹³⁴, A.C. Forti ¹⁰⁰, E. Fortin ¹⁰¹, A.W. Fortman ⁶¹, M.G. Foti ^{17a}, L. Fountas ⁹, D. Fournier ⁶⁶, H. Fox ⁹⁰, P. Francavilla ^{73a,73b}, S. Francescato ⁶¹, M. Franchini ^{23b,23a}, S. Franchino ^{63a}, D. Francis ³⁶, L. Franco ⁴, L. Franconi ¹⁹, M. Franklin ⁶¹, G. Frattari ²⁶, A.C. Freegard ⁹³, P.M. Freeman ²⁰, W.S. Freund ^{81b}, N. Fritzsche ⁵⁰, A. Froch ⁵⁴, D. Froidevaux ³⁶, J.A. Frost ¹²⁵, Y. Fu ^{62a}, M. Fujimoto ¹¹⁷, E. Fullana Torregrosa ^{162,*}, J. Fuster ¹⁶², A. Gabrielli ^{23b,23a}, A. Gabrielli ³⁶, P. Gadow ⁴⁸, G. Gagliardi ^{57b,57a}, L.G. Gagnon ^{17a}, G.E. Gallardo ¹²⁵, E.J. Gallas ¹²⁵, B.J. Gallop ¹³³, R. Gamboa Goni ⁹³, K.K. Gan ¹¹⁸, S. Ganguly ¹⁵², J. Gao ^{62a}, Y. Gao ⁵², F.M. Garay Walls ^{136a,136b}, B. Garcia ^{29,ag}, C. García ¹⁶², J.E. García Navarro ¹⁶², J.A. García Pascual ^{14a}, M. Garcia-Sciveres ^{17a}, R.W. Gardner ³⁹, D. Garg ⁷⁹, R.B. Garg ¹⁴², S. Gargiulo ⁵⁴, C.A. Garner ¹⁵⁴, V. Garonne ²⁹, S.J. Gasiorowski ¹³⁷, P. Gaspar ^{81b}, G. Gaudio ^{72a}, P. Gauzzi ^{74a,74b}, I.L. Gavrilenco ³⁷, A. Gavriluk ³⁷, C. Gay ¹⁶³, G. Gaycken ⁴⁸, E.N. Gazis ¹⁰,

- A.A. Geanta ^{27b}, C.M. Gee ¹³⁵, J. Geisen ⁹⁷, M. Geisen ⁹⁹, C. Gemme ^{57b}, M.H. Genest ⁶⁰, S. Gentile ^{74a,74b}, S. George ⁹⁴, W.F. George ²⁰, T. Geralis ⁴⁶, L.O. Gerlach ⁵⁵, P. Gessinger-Befurt ³⁶, M. Ghasemi Bostanabad ¹⁶⁴, M. Ghneimat ¹⁴⁰, A. Ghosal ¹⁴⁰, A. Ghosh ¹⁵⁹, A. Ghosh ⁷, B. Giacobbe ^{23b}, S. Giagu ^{74a,74b}, N. Giangiacomi ¹⁵⁴, P. Giannetti ^{73a}, A. Giannini ^{62a}, S.M. Gibson ⁹⁴, M. Gignac ¹³⁵, D.T. Gil ^{84b}, A.K. Gilbert ^{84a}, B.J. Gilbert ⁴¹, D. Gillberg ³⁴, G. Gilles ¹¹³, N.E.K. Gillwald ⁴⁸, L. Ginabat ¹²⁶, D.M. Gingrich ^{2,ad}, M.P. Giordani ^{68a,68c}, P.F. Giraud ¹³⁴, G. Giugliarelli ^{68a,68c}, D. Giugni ^{70a}, F. Giulii ²⁶, I. Gkalias ^{9,i}, L.K. Gladilin ³⁷, C. Glasman ⁹⁸, G.R. Gledhill ¹²², M. Glisic ¹²², I. Gnesi ^{43b,e}, Y. Go ^{29,ag}, M. Goblirsch-Kolb ²⁶, B. Gocke ⁴⁹, D. Godin ¹⁰⁷, S. Goldfarb ¹⁰⁴, T. Golling ⁵⁶, M.G.D. Gololo ^{33g}, D. Golubkov ³⁷, J.P. Gombas ¹⁰⁶, A. Gomes ^{129a,129b}, A.J. Gomez Delegido ¹⁶², R. Goncalves Gama ⁵⁵, R. Gonçalo ^{129a,129c}, G. Gonella ¹²², L. Gonella ²⁰, A. Gongadze ³⁸, F. Gonnella ²⁰, J.L. Gonski ⁴¹, R.Y. González Andana ⁵², S. González de la Hoz ¹⁶², S. Gonzalez Fernandez ¹³, R. Gonzalez Lopez ⁹¹, C. Gonzalez Renteria ^{17a}, R. Gonzalez Suarez ¹⁶⁰, S. Gonzalez-Sevilla ⁵⁶, G.R. Gonzalvo Rodriguez ¹⁶², L. Goossens ³⁶, N.A. Gorasia ²⁰, P.A. Gorbounov ³⁷, B. Gorini ³⁶, E. Gorini ^{69a,69b}, A. Gorišek ⁹², A.T. Goshaw ⁵¹, M.I. Gostkin ³⁸, C.A. Gottardo ¹¹², M. Gouighri ^{35b}, V. Goumarre ⁴⁸, A.G. Goussiou ¹³⁷, N. Govender ^{33c}, C. Goy ⁴, I. Grabowska-Bold ^{84a}, K. Graham ³⁴, E. Gramstad ¹²⁴, S. Grancagnolo ¹⁸, M. Grandi ¹⁴⁵, V. Gratchev ^{37,*}, P.M. Gravila ^{27f}, F.G. Gravili ^{69a,69b}, H.M. Gray ^{17a}, M. Greco ^{69a,69b}, C. Grefe ²⁴, I.M. Gregor ⁴⁸, P. Grenier ¹⁴², C. Grieco ¹³, A.A. Grillo ¹³⁵, K. Grimm ^{31,m}, S. Grinstein ^{13,t}, J.-F. Grivaz ⁶⁶, E. Gross ¹⁶⁸, J. Grosse-Knetter ⁵⁵, C. Grud ¹⁰⁵, A. Grummer ¹¹¹, J.C. Grundy ¹²⁵, L. Guan ¹⁰⁵, W. Guan ¹⁶⁹, C. Gubbels ¹⁶³, J.G.R. Guerrero Rojas ¹⁶², G. Guerrieri ^{68a,68c}, F. Guescini ¹⁰⁹, R. Gugel ⁹⁹, J.A.M. Guhit ¹⁰⁵, A. Guida ⁴⁸, T. Guillemin ⁴, E. Guilloton ^{166,133}, S. Guindon ³⁶, F. Guo ^{14a,14d}, J. Guo ^{62c}, L. Guo ⁶⁶, Y. Guo ¹⁰⁵, R. Gupta ⁴⁸, S. Gurbuz ²⁴, G. Gustavino ³⁶, M. Guth ⁵⁶, P. Gutierrez ¹¹⁹, L.F. Gutierrez Zagazeta ¹²⁷, C. Gutschow ⁹⁵, C. Guyot ¹³⁴, C. Gwenlan ¹²⁵, C.B. Gwilliam ⁹¹, E.S. Haaland ¹²⁴, A. Haas ¹¹⁶, M. Habedank ⁴⁸, C. Haber ^{17a}, H.K. Hadavand ⁸, A. Hadef ⁹⁹, S. Hadzic ¹⁰⁹, M. Haleem ¹⁶⁵, J. Haley ¹²⁰, J.J. Hall ¹³⁸, G.D. Hallewell ¹⁰¹, L. Halser ¹⁹, K. Hamano ¹⁶⁴, H. Hamdaoui ^{35e}, M. Hamer ²⁴, G.N. Hamity ⁵², J. Han ^{62b}, K. Han ^{62a}, L. Han ^{14c}, L. Han ^{62a}, S. Han ^{17a}, Y.F. Han ¹⁵⁴, K. Hanagaki ⁸², M. Hance ¹³⁵, D.A. Hangal ^{41,y}, M.D. Hank ³⁹, R. Hankache ¹⁰⁰, J.B. Hansen ⁴², J.D. Hansen ⁴², P.H. Hansen ⁴², K. Hara ¹⁵⁶, D. Harada ⁵⁶, T. Harenberg ¹⁷⁰, S. Harkusha ³⁷, Y.T. Harris ¹²⁵, P.F. Harrison ¹⁶⁶, N.M. Hartman ¹⁴², N.M. Hartmann ¹⁰⁸, Y. Hasegawa ¹³⁹, A. Hasib ⁵², S. Haug ¹⁹, R. Hauser ¹⁰⁶, M. Havranek ¹³¹, C.M. Hawkes ²⁰, R.J. Hawkings ³⁶, S. Hayashida ¹¹⁰, D. Hayden ¹⁰⁶, C. Hayes ¹⁰⁵, R.L. Hayes ¹⁶³, C.P. Hays ¹²⁵, J.M. Hays ⁹³, H.S. Hayward ⁹¹, F. He ^{62a}, Y. He ¹⁵³, Y. He ¹²⁶, M.P. Heath ⁵², V. Hedberg ⁹⁷, A.L. Heggelund ¹²⁴, N.D. Hehir ⁹³, C. Heidegger ⁵⁴, K.K. Heidegger ⁵⁴, W.D. Heidorn ⁸⁰, J. Heilman ³⁴, S. Heim ⁴⁸, T. Heim ^{17a}, B. Heinemann ^{48,aa}, J.G. Heinlein ¹²⁷, J.J. Heinrich ¹²², L. Heinrich ³⁶, J. Hejbal ¹³⁰, L. Helary ⁴⁸, A. Held ¹¹⁶, S. Hellesund ¹²⁴, C.M. Helling ¹⁶³, S. Hellman ^{47a,47b}, C. Helsens ³⁶, R.C.W. Henderson ⁹⁰, L. Henkelmann ³², A.M. Henriques Correia ³⁶, H. Herde ¹⁴², Y. Hernández Jiménez ¹⁴⁴, H. Herr ⁹⁹, M.G. Herrmann ¹⁰⁸, T. Herrmann ⁵⁰, G. Herten ⁵⁴, R. Hertenberger ¹⁰⁸, L. Hervas ³⁶, N.P. Hessey ^{155a}, H. Hibi ⁸³, E. Higón-Rodriguez ¹⁶², S.J. Hillier ²⁰, I. Hincliffe ^{17a}, F. Hinterkeuser ²⁴, M. Hirose ¹²³, S. Hirose ¹⁵⁶, D. Hirschbuehl ¹⁷⁰, B. Hiti ⁹², J. Hobbs ¹⁴⁴, R. Hobincu ^{27e}, N. Hod ¹⁶⁸, M.C. Hodgkinson ¹³⁸, B.H. Hodgkinson ³², A. Hoecker ³⁶, J. Hofer ⁴⁸, D. Hohn ⁵⁴, T. Holm ²⁴, M. Holzbock ¹⁰⁹, L.B.A.H. Hommels ³², B.P. Honan ¹⁰⁰, J. Hong ^{62c}, T.M. Hong ¹²⁸, Y. Hong ⁵⁵, J.C. Honig ⁵⁴, A. Höngle ¹⁰⁹, B.H. Hooberman ¹⁶¹, W.H. Hopkins ⁶, Y. Horii ¹¹⁰, S. Hou ¹⁴⁷, J. Howarth ⁵⁹, J. Hoya ⁸⁹, M. Hrabovsky ¹²¹, A. Hrynevich ³⁷, T. Hryna'ova ⁴, P.J. Hsu ⁶⁵, S.-C. Hsu ¹³⁷, Q. Hu ^{41,y}, Y.F. Hu ^{14a,14d,af}, D.P. Huang ⁹⁵, S. Huang ^{64b}, X. Huang ^{14c}, Y. Huang ^{62a}, Y. Huang ^{14a}, Z. Huang ¹⁰⁰, Z. Hubacek ¹³¹, M. Huebner ²⁴, F. Huegging ²⁴, T.B. Huffman ¹²⁵, M. Huhtinen ³⁶, S.K. Huiberts ¹⁶, R. Hulsken ¹⁰³, N. Huseynov ^{12,a}, J. Huston ¹⁰⁶, J. Huth ⁶¹, R. Hyneman ¹⁴², S. Hyrych ^{28a}, G. Iacobucci ⁵⁶, G. Iakovidis ²⁹, I. Ibragimov ¹⁴⁰, L. Iconomidou-Fayard ⁶⁶, P. Iengo ^{71a,71b}, R. Iguchi ¹⁵², T. Iizawa ⁵⁶, Y. Ikegami ⁸², A. Ilg ¹⁹, N. Ilic ¹⁵⁴, H. Imam ^{35a}, T. Ingebretsen Carlson ^{47a,47b}, G. Introzzi ^{72a,72b}, M. Iodice ^{76a}, V. Ippolito ^{74a,74b}, M. Ishino ¹⁵², W. Islam ¹⁶⁹, C. Issever ^{18,48}, S. Istin ^{21a,ah}, H. Ito ¹⁶⁷, J.M. Iturbe Ponce ^{64a}, R. Iuppa ^{77a,77b}, A. Ivina ¹⁶⁸, J.M. Izen ⁴⁵, V. Izzo ^{71a}, P. Jacka ^{130,131}, P. Jackson ¹, R.M. Jacobs ⁴⁸, B.P. Jaeger ¹⁴¹, C.S. Jagfeld ¹⁰⁸, G. Jäkel ¹⁷⁰, K. Jakobs ⁵⁴, T. Jakoubek ¹⁶⁸, J. Jamieson ⁵⁹, K.W. Janas ^{84a}, G. Jarlskog ⁹⁷, A.E. Jaspan ⁹¹, T. Javůrek ³⁶, M. Javurkova ¹⁰², F. Jeanneau ¹³⁴, L. Jeanty ¹²², J. Jejelava ^{148a,x}, P. Jenni ^{54,f}, C.E. Jessiman ³⁴, S. Jézéquel ⁴, J. Jia ¹⁴⁴, X. Jia ⁶¹, X. Jia ^{14a,14d}, Z. Jia ^{14c}, Y. Jiang ^{62a}, S. Jiggins ⁵², J. Jimenez Pena ¹⁰⁹, S. Jin ^{14c}, A. Jinaru ^{27b}, O. Jinnouchi ¹⁵³, H. Jivan ^{33g}, P. Johansson ¹³⁸, K.A. Johns ⁷, C.A. Johnson ⁶⁷, D.M. Jones ³², E. Jones ¹⁶⁶, R.W.L. Jones ⁹⁰, T.J. Jones ⁹¹,

- J. Jovicevic ¹⁵, X. Ju ^{17a}, J.J. Junggeburth ³⁶, A. Juste Rozas ^{13,t}, S. Kabana ^{136e}, A. Kaczmarska ⁸⁵,
 M. Kado ^{74a,74b}, H. Kagan ¹¹⁸, M. Kagan ¹⁴², A. Kahn ⁴¹, A. Kahn ¹²⁷, C. Kahra ⁹⁹, T. Kaji ¹⁶⁷,
 E. Kajomovitz ¹⁴⁹, N. Kakati ¹⁶⁸, C.W. Kalderon ²⁹, A. Kamenshchikov ¹⁵⁴, N.J. Kang ¹³⁵, Y. Kano ¹¹⁰,
 D. Kar ^{33g}, K. Karava ¹²⁵, M.J. Kareem ^{155b}, E. Karentzos ⁵⁴, I. Karkanias ¹⁵¹, S.N. Karpov ³⁸, Z.M. Karpova ³⁸,
 V. Kartvelishvili ⁹⁰, A.N. Karyukhin ³⁷, E. Kasimi ¹⁵¹, C. Kato ^{62d}, J. Katzy ⁴⁸, S. Kaur ³⁴, K. Kawade ¹³⁹,
 K. Kawagoe ⁸⁸, T. Kawaguchi ¹¹⁰, T. Kawamoto ¹³⁴, G. Kawamura ⁵⁵, E.F. Kay ¹⁶⁴, F.I. Kaya ¹⁵⁷, S. Kazakos ¹³,
 V.F. Kazanin ³⁷, Y. Ke ¹⁴⁴, J.M. Keaveney ^{33a}, R. Keeler ¹⁶⁴, G.V. Kehris ⁶¹, J.S. Keller ³⁴, A.S. Kelly ⁹⁵,
 D. Kelsey ¹⁴⁵, J.J. Kempster ²⁰, J. Kendrick ²⁰, K.E. Kennedy ⁴¹, O. Kepka ¹³⁰, B.P. Kerridge ¹⁶⁶, S. Kersten ¹⁷⁰,
 B.P. Kerševan ⁹², L. Keszeghova ^{28a}, S. Ketabchi Haghigat ¹⁵⁴, M. Khandoga ¹²⁶, A. Khanov ¹²⁰,
 A.G. Kharlamov ³⁷, T. Kharlamova ³⁷, E.E. Khoda ¹³⁷, T.J. Khoo ¹⁸, G. Khoriauli ¹⁶⁵, J. Khubua ^{148b},
 Y.A.R. Khwaira ⁶⁶, M. Kiehn ³⁶, A. Kilgallon ¹²², E. Kim ¹⁵³, Y.K. Kim ³⁹, N. Kimura ⁹⁵, A. Kirchhoff ⁵⁵,
 D. Kirchmeier ⁵⁰, C. Kirfel ²⁴, J. Kirk ¹³³, A.E. Kiryunin ¹⁰⁹, T. Kishimoto ¹⁵², D.P. Kisliuk ¹⁵⁴, C. Kitsaki ¹⁰,
 O. Kivernyk ²⁴, M. Klassen ^{63a}, C. Klein ³⁴, L. Klein ¹⁶⁵, M.H. Klein ¹⁰⁵, M. Klein ⁹¹, U. Klein ⁹¹, P. Klimek ³⁶,
 A. Klimentov ²⁹, F. Klimpel ¹⁰⁹, T. Klingl ²⁴, T. Klioutchnikova ³⁶, F.F. Klitzner ¹⁰⁸, P. Kluit ¹¹³, S. Kluth ¹⁰⁹,
 E. Kneringer ⁷⁸, T.M. Knight ¹⁵⁴, A. Knue ⁵⁴, D. Kobayashi ⁸⁸, R. Kobayashi ⁸⁶, M. Kocian ¹⁴², T. Kodama ¹⁵²,
 P. Kodyš ¹³², D.M. Koeck ¹⁴⁵, P.T. Koenig ²⁴, T. Koffas ³⁴, N.M. Köhler ³⁶, M. Kolb ¹³⁴, I. Koletsou ⁴,
 T. Komarek ¹²¹, K. Köneke ⁵⁴, A.X.Y. Kong ¹, T. Kono ¹¹⁷, N. Konstantinidis ⁹⁵, B. Konya ⁹⁷,
 R. Kopeliansky ⁶⁷, S. Koperny ^{84a}, K. Korcyl ⁸⁵, K. Kordas ¹⁵¹, G. Koren ¹⁵⁰, A. Korn ⁹⁵, S. Korn ⁵⁵,
 I. Korolkov ¹³, N. Korotkova ³⁷, B. Kortman ¹¹³, O. Kortner ¹⁰⁹, S. Kortner ¹⁰⁹, W.H. Kostecka ¹¹⁴,
 V.V. Kostyukhin ^{140,37}, A. Kotsokechagia ⁶⁶, A. Kotwal ⁵¹, A. Koulouris ³⁶,
 A. Kourkoumeli-Charalampidi ^{72a,72b}, C. Kourkoumelis ⁹, E. Kourlitis ⁶, O. Kovanda ¹⁴⁵, R. Kowalewski ¹⁶⁴,
 W. Kozanecki ¹³⁴, A.S. Kozhin ³⁷, V.A. Kramarenko ³⁷, G. Kramberger ⁹², P. Kramer ⁹⁹, M.W. Krasny ¹²⁶,
 A. Krasznahorkay ³⁶, J.A. Kremer ⁹⁹, J. Kretzschmar ⁹¹, K. Kreul ¹⁸, P. Krieger ¹⁵⁴, F. Krieter ¹⁰⁸,
 S. Krishnamurthy ¹⁰², A. Krishnan ^{63b}, M. Krivos ¹³², K. Krizka ^{17a}, K. Kroeninger ⁴⁹, H. Kroha ¹⁰⁹,
 J. Kroll ¹³⁰, J. Kroll ¹²⁷, K.S. Krowppman ¹⁰⁶, U. Kruchonak ³⁸, H. Krüger ²⁴, N. Krumnack ⁸⁰, M.C. Kruse ⁵¹,
 J.A. Krzysiak ⁸⁵, A. Kubota ¹⁵³, O. Kuchinskaia ³⁷, S. Kuday ^{3a}, D. Kuechler ⁴⁸, J.T. Kuechler ⁴⁸, S. Kuehn ³⁶,
 T. Kuhl ⁴⁸, V. Kukhtin ³⁸, Y. Kulchitsky ^{37,a}, S. Kuleshov ^{136d,136b}, M. Kumar ^{33g}, N. Kumari ¹⁰¹, M. Kuna ⁶⁰,
 A. Kupco ¹³⁰, T. Kupfer ⁴⁹, A. Kupich ³⁷, O. Kuprash ⁵⁴, H. Kurashige ⁸³, L.L. Kurchaninov ^{155a},
 Y.A. Kurochkin ³⁷, A. Kurova ³⁷, E.S. Kuwertz ³⁶, M. Kuze ¹⁵³, A.K. Kvam ¹³⁷, J. Kvita ¹²¹, T. Kwan ¹⁰³,
 K.W. Kwok ^{64a}, C. Lacasta ¹⁶², F. Lacava ^{74a,74b}, H. Lacker ¹⁸, D. Lacour ¹²⁶, N.N. Lad ⁹⁵, E. Ladygin ³⁸,
 B. Laforge ¹²⁶, T. Lagouri ^{136e}, S. Lai ⁵⁵, I.K. Lakomiec ^{84a}, N. Lalloue ⁶⁰, J.E. Lambert ¹¹⁹, S. Lammers ⁶⁷,
 W. Lampl ⁷, C. Lampoudis ¹⁵¹, A.N. Lancaster ¹¹⁴, E. Lançon ²⁹, U. Landgraf ⁵⁴, M.P.J. Landon ⁹³,
 V.S. Lang ⁵⁴, R.J. Langenberg ¹⁰², A.J. Lankford ¹⁵⁹, F. Lanni ²⁹, K. Lantzs ²⁴, A. Lanza ^{72a},
 A. Lapertosa ^{57b,57a}, J.F. Laporte ¹³⁴, T. Lari ^{70a}, F. Lasagni Manghi ^{23b}, M. Lassnig ³⁶, V. Latonova ¹³⁰,
 T.S. Lau ^{64a}, A. Laudrain ⁹⁹, A. Laurier ³⁴, S.D. Lawlor ⁹⁴, Z. Lawrence ¹⁰⁰, M. Lazzaroni ^{70a,70b}, B. Le ¹⁰⁰,
 B. Leban ⁹², A. Lebedev ⁸⁰, M. LeBlanc ³⁶, T. LeCompte ⁶, F. Ledroit-Guillon ⁶⁰, A.C.A. Lee ⁹⁵, G.R. Lee ¹⁶,
 L. Lee ⁶¹, S.C. Lee ¹⁴⁷, S. Lee ^{47a,47b}, L.L. Leeuw ^{33c}, B. Lefebvre ^{155a}, H.P. Lefebvre ⁹⁴, M. Lefebvre ¹⁶⁴,
 C. Leggett ^{17a}, K. Lehmann ¹⁴¹, G. Lehmann Miotto ³⁶, W.A. Leight ¹⁰², A. Leisos ^{151,s}, M.A.L. Leite ^{81c},
 C.E. Leitgeb ⁴⁸, R. Leitner ¹³², K.J.C. Leney ⁴⁴, T. Lenz ²⁴, S. Leone ^{73a}, C. Leonidopoulos ⁵², A. Leopold ¹⁴³,
 C. Leroy ¹⁰⁷, R. Les ¹⁰⁶, C.G. Lester ³², M. Levchenko ³⁷, J. Levêque ⁴, D. Levin ¹⁰⁵, L.J. Levinson ¹⁶⁸,
 D.J. Lewis ²⁰, B. Li ^{14b}, B. Li ^{62b}, C. Li ^{62a}, C.-Q. Li ^{62c,62d}, H. Li ^{62a}, H. Li ^{62b}, H. Li ^{14c}, H. Li ^{62b}, J. Li ^{62c},
 K. Li ¹³⁷, L. Li ^{62c}, M. Li ^{14a,14d}, Q.Y. Li ^{62a}, S. Li ^{62d,62c,d}, T. Li ^{62b}, X. Li ¹⁰³, Z. Li ^{62b}, Z. Li ¹²⁵, Z. Li ¹⁰³, Z. Li ⁹¹,
 Z. Liang ^{14a}, M. Liberatore ⁴⁸, B. Liberti ^{75a}, K. Lie ^{64c}, J. Lieber Marin ^{81b}, K. Lin ¹⁰⁶, R.A. Linck ⁶⁷,
 R.E. Lindley ⁷, J.H. Lindon ², A. Linss ⁴⁸, E. Lipeles ¹²⁷, A. Lipniacka ¹⁶, T.M. Liss ^{161,ab}, A. Lister ¹⁶³,
 J.D. Little ⁴, B. Liu ^{14a}, B.X. Liu ¹⁴¹, D. Liu ^{62d,62c}, J.B. Liu ^{62a}, J.K.K. Liu ³², K. Liu ^{62d,62c}, M. Liu ^{62a},
 M.Y. Liu ^{62a}, P. Liu ^{14a}, Q. Liu ^{62d,137,62c}, X. Liu ^{62a}, Y. Liu ⁴⁸, Y. Liu ^{14c,14d}, Y.L. Liu ¹⁰⁵, Y.W. Liu ^{62a},
 M. Livan ^{72a,72b}, J. Llorente Merino ¹⁴¹, S.L. Lloyd ⁹³, E.M. Lobodzinska ⁴⁸, P. Loch ⁷, S. Loffredo ^{75a,75b},
 T. Lohse ¹⁸, K. Lohwasser ¹³⁸, M. Lokajicek ¹³⁰, J.D. Long ¹⁶¹, I. Longarini ^{74a,74b}, L. Longo ^{69a,69b},
 R. Longo ¹⁶¹, I. Lopez Paz ³⁶, A. Lopez Solis ⁴⁸, J. Lorenz ¹⁰⁸, N. Lorenzo Martinez ⁴, A.M. Lory ¹⁰⁸,
 A. Lösle ⁵⁴, X. Lou ^{47a,47b}, X. Lou ^{14a,14d}, A. Lounis ⁶⁶, J. Love ⁶, P.A. Love ⁹⁰, J.J. Lozano Bahilo ¹⁶²,
 G. Lu ^{14a,14d}, M. Lu ⁷⁹, S. Lu ¹²⁷, Y.J. Lu ⁶⁵, H.J. Lubatti ¹³⁷, C. Luci ^{74a,74b}, F.L. Lucio Alves ^{14c}, A. Lucotte ⁶⁰,
 F. Luehring ⁶⁷, I. Luise ¹⁴⁴, O. Lukianchuk ⁶⁶, O. Lundberg ¹⁴³, B. Lund-Jensen ¹⁴³, N.A. Luongo ¹²²,
 M.S. Lutz ¹⁵⁰, D. Lynn ²⁹, H. Lyons ⁹¹, R. Lysak ¹³⁰, E. Lytken ⁹⁷, F. Lyu ^{14a}, V. Lyubushkin ³⁸,

- T. Lyubushkina ³⁸, H. Ma ²⁹, L.L. Ma ^{62b}, Y. Ma ⁹⁵, D.M. Mac Donell ¹⁶⁴, G. Maccarrone ⁵³,
 J.C. MacDonald ¹³⁸, R. Madar ⁴⁰, W.F. Mader ⁵⁰, J. Maeda ⁸³, T. Maeno ²⁹, M. Maerker ⁵⁰, V. Magerl ⁵⁴,
 J. Magro ^{68a,68c}, D.J. Mahon ⁴¹, C. Maidantchik ^{81b}, A. Maio ^{129a,129b,129d}, K. Maj ^{84a}, O. Majersky ^{28a},
 S. Majewski ¹²², N. Makovec ⁶⁶, V. Maksimovic ¹⁵, B. Malaescu ¹²⁶, Pa. Malecki ⁸⁵, V.P. Maleev ³⁷,
 F. Malek ⁶⁰, D. Malito ^{43b,43a}, U. Mallik ⁷⁹, C. Malone ³², S. Maltezos ¹⁰, S. Malyukov ³⁸, J. Mamuzic ¹¹⁹,
 G. Mancini ⁵³, J.P. Mandalia ⁹³, I. Mandić ⁹², L. Manhaes de Andrade Filho ^{81a}, I.M. Maniatis ¹⁵¹,
 M. Manisha ¹³⁴, J. Manjarres Ramos ⁵⁰, D.C. Mankad ¹⁶⁸, K.H. Mankinen ⁹⁷, A. Mann ¹⁰⁸, A. Manousos ⁷⁸,
 B. Mansoulie ¹³⁴, S. Manzoni ³⁶, A. Marantis ¹⁵¹, G. Marchiori ⁵, M. Marcisovsky ¹³⁰, L. Marcoccia ^{75a,75b},
 C. Marcon ⁹⁷, M. Marinescu ²⁰, M. Marjanovic ¹¹⁹, Z. Marshall ^{17a}, S. Marti-Garcia ¹⁶², T.A. Martin ¹⁶⁶,
 V.J. Martin ⁵², B. Martin dit Latour ¹⁶, L. Martinelli ^{74a,74b}, M. Martinez ^{13,t}, P. Martinez Agullo ¹⁶²,
 V.I. Martinez Outschoorn ¹⁰², P. Martinez Suarez ¹³, S. Martin-Haugh ¹³³, V.S. Martoiu ^{27b},
 A.C. Martyniuk ⁹⁵, A. Marzin ³⁶, S.R. Maschek ¹⁰⁹, L. Masetti ⁹⁹, T. Mashimo ¹⁵², J. Masik ¹⁰⁰,
 A.L. Maslennikov ³⁷, L. Massa ^{23b}, P. Massarotti ^{71a,71b}, P. Mastrandrea ^{73a,73b}, A. Mastroberardino ^{43b,43a},
 T. Masubuchi ¹⁵², T. Mathisen ¹⁶⁰, A. Matic ¹⁰⁸, N. Matsuzawa ¹⁵², J. Maurer ^{27b}, F.A. Mausolf ⁴⁹,
 B. Maček ⁹², D.A. Maximov ³⁷, R. Mazini ¹⁴⁷, I. Maznás ¹⁵¹, M. Mazza ¹⁰⁶, S.M. Mazza ¹³⁵, C. Mc Ginn ^{29,ag},
 J.P. Mc Gowan ¹⁰³, S.P. Mc Kee ¹⁰⁵, T.G. McCarthy ¹⁰⁹, W.P. McCormack ^{17a}, E.F. McDonald ¹⁰⁴,
 A.E. McDougall ¹¹³, J.A. McFayden ¹⁴⁵, G. Mchedlidze ^{148b}, R.P. Mckenzie ^{33g}, D.J. McLaughlin ⁹⁵,
 K.D. McLean ¹⁶⁴, S.J. McMahon ¹³³, P.C. McNamara ¹⁰⁴, R.A. McPherson ^{164,v}, J.E. Mdhluli ^{33g}, S. Meehan ³⁶,
 T. Megy ⁴⁰, S. Mehlhase ¹⁰⁸, A. Mehta ⁹¹, B. Meirose ⁴⁵, D. Melini ¹⁴⁹, B.R. Mellado Garcia ^{33g}, A.H. Melo ⁵⁵,
 F. Meloni ⁴⁸, E.D. Mendes Gouveia ^{129a}, A.M. Mendes Jacques Da Costa ²⁰, H.Y. Meng ¹⁵⁴, L. Meng ⁹⁰,
 S. Menke ¹⁰⁹, M. Mentink ³⁶, E. Meoni ^{43b,43a}, C. Merlassino ¹²⁵, L. Merola ^{71a,71b}, C. Meroni ^{70a},
 G. Merz ¹⁰⁵, O. Meshkov ³⁷, J.K.R. Meshreki ¹⁴⁰, J. Metcalfe ⁶, A.S. Mete ⁶, C. Meyer ⁶⁷, J-P. Meyer ¹³⁴,
 M. Michetti ¹⁸, R.P. Middleton ¹³³, L. Mijović ⁵², G. Mikenberg ¹⁶⁸, M. Mikestikova ¹³⁰, M. Mikuž ⁹²,
 H. Mildner ¹³⁸, A. Milic ¹⁵⁴, C.D. Milke ⁴⁴, D.W. Miller ³⁹, L.S. Miller ³⁴, A. Milov ¹⁶⁸, D.A. Milstead ^{47a,47b},
 T. Min ^{14c}, A.A. Minaenko ³⁷, I.A. Minashvili ^{148b}, L. Mince ⁵⁹, A.I. Mincer ¹¹⁶, B. Mindur ^{84a}, M. Mineev ³⁸,
 Y. Minegishi ¹⁵², Y. Mino ⁸⁶, L.M. Mir ¹³, M. Miralles Lopez ¹⁶², M. Mironova ¹²⁵, T. Mitani ¹⁶⁷, A. Mitra ¹⁶⁶,
 V.A. Mitsou ¹⁶², O. Miu ¹⁵⁴, P.S. Miyagawa ⁹³, Y. Miyazaki ⁸⁸, A. Mizukami ⁸², J.U. Mjörnmark ⁹⁷,
 T. Mkrtchyan ^{63a}, M. Mlynárikova ¹¹⁴, T. Moa ^{47a,47b}, S. Mobius ⁵⁵, K. Mochizuki ¹⁰⁷, P. Moder ⁴⁸,
 P. Mogg ¹⁰⁸, A.F. Mohammed ^{14a,14d}, S. Mohapatra ⁴¹, G. Mokgatitswane ^{33g}, B. Mondal ¹⁴⁰, S. Mondal ¹³¹,
 K. Mönig ⁴⁸, E. Monnier ¹⁰¹, L. Monsonis Romero ¹⁶², J. Montejo Berlingen ³⁶, M. Montella ¹¹⁸,
 F. Monticelli ⁸⁹, N. Morange ⁶⁶, A.L. Moreira De Carvalho ^{129a}, M. Moreno Llácer ¹⁶²,
 C. Moreno Martinez ¹³, P. Morettini ^{57b}, S. Morgenstern ¹⁶⁶, M. Morii ⁶¹, M. Morinaga ¹⁵², V. Morisbak ¹²⁴,
 A.K. Morley ³⁶, F. Morodei ^{74a,74b}, L. Morvaj ³⁶, P. Moschovakos ³⁶, B. Moser ¹¹³, M. Mosidze ^{148b},
 T. Moskalets ⁵⁴, P. Moskvitina ¹¹², J. Moss ^{31,n}, E.J.W. Moyse ¹⁰², S. Muanza ¹⁰¹, J. Mueller ¹²⁸,
 D. Muenstermann ⁹⁰, R. Müller ¹⁹, G.A. Mullier ⁹⁷, J.J. Mullin ¹²⁷, D.P. Mungo ^{70a,70b},
 J.L. Munoz Martinez ¹³, F.J. Munoz Sanchez ¹⁰⁰, M. Murin ¹⁰⁰, W.J. Murray ^{166,133}, A. Murrone ^{70a,70b},
 J.M. Muse ¹¹⁹, M. Muškinja ^{17a}, C. Mwewa ²⁹, A.G. Myagkov ^{37,a}, A.J. Myers ⁸, A.A. Myers ¹²⁸, G. Myers ⁶⁷,
 M. Myska ¹³¹, B.P. Nachman ^{17a}, O. Nackenhorst ⁴⁹, A. Nag ⁵⁰, K. Nagai ¹²⁵, K. Nagano ⁸², J.L. Nagle ^{29,ag},
 E. Nagy ¹⁰¹, A.M. Nairz ³⁶, Y. Nakahama ⁸², K. Nakamura ⁸², H. Nanjo ¹²³, R. Narayan ⁴⁴,
 E.A. Narayanan ¹¹¹, I. Naryshkin ³⁷, M. Naseri ³⁴, C. Nass ²⁴, G. Navarro ^{22a}, J. Navarro-Gonzalez ¹⁶²,
 R. Nayak ¹⁵⁰, P.Y. Nechaeva ³⁷, F. Nechansky ⁴⁸, T.J. Neep ²⁰, A. Negri ^{72a,72b}, M. Negrini ^{23b}, C. Nellist ¹¹²,
 C. Nelson ¹⁰³, K. Nelson ¹⁰⁵, S. Nemecek ¹³⁰, M. Nessi ^{36,g}, M.S. Neubauer ¹⁶¹, F. Neuhaus ⁹⁹, J. Neundorf ⁴⁸,
 R. Newhouse ¹⁶³, P.R. Newman ²⁰, C.W. Ng ¹²⁸, Y.S. Ng ¹⁸, Y.W.Y. Ng ¹⁵⁹, B. Ngair ^{35e}, H.D.N. Nguyen ¹⁰⁷,
 R.B. Nickerson ¹²⁵, R. Nicolaïdou ¹³⁴, J. Nielsen ¹³⁵, M. Niemeyer ⁵⁵, N. Nikiforou ³⁶, V. Nikolaenko ^{37,a},
 I. Nikolic-Audit ¹²⁶, K. Nikolopoulos ²⁰, P. Nilsson ²⁹, H.R. Nindhito ⁵⁶, A. Nisati ^{74a}, N. Nishu ²,
 R. Nisius ¹⁰⁹, J-E. Nitschke ⁵⁰, E.K. Nkadimeng ^{33g}, S.J. Noacco Rosende ⁸⁹, T. Nobe ¹⁵², D.L. Noel ³²,
 Y. Noguchi ⁸⁶, M.A. Nomura ²⁹, M.B. Norfolk ¹³⁸, R.R.B. Norisam ⁹⁵, B.J. Norman ³⁴, J. Novak ⁹², T. Novak ⁴⁸,
 O. Novgorodova ⁵⁰, L. Novotny ¹³¹, R. Novotny ¹¹¹, L. Nozka ¹²¹, K. Ntekas ¹⁵⁹, E. Nurse ⁹⁵,
 F.G. Oakham ^{34,ad}, J. Ocariz ¹²⁶, A. Ochi ⁸³, I. Ochoa ^{129a}, S. Oda ⁸⁸, S. Oerdekk ¹⁶⁰, A. Ogrodnik ^{84a}, A. Oh ¹⁰⁰,
 C.C. Ohm ¹⁴³, H. Oide ¹⁵³, R. Oishi ¹⁵², M.L. Ojeda ⁴⁸, Y. Okazaki ⁸⁶, M.W. O'Keefe ⁹¹, Y. Okumura ¹⁵²,
 A. Olariu ^{27b}, L.F. Oleiro Seabra ^{129a}, S.A. Olivares Pino ^{136e}, D. Oliveira Damazio ²⁹,
 D. Oliveira Goncalves ^{81a}, J.L. Oliver ¹⁵⁹, M.J.R. Olsson ¹⁵⁹, A. Olszewski ⁸⁵, J. Olszowska ^{85,*}, Ö.O. Öncel ⁵⁴,
 D.C. O'Neil ¹⁴¹, A.P. O'Neill ¹⁹, A. Onofre ^{129a,129e}, P.U.E. Onyisi ¹¹, M.J. Oreglia ³⁹, G.E. Orellana ⁸⁹,

- D. Orestano 76a, 76b, N. Orlando 13, R.S. Orr 154, V. O'Shea 59, R. Ospanov 62a, G. Otero y Garzon 30,
 H. Otono 88, P.S. Ott 63a, G.J. Ottino 17a, M. Ouchrif 35d, J. Ouellette 29, ag, F. Ould-Saada 124, M. Owen 59,
 R.E. Owen 133, K.Y. Oyulmaz 21a, V.E. Ozcan 21a, N. Ozturk 8, S. Ozturk 21d, J. Pacalt 121, H.A. Pacey 32,
 K. Pachal 51, A. Pacheco Pages 13, C. Padilla Aranda 13, G. Padovano 74a, 74b, S. Pagan Griso 17a,
 G. Palacino 67, A. Palazzo 69a, 69b, S. Palazzo 52, S. Palestini 36, M. Palka 84b, J. Pan 171, D.K. Panchal 11,
 C.E. Pandini 113, J.G. Panduro Vazquez 94, P. Pani 48, G. Panizzo 68a, 68c, L. Paolozzi 56, C. Papadatos 107,
 S. Parajuli 44, A. Paramonov 6, C. Paraskevopoulos 10, D. Paredes Hernandez 64b, T.H. Park 154,
 M.A. Parker 32, F. Parodi 57b, 57a, E.W. Parrish 114, V.A. Parrish 52, J.A. Parsons 41, U. Parzefall 54,
 B. Pascual Dias 107, L. Pascual Dominguez 150, V.R. Pascuzzi 17a, F. Pasquali 113, E. Pasqualucci 74a,
 S. Passaggio 57b, F. Pastore 94, P. Pasuwan 47a, 47b, J.R. Pater 100, J. Patton 91, T. Pauly 36, J. Pearkes 142,
 M. Pedersen 124, R. Pedro 129a, S.V. Peleganchuk 37, O. Penc 130, C. Peng 64b, H. Peng 62a, M. Penzin 37,
 B.S. Peralva 81a, A.P. Pereira Peixoto 60, L. Pereira Sanchez 47a, 47b, D.V. Perepelitsa 29, ag,
 E. Perez Codina 155a, M. Perganti 10, L. Perini 70a, 70b, *, H. Pernegger 36, S. Perrella 36, A. Perrevoort 112,
 O. Perrin 40, K. Peters 48, R.F.Y. Peters 100, B.A. Petersen 36, T.C. Petersen 42, E. Petit 101, V. Petousis 131,
 C. Petridou 151, A. Petrukhan 140, M. Pettee 17a, N.E. Pettersson 36, A. Petukhov 37, K. Petukhova 132,
 A. Peyaud 134, R. Pezoa 136f, L. Pezzotti 36, G. Pezzullo 171, T. Pham 104, P.W. Phillips 133, M.W. Phipps 161,
 G. Piacquadio 144, E. Pianori 17a, F. Piazza 70a, 70b, R. Piegaia 30, D. Pietreanu 27b, A.D. Pilkington 100,
 M. Pinamonti 68a, 68c, J.L. Pinfold 2, C. Pitman Donaldson 95, D.A. Pizzi 34, L. Pizzimento 75a, 75b,
 A. Pizzini 113, M.-A. Pleier 29, V. Plesanovs 54, V. Pleskot 132, E. Plotnikova 38, G. Poddar 4, R. Poettgen 97,
 R. Poggi 56, L. Poggiali 126, I. Pogrebnyak 106, D. Pohl 24, I. Pokharel 55, S. Polacek 132, G. Polesello 72a,
 A. Poley 141, 155a, R. Polifka 131, A. Polini 23b, C.S. Pollard 125, Z.B. Pollock 118, V. Polychronakos 29,
 D. Ponomarenko 37, L. Pontecorvo 36, S. Popa 27a, G.A. Popeneciu 27d, D.M. Portillo Quintero 155a,
 S. Pospisil 131, P. Postolache 27c, K. Potamianos 125, I.N. Potrap 38, C.J. Potter 32, H. Potti 1, T. Poulsen 48,
 J. Poveda 162, G. Pownall 48, M.E. Pozo Astigarraga 36, A. Prades Ibanez 162, M.M. Prapa 46, J. Pretel 54,
 D. Price 100, M. Primavera 69a, M.A. Principe Martin 98, M.L. Proffitt 137, N. Proklova 37, K. Prokofiev 64c,
 G. Proto 75a, 75b, S. Protopopescu 29, J. Proudfoot 6, M. Przybycien 84a, J.E. Puddefoot 138, D. Pudzha 37,
 P. Puzo 66, D. Pyatiizbyantseva 37, J. Qian 105, Y. Qin 100, T. Qiu 93, A. Quadt 55, M. Queitsch-Maitland 24,
 G. Rabanal Bolanos 61, D. Rafanoharana 54, F. Ragusa 70a, 70b, J.L. Rainbolt 39, J.A. Raine 56, S. Rajagopalan 29,
 E. Ramakoti 37, K. Ran 14a, 14d, V. Raskina 126, D.F. Rassloff 63a, S. Rave 99, B. Ravina 59, I. Ravinovich 168,
 M. Raymond 36, A.L. Read 124, N.P. Readioff 138, D.M. Rebuzzi 72a, 72b, G. Redlinger 29, K. Reeves 45,
 J.A. Reidelsturz 170, D. Reikher 150, A. Reiss 99, A. Rej 140, C. Rembser 36, A. Renardi 48, M. Renda 27b,
 M.B. Rendel 109, A.G. Rennie 59, S. Resconi 70a, M. Ressegotti 57b, 57a, E.D. Resseguei 17a, S. Rettie 95,
 B. Reynolds 118, E. Reynolds 17a, M. Rezaei Estabragh 170, O.L. Rezanova 37, P. Reznicek 132, E. Ricci 77a, 77b,
 R. Richter 109, S. Richter 47a, 47b, E. Richter-Was 84b, M. Ridel 126, P. Rieck 116, P. Riedler 36,
 M. Rijssenbeek 144, A. Rimoldi 72a, 72b, M. Rimoldi 48, L. Rinaldi 23b, 23a, T.T. Rinn 161, M.P. Rinnagel 108,
 G. Ripellino 143, I. Riu 13, P. Rivadeneira 48, J.C. Rivera Vergara 164, F. Rizatdinova 120, E. Rizvi 93, C. Rizzi 56,
 B.A. Roberts 166, B.R. Roberts 17a, S.H. Robertson 103, v, M. Robin 48, D. Robinson 32,
 C.M. Robles Gajardo 136f, M. Robles Manzano 99, A. Robson 59, A. Rocchi 75a, 75b, C. Roda 73a, 73b,
 S. Rodriguez Bosca 63a, Y. Rodriguez Garcia 22a, A. Rodriguez Rodriguez 54, A.M. Rodríguez Vera 155b,
 S. Roe 36, J.T. Roemer 159, A.R. Roepe-Gier 119, J. Roggel 170, O. Røhne 124, R.A. Rojas 164, B. Roland 54,
 C.P.A. Roland 67, J. Roloff 29, A. Romanouk 37, M. Romano 23b, A.C. Romero Hernandez 161, N. Rompotis 91,
 L. Roos 126, S. Rosati 74a, B.J. Rosser 39, E. Rossi 4, E. Rossi 71a, 71b, L.P. Rossi 57b, L. Rossini 48, R. Rosten 118,
 M. Rotaru 27b, B. Rottler 54, D. Rousseau 66, D. Rousso 32, G. Rovelli 72a, 72b, A. Roy 161, A. Rozanov 101,
 Y. Rozen 149, X. Ruan 33g, A. Rubio Jimenez 162, A.J. Ruby 91, T.A. Ruggeri 1, F. Rühr 54, A. Ruiz-Martinez 162,
 A. Rummler 36, Z. Rurikova 54, N.A. Rusakovich 38, H.L. Russell 164, J.P. Rutherford 7, E.M. Rüttinger 138,
 K. Rybacki 90, M. Rybar 132, E.B. Rye 124, A. Ryzhov 37, J.A. Sabater Iglesias 56, P. Sabatini 162,
 L. Sabetta 74a, 74b, H.F-W. Sadrozinski 135, F. Safai Tehrani 74a, B. Safarzadeh Samani 145, M. Safdari 142,
 S. Saha 103, M. Sahinsoy 109, M. Saimpert 134, M. Saito 152, T. Saito 152, D. Salamani 36,
 G. Salamanna 76a, 76b, A. Salnikov 142, J. Salt 162, A. Salvador Salas 13, D. Salvatore 43b, 43a, F. Salvatore 145,
 A. Salzburger 36, D. Sammel 54, D. Sampsonidis 151, D. Sampsonidou 62d, 62c, J. Sánchez 162,
 A. Sanchez Pineda 4, V. Sanchez Sebastian 162, H. Sandaker 124, C.O. Sander 48, J.A. Sandesara 102,
 M. Sandhoff 170, C. Sandoval 22b, D.P.C. Sankey 133, A. Sansoni 53, C. Santoni 40, H. Santos 129a, 129b,
 S.N. Santpur 17a, A. Santra 168, K.A. Saoucha 138, J.G. Saraiva 129a, 129d, J. Sardain 101, O. Sasaki 82,

- K. Sato 156, C. Sauer 63b, F. Sauerburger 54, E. Sauvan 4, P. Savard 154,ad, R. Sawada 152, C. Sawyer 133, L. Sawyer 96, I. Sayago Galvan 162, C. Sbarra 23b, A. Sbrizzi 23b,23a, T. Scanlon 95, J. Schaarschmidt 137, P. Schacht 109, D. Schaefer 39, U. Schäfer 99, A.C. Schaffer 66, D. Schaile 108, R.D. Schamberger 144, E. Schanet 108, C. Scharf 18, V.A. Schegelsky 37, D. Scheirich 132, F. Schenck 18, M. Schernau 159, C. Scheulen 55, C. Schiavi 57b,57a, Z.M. Schillaci 26, E.J. Schioppa 69a,69b, M. Schioppa 43b,43a, B. Schlag 99, K.E. Schleicher 54, S. Schlenker 36, K. Schmieden 99, C. Schmitt 99, S. Schmitt 48, L. Schoeffel 134, A. Schoening 63b, P.G. Scholer 54, E. Schopf 125, M. Schott 99, J. Schovancova 36, S. Schramm 56, F. Schroeder 170, H-C. Schultz-Coulon 63a, M. Schumacher 54, B.A. Schumm 135, Ph. Schune 134, A. Schwartzman 142, T.A. Schwarz 105, Ph. Schwemling 134, R. Schwienhorst 106, A. Sciandra 135, G. Sciolla 26, F. Scuri 73a, F. Scutti 104, C.D. Sebastiani 91, K. Sedlaczek 49, P. Seema 18, S.C. Seidel 111, A. Seiden 135, B.D. Seidlitz 41, T. Seiss 39, C. Seitz 48, J.M. Seixas 81b, G. Sekhniaidze 71a, S.J. Sekula 44, L. Selem 4, N. Semprini-Cesari 23b,23a, S. Sen 51, V. Senthilkumar 162, L. Serin 66, L. Serkin 68a,68b, M. Sessa 76a,76b, H. Severini 119, S. Sevova 142, F. Sforza 57b,57a, A. Sfyrla 56, E. Shabalina 55, R. Shaheen 143, J.D. Shahinian 127, N.W. Shaikh 47a,47b, D. Shaked Renous 168, L.Y. Shan 14a, M. Shapiro 17a, A. Sharma 36, A.S. Sharma 163, P. Sharma 79, S. Sharma 48, P.B. Shatalov 37, K. Shaw 145, S.M. Shaw 100, P. Sherwood 95, L. Shi 95, C.O. Shimmin 171, Y. Shimogama 167, J.D. Shinner 94, I.P.J. Shipsey 125, S. Shirabe 60, M. Shiyakova 38, J. Shlomi 168, M.J. Shochet 39, J. Shojaei 104, D.R. Shope 143, S. Shrestha 118, E.M. Shrif 33g, M.J. Shroff 164, P. Sicho 130, A.M. Sickles 161, E. Sideras Haddad 33g, O. Sidiropoulou 36, A. Sidoti 23b, F. Siegert 50, Dj. Sijacki 15, R. Sikora 84a, F. Sili 89, J.M. Silva 20, M.V. Silva Oliveira 36, S.B. Silverstein 47a, S. Simion 66, R. Simoniello 36, E.L. Simpson 59, N.D. Simpson 97, S. Simsek 21d, S. Sindhu 55, P. Sinervo 154, V. Sinetckii 37, S. Singh 141, S. Singh 154, S. Sinha 48, S. Sinha 33g, M. Sioli 23b,23a, I. Siral 122, S.Yu. Sivoklokov 37,* J. Sjölin 47a,47b, A. Skaf 55, E. Skorda 97, P. Skubic 119, M. Slawinska 85, V. Smakhtin 168, B.H. Smart 133, J. Smiesko 132, S.Yu. Smirnov 37, Y. Smirnov 37, L.N. Smirnova 37,a, O. Smirnova 97, E.A. Smith 39, H.A. Smith 125, J.L. Smith 91, R. Smith 142, M. Smizanska 90, K. Smolek 131, A. Smykiewicz 85, A.A. Snesarev 37, H.L. Snoek 113, S. Snyder 29, R. Sobie 164,v, A. Soffer 150, C.A. Solans Sanchez 36, E.Yu. Soldatov 37, U. Soldevila 162, A.A. Solodkov 37, S. Solomon 54, A. Soloshenko 38, K. Solovieva 54, O.V. Solovyanov 37, V. Solovyev 37, P. Sommer 138, A. Sonay 13, W.Y. Song 155b, A. Sopczak 131, A.L. Sopio 95, F. Sopkova 28b, V. Sothilingam 63a, S. Sottocornola 72a,72b, R. Soualah 115b, Z. Soumaimi 35e, D. South 48, S. Spagnolo 69a,69b, M. Spalla 109, F. Spanò 94, D. Sperlich 54, G. Spigo 36, M. Spina 145, S. Spinali 90, D.P. Spiteri 59, M. Spousta 132, E.J. Staats 34, A. Stabile 70a,70b, R. Stamen 63a, M. Stamenkovic 113, A. Stampeki 20, M. Standke 24, E. Stanecka 85, B. Stanislaus 17a, M.M. Stanitzki 48, M. Stankaityte 125, B. Stapf 48, E.A. Starchenko 37, G.H. Stark 135, J. Stark 101, D.M. Starko 155b, P. Staroba 130, P. Starovoitov 63a, S. Stärz 103, R. Staszewski 85, G. Stavropoulos 46, J. Steentoft 160, P. Steinberg 29, A.L. Steinhebel 122, B. Stelzer 141,155a, H.J. Stelzer 128, O. Stelzer-Chilton 155a, H. Stenzel 58, T.J. Stevenson 145, G.A. Stewart 36, M.C. Stockton 36, G. Stoica 27b, M. Stolarski 129a, S. Stonjek 109, A. Straessner 50, J. Strandberg 143, S. Strandberg 47a,47b, M. Strauss 119, T. Strebler 101, P. Strizenec 28b, R. Ströhmer 165, D.M. Strom 122, L.R. Strom 48, R. Stroynowski 44, A. Strubig 47a,47b, S.A. Stucci 29, B. Stugu 16, J. Stupak 119, N.A. Styles 48, D. Su 142, S. Su 62a, W. Su 62d,137,62c, X. Su 62a,66, K. Sugizaki 152, V.V. Sulin 37, M.J. Sullivan 91, D.M.S. Sultan 77a,77b, L. Sultanaliyeva 37, S. Sultansoy 3b, T. Sumida 86, S. Sun 105, S. Sun 169, O. Sunneborn Gudnadottir 160, M.R. Sutton 145, M. Svatos 130, M. Swiatlowski 155a, T. Swirski 165, I. Sykora 28a, M. Sykora 132, T. Sykora 132, D. Ta 99, K. Tackmann 48,u, A. Taffard 159, R. Tafirout 155a, J.S. Tafoya Vargas 66, R.H.M. Taibah 126, R. Takashima 87, K. Takeda 83, E.P. Takeva 52, Y. Takubo 82, M. Talby 101, A.A. Talyshев 37, K.C. Tam 64b, N.M. Tamir 150, A. Tanaka 152, J. Tanaka 152, R. Tanaka 66, M. Tanasini 57b,57a, J. Tang 62c, Z. Tao 163, S. Tapia Araya 80, S. Tapprogge 99, A. Tarek Abouelfadl Mohamed 106, S. Tarem 149, K. Tariq 62b, G. Tarna 27b, G.F. Tartarelli 70a, P. Tas 132, M. Tasevsky 130, E. Tassi 43b,43a, A.C. Tate 161, G. Tateno 152, Y. Tayalati 35e, G.N. Taylor 104, W. Taylor 155b, H. Teagle 91, A.S. Tee 169, R. Teixeira De Lima 142, P. Teixeira-Dias 94, J.J. Teoh 154, K. Terashi 152, J. Terron 98, S. Terzo 13, M. Testa 53, R.J. Teuscher 154,v, N. Themistokleous 52, T. Theveneaux-Pelzer 18, O. Thielmann 170, D.W. Thomas 94, J.P. Thomas 20, E.A. Thompson 48, P.D. Thompson 20, E. Thomson 127, E.J. Thorpe 93, Y. Tian 55, V. Tikhomirov 37,a, Yu.A. Tikhonov 37, S. Timoshenko 37, E.X.L. Ting 1, P. Tipton 171, S. Tisserant 101, S.H. Tlou 33g, A. Tnourji 40, K. Todome 23b,23a, S. Todorova-Nova 132, S. Todt 50, M. Togawa 82, J. Tojo 88, S. Tokár 28a, K. Tokushuku 82, R. Tombs 32, M. Tomoto 82,110, L. Tompkins 142, P. Tornambe 102, E. Torrence 122, H. Torres 50, E. Torró Pastor 162, M. Toscani 30,

- C. Tosciri ³⁹, D.R. Tovey ¹³⁸, A. Traeet ¹⁶, I.S. Trandafir ^{27b}, T. Trefzger ¹⁶⁵, A. Tricoli ²⁹, I.M. Trigger ^{155a}, S. Trincaz-Duvold ¹²⁶, D.A. Trischuk ¹⁶³, B. Trocmé ⁶⁰, A. Trofymov ⁶⁶, C. Troncon ^{70a}, L. Truong ^{33c}, M. Trzebinski ⁸⁵, A. Trzupek ⁸⁵, F. Tsai ¹⁴⁴, M. Tsai ¹⁰⁵, A. Tsiamis ¹⁵¹, P.V. Tsiareshka ³⁷, A. Tsirigotis ^{151s}, V. Tsiskaridze ¹⁴⁴, E.G. Tskhadadze ^{148a}, M. Tsopoulou ¹⁵¹, Y. Tsujikawa ⁸⁶, I.I. Tsukerman ³⁷, V. Tsulaia ^{17a}, S. Tsuno ⁸², O. Tsur ¹⁴⁹, D. Tsybychev ¹⁴⁴, Y. Tu ^{64b}, A. Tudorache ^{27b}, V. Tudorache ^{27b}, A.N. Tuna ³⁶, S. Turchikhin ³⁸, I. Turk Cakir ^{3a}, R. Turra ^{70a}, P.M. Tuts ⁴¹, S. Tzamarias ¹⁵¹, P. Tzanis ¹⁰, E. Tzovara ⁹⁹, K. Uchida ¹⁵², F. Ukegawa ¹⁵⁶, P.A. Ulloa Poblete ^{136c}, G. Unal ³⁶, M. Unal ¹¹, A. Undrus ²⁹, G. Unel ¹⁵⁹, K. Uno ¹⁵², J. Urban ^{28b}, P. Urquijo ¹⁰⁴, G. Usai ⁸, R. Ushioda ¹⁵³, M. Usman ¹⁰⁷, Z. Uysal ^{21b}, V. Vacek ¹³¹, B. Vachon ¹⁰³, K.O.H. Vadla ¹²⁴, T. Vafeiadis ³⁶, C. Valderanis ¹⁰⁸, E. Valdes Santurio ^{47a,47b}, M. Valente ^{155a}, S. Valentini ^{23b,23a}, A. Valero ¹⁶², A. Vallier ¹⁰¹, J.A. Valls Ferrer ¹⁶², T.R. Van Daalen ¹³⁷, P. Van Gemmeren ⁶, S. Van Stroud ⁹⁵, I. Van Vulpen ¹¹³, M. Vanadia ^{75a,75b}, W. Vandelli ³⁶, M. Vandenbroucke ¹³⁴, E.R. Vandewall ¹²⁰, D. Vannicola ¹⁵⁰, L. Vannoli ^{57b,57a}, R. Vari ^{74a}, E.W. Varnes ⁷, C. Varni ^{17a}, T. Varol ¹⁴⁷, D. Varouchas ⁶⁶, L. Varriale ¹⁶², K.E. Varvell ¹⁴⁶, M.E. Vasile ^{27b}, L. Vaslin ⁴⁰, G.A. Vasquez ¹⁶⁴, F. Vazeille ⁴⁰, D. Vazquez Furelos ¹³, T. Vazquez Schroeder ³⁶, J. Veatch ³¹, V. Vecchio ¹⁰⁰, M.J. Veen ¹¹³, I. Veliscek ¹²⁵, L.M. Veloce ¹⁵⁴, F. Veloso ^{129a,129c}, S. Veneziano ^{74a}, A. Ventura ^{69a,69b}, A. Verbytskyi ¹⁰⁹, M. Verducci ^{73a,73b}, C. Vergis ²⁴, M. Verissimo De Araujo ^{81b}, W. Verkerke ¹¹³, J.C. Vermeulen ¹¹³, C. Vernieri ¹⁴², P.J. Verschuuren ⁹⁴, M. Vessella ¹⁰², M.L. Vesterbacka ¹¹⁶, M.C. Vetterli ^{141,ad}, A. Vgenopoulos ¹⁵¹, N. Viaux Maira ^{136f}, T. Vickey ¹³⁸, O.E. Vickey Boeriu ¹³⁸, G.H.A. Viehhäuser ¹²⁵, L. Vigani ^{63b}, M. Villa ^{23b,23a}, M. Villaplana Perez ¹⁶², E.M. Villhauer ⁵², E. Vilucchi ⁵³, M.G. Vincter ³⁴, G.S. Virdee ²⁰, A. Vishwakarma ⁵², C. Vittori ^{23b,23a}, I. Vivarelli ¹⁴⁵, V. Vladimirov ¹⁶⁶, E. Voevodina ¹⁰⁹, F. Vogel ¹⁰⁸, P. Vokac ¹³¹, J. Von Ahnen ⁴⁸, E. Von Toerne ²⁴, B. Vormwald ³⁶, V. Vorobel ¹³², K. Vorobev ³⁷, M. Vos ¹⁶², J.H. Vossebeld ⁹¹, M. Vozak ¹¹³, L. Vozdecky ⁹³, N. Vranjes ¹⁵, M. Vranjes Milosavljevic ¹⁵, M. Vreeswijk ¹¹³, R. Vuillermet ³⁶, O. Vujinovic ⁹⁹, I. Vukotic ³⁹, S. Wada ¹⁵⁶, C. Wagner ¹⁰², W. Wagner ¹⁷⁰, S. Wahdan ¹⁷⁰, H. Wahlberg ⁸⁹, R. Wakasa ¹⁵⁶, M. Wakida ¹¹⁰, V.M. Walbrecht ¹⁰⁹, J. Walder ¹³³, R. Walker ¹⁰⁸, W. Walkowiak ¹⁴⁰, A.M. Wang ⁶¹, A.Z. Wang ¹⁶⁹, C. Wang ^{62a}, C. Wang ^{62c}, H. Wang ^{17a}, J. Wang ^{64a}, P. Wang ⁴⁴, R.-J. Wang ⁹⁹, R. Wang ⁶¹, R. Wang ⁶, S.M. Wang ¹⁴⁷, S. Wang ^{62b}, T. Wang ^{62a}, W.T. Wang ⁷⁹, W.X. Wang ^{62a}, X. Wang ^{14c}, X. Wang ¹⁶¹, X. Wang ^{62c}, Y. Wang ^{62d}, Y. Wang ^{14c}, Z. Wang ¹⁰⁵, Z. Wang ^{62d,51,62c}, Z. Wang ¹⁰⁵, A. Warburton ¹⁰³, R.J. Ward ²⁰, N. Warrack ⁵⁹, A.T. Watson ²⁰, M.F. Watson ²⁰, G. Watts ¹³⁷, B.M. Waugh ⁹⁵, A.F. Webb ¹¹, C. Weber ²⁹, M.S. Weber ¹⁹, S.A. Weber ³⁴, S.M. Weber ^{63a}, C. Wei ^{62a}, Y. Wei ¹²⁵, A.R. Weidberg ¹²⁵, J. Weingarten ⁴⁹, M. Weirich ⁹⁹, C. Weiser ⁵⁴, C.J. Wells ⁴⁸, T. Wenaus ²⁹, B. Wendland ⁴⁹, T. Wengler ³⁶, N.S. Wenke ¹⁰⁹, N. Wermes ²⁴, M. Wessels ^{63a}, K. Whalen ¹²², A.M. Wharton ⁹⁰, A.S. White ⁶¹, A. White ⁸, M.J. White ¹, D. Whiteson ¹⁵⁹, L. Wickremasinghe ¹²³, W. Wiedenmann ¹⁶⁹, C. Wiel ⁵⁰, M. Wielaers ¹³³, N. Wieseotte ⁹⁹, C. Wiglesworth ⁴², L.A.M. Wiik-Fuchs ⁵⁴, D.J. Wilbern ¹¹⁹, H.G. Wilkens ³⁶, D.M. Williams ⁴¹, H.H. Williams ¹²⁷, S. Williams ³², S. Willocq ¹⁰², P.J. Windischhofer ¹²⁵, F. Winklmeier ¹²², B.T. Winter ⁵⁴, M. Wittgen ¹⁴², M. Wobisch ⁹⁶, A. Wolf ⁹⁹, R. Wölker ¹²⁵, J. Wollrath ¹⁵⁹, M.W. Wolter ⁸⁵, H. Wolters ^{129a,129c}, V.W.S. Wong ¹⁶³, A.F. Wongel ⁴⁸, S.D. Worm ⁴⁸, B.K. Wosiek ⁸⁵, K.W. Woźniak ⁸⁵, K. Wraight ⁵⁹, J. Wu ^{14a,14d}, M. Wu ^{64a}, S.L. Wu ¹⁶⁹, X. Wu ⁵⁶, Y. Wu ^{62a}, Z. Wu ^{134,62a}, J. Wuerzinger ¹²⁵, T.R. Wyatt ¹⁰⁰, B.M. Wynne ⁵², S. Xella ⁴², L. Xia ^{14c}, M. Xia ^{14b}, J. Xiang ^{64c}, X. Xiao ¹⁰⁵, M. Xie ^{62a}, X. Xie ^{62a}, I. Xiotidis ¹⁴⁵, D. Xu ^{14a}, H. Xu ^{62a}, H. Xu ^{62a}, L. Xu ^{62a}, R. Xu ¹²⁷, T. Xu ^{62a}, W. Xu ¹⁰⁵, Y. Xu ^{14b}, Z. Xu ^{62b}, Z. Xu ¹⁴², B. Yabsley ¹⁴⁶, S. Yacoob ^{33a}, N. Yamaguchi ⁸⁸, Y. Yamaguchi ¹⁵³, H. Yamauchi ¹⁵⁶, T. Yamazaki ^{17a}, Y. Yamazaki ⁸³, J. Yan ^{62c}, S. Yan ¹²⁵, Z. Yan ²⁵, H.J. Yang ^{62c,62d}, H.T. Yang ^{17a}, S. Yang ^{62a}, T. Yang ^{64c}, X. Yang ^{62a}, X. Yang ^{14a}, Y. Yang ⁴⁴, Z. Yang ^{62a,105}, W.-M. Yao ^{17a}, Y.C. Yap ⁴⁸, H. Ye ^{14c}, J. Ye ⁴⁴, S. Ye ²⁹, X. Ye ^{62a}, I. Yeletskikh ³⁸, M.R. Yexley ⁹⁰, P. Yin ⁴¹, K. Yorita ¹⁶⁷, C.J.S. Young ⁵⁴, C. Young ¹⁴², M. Yuan ¹⁰⁵, R. Yuan ^{62b,j}, X. Yue ^{63a}, M. Zaazoua ^{35e}, B. Zabinski ⁸⁵, E. Zaid ⁵², T. Zakareishvili ^{148b}, N. Zakharchuk ³⁴, S. Zambito ⁵⁶, J. Zang ¹⁵², D. Zanzi ⁵⁴, O. Zaplatilek ¹³¹, S.V. Zeißner ⁴⁹, C. Zeitnitz ¹⁷⁰, J.C. Zeng ¹⁶¹, D.T. Zenger Jr ²⁶, O. Zenin ³⁷, T. Ženiš ^{28a}, S. Zenz ⁹³, S. Zerradi ^{35a}, D. Zerwas ⁶⁶, B. Zhang ^{14c}, D.F. Zhang ¹³⁸, G. Zhang ^{14b}, J. Zhang ⁶, K. Zhang ^{14a,14d}, L. Zhang ^{14c}, R. Zhang ¹⁶⁹, S. Zhang ¹⁰⁵, T. Zhang ¹⁵², X. Zhang ^{62c}, X. Zhang ^{62b}, Z. Zhang ⁶⁶, H. Zhao ¹³⁷, P. Zhao ⁵¹, T. Zhao ^{62b}, Y. Zhao ¹³⁵, Z. Zhao ^{62a}, A. Zhemchugov ³⁸, Z. Zheng ¹⁴², D. Zhong ¹⁶¹, B. Zhou ¹⁰⁵, C. Zhou ¹⁶⁹, H. Zhou ⁷, N. Zhou ^{62c}, Y. Zhou ⁷, C.G. Zhu ^{62b}, C. Zhu ^{14a,14d}, H.L. Zhu ^{62a}, H. Zhu ^{14a}, J. Zhu ¹⁰⁵, Y. Zhu ^{62a}, X. Zhuang ^{14a}, K. Zhukov ³⁷, V. Zhulanov ³⁷, N.I. Zimine ³⁸, J. Zinsser ^{63b},

M. Ziolkowski ¹⁴⁰, L. Živković ¹⁵, A. Zoccoli ^{23b,23a}, K. Zoch ⁵⁶, T.G. Zorbas ¹³⁸, O. Zormpa ⁴⁶, W. Zou ⁴¹,
L. Zwalinski ³⁶

¹ Department of Physics, University of Adelaide, Adelaide; Australia

² Department of Physics, University of Alberta, Edmonton AB; Canada

³ ^(a) Department of Physics, Ankara University, Ankara; ^(b) Division of Physics, TOBB University of Economics and Technology, Ankara; Türkiye

⁴ LAPP, Univ. Savoie Mont Blanc, CNRS/IN2P3, Annecy; France

⁵ APC, Université Paris Cité, CNRS/IN2P3, Paris; France

⁶ High Energy Physics Division, Argonne National Laboratory, Argonne IL; United States of America

⁷ Department of Physics, University of Arizona, Tucson AZ; United States of America

⁸ Department of Physics, University of Texas at Arlington, Arlington TX; United States of America

⁹ Physics Department, National and Kapodistrian University of Athens, Athens; Greece

¹⁰ Physics Department, National Technical University of Athens, Zografou; Greece

¹¹ Department of Physics, University of Texas at Austin, Austin TX; United States of America

¹² Institute of Physics, Azerbaijan Academy of Sciences, Baku; Azerbaijan

¹³ Institut de Física d'Altes Energies (IFAE), Barcelona Institute of Science and Technology, Barcelona; Spain

¹⁴ ^(a) Institute of High Energy Physics, Chinese Academy of Sciences, Beijing; ^(b) Physics Department, Tsinghua University, Beijing; ^(c) Department of Physics, Nanjing University, Nanjing;

^(d) University of Chinese Academy of Science (UCAS), Beijing; China

¹⁵ Institute of Physics, University of Belgrade, Belgrade; Serbia

¹⁶ Department for Physics and Technology, University of Bergen, Bergen; Norway

¹⁷ ^(a) Physics Division, Lawrence Berkeley National Laboratory, Berkeley CA; ^(b) University of California, Berkeley CA; United States of America

¹⁸ Institut für Physik, Humboldt Universität zu Berlin, Berlin; Germany

¹⁹ Albert Einstein Center for Fundamental Physics and Laboratory for High Energy Physics, University of Bern, Bern; Switzerland

²⁰ School of Physics and Astronomy, University of Birmingham, Birmingham; United Kingdom

²¹ ^(a) Department of Physics, Bogazici University, Istanbul; ^(b) Department of Physics Engineering, Gaziantep University, Gaziantep; ^(c) Department of Physics, Istanbul University, Istanbul;

^(d) Istanufe University, Sariyer, Istanbul; Türkiye

²² ^(a) Facultad de Ciencias y Centro de Investigaciones, Universidad Antonio Nariño, Bogotá; ^(b) Departamento de Física, Universidad Nacional de Colombia, Bogotá; Colombia

²³ ^(a) Dipartimento di Fisica e Astronomia A. Righi, Università di Bologna, Bologna; ^(b) INFN Sezione di Bologna; Italy

²⁴ Physikalisch-es Institut, Universität Bonn, Bonn; Germany

²⁵ Department of Physics, Boston University, Boston MA; United States of America

²⁶ Department of Physics, Brandeis University, Waltham MA; United States of America

²⁷ ^(a) Transilvania University of Brasov, Brasov; ^(b) Horia Hulubei National Institute of Physics and Nuclear Engineering, Bucharest; ^(c) Department of Physics, Alexandru Ioan Cuza University of Iasi, Iasi; ^(d) National Institute for Research and Development of Isotopic and Molecular Technologies, Physics Department, Cluj-Napoca; ^(e) University Politehnica Bucharest, Bucharest; ^(f) West University in Timisoara, Timisoara; Romania

²⁸ ^(a) Faculty of Mathematics, Physics and Informatics, Comenius University, Bratislava; ^(b) Department of Subnuclear Physics, Institute of Experimental Physics of the Slovak Academy of Sciences, Kosice; Slovak Republic

²⁹ Physics Department, Brookhaven National Laboratory, Upton NY; United States of America

³⁰ Universidad de Buenos Aires, Facultad de Ciencias Exactas y Naturales, Departamento de Física, y CONICET, Instituto de Física de Buenos Aires (IFIBA), Buenos Aires; Argentina

³¹ California State University, CA; United States of America

³² Cavendish Laboratory, University of Cambridge, Cambridge; United Kingdom

³³ ^(a) Department of Physics, University of Cape Town, Cape Town; ^(b) iThemba Labs, Western Cape; ^(c) Department of Mechanical Engineering Science, University of Johannesburg, Johannesburg; ^(d) National Institute of Physics, University of the Philippines Diliman (Philippines); ^(e) University of South Africa, Department of Physics, Pretoria; ^(f) University of Zululand, KwaDlangezwa; ^(g) School of Physics, University of the Witwatersrand, Johannesburg; South Africa

³⁴ Department of Physics, Carleton University, Ottawa ON; Canada

³⁵ ^(a) Faculté des Sciences Ain Chock, Réseau Universitaire de Physique des Hautes Energies – Université Hassan II, Casablanca; ^(b) Faculté des Sciences, Université Ibn-Tofail, Kénitra;

^(c) Faculté des Sciences Semlalia, Université Cadi Ayyad, LPHEA, Marrakech; ^(d) LPMR, Faculté des Sciences, Université Mohamed Premier, Oujda; ^(e) Faculté des sciences, Université Mohammed V, Rabat; ^(f) Institute of Applied Physics, Mohammed VI Polytechnic University, Ben Guerir; Morocco

³⁶ CERN, Geneva; Switzerland

³⁷ Affiliated with an institute covered by a cooperation agreement with CERN

³⁸ Affiliated with an international laboratory covered by a cooperation agreement with CERN

³⁹ Enrico Fermi Institute, University of Chicago, Chicago IL; United States of America

⁴⁰ LPC, Université Clermont Auvergne, CNRS/IN2P3, Clermont-Ferrand; France

⁴¹ Nevis Laboratory, Columbia University, Irvington NY; United States of America

⁴² Niels Bohr Institute, University of Copenhagen, Copenhagen; Denmark

⁴³ ^(a) Dipartimento di Fisica, Università della Calabria, Rende; ^(b) INFN Gruppo Collegato di Cosenza, Laboratori Nazionali di Frascati; Italy

⁴⁴ Physics Department, Southern Methodist University, Dallas TX; United States of America

⁴⁵ Physics Department, University of Texas at Dallas, Richardson TX; United States of America

⁴⁶ National Centre for Scientific Research "Demokritos", Agia Paraskevi; Greece

⁴⁷ ^(a) Department of Physics, Stockholm University; ^(b) Oskar Klein Centre, Stockholm; Sweden

⁴⁸ Deutsches Elektronen-Synchrotron DESY, Hamburg and Zeuthen; Germany

⁴⁹ Fakultät Physik, Technische Universität Dortmund, Dortmund; Germany

⁵⁰ Institut für Kern- und Teilchenphysik, Technische Universität Dresden, Dresden; Germany

⁵¹ Department of Physics, Duke University, Durham NC; United States of America

⁵² SUPA – School of Physics and Astronomy, University of Edinburgh, Edinburgh; United Kingdom

⁵³ INFN e Laboratori Nazionali di Frascati, Frascati; Italy

⁵⁴ Physikalisches Institut, Albert-Ludwigs-Universität Freiburg, Freiburg; Germany

⁵⁵ II. Physikalisches Institut, Georg-August-Universität Göttingen, Göttingen; Germany

⁵⁶ Département de Physique Nucléaire et Corpusculaire, Université de Genève, Genève; Switzerland

⁵⁷ ^(a) Dipartimento di Fisica, Università di Genova, Genova; ^(b) INFN Sezione di Genova; Italy

⁵⁸ II. Physikalisches Institut, Justus-Liebig-Universität Giessen, Giessen; Germany

⁵⁹ SUPA – School of Physics and Astronomy, University of Glasgow, Glasgow; United Kingdom

⁶⁰ LPSC, Université Grenoble Alpes, CNRS/IN2P3, Grenoble INP, Grenoble; France

⁶¹ Laboratory for Particle Physics and Cosmology, Harvard University, Cambridge MA; United States of America

⁶² ^(a) Department of Modern Physics and State Key Laboratory of Particle Detection and Electronics, University of Science and Technology of China, Hefei; ^(b) Institute of Frontier and Interdisciplinary Science and Key Laboratory of Particle Physics and Particle Irradiation (MOE), Shandong University, Qingdao; ^(c) School of Physics and Astronomy, Shanghai Jiao Tong University, Key Laboratory for Particle Astrophysics and Cosmology (MOE), SKLPPC, Shanghai; ^(d) Tsung-Dao Lee Institute, Shanghai; China

⁶³ ^(a) Kirchhoff-Institut für Physik, Ruprecht-Karls-Universität Heidelberg, Heidelberg; ^(b) Physikalisches Institut, Ruprecht-Karls-Universität Heidelberg, Heidelberg; Germany

⁶⁴ ^(a) Department of Physics, Chinese University of Hong Kong, Shatin, N.T., Hong Kong; ^(b) Department of Physics, University of Hong Kong, Hong Kong; ^(c) Department of Physics and Institute for Advanced Study, Hong Kong University of Science and Technology, Clear Water Bay, Kowloon, Hong Kong; China

- ⁶⁵ Department of Physics, National Tsing Hua University, Hsinchu; Taiwan
⁶⁶ IJCLab, Université Paris-Saclay, CNRS/IN2P3, 91405, Orsay; France
⁶⁷ Department of Physics, Indiana University, Bloomington IN; United States of America
⁶⁸ ^(a) INFN Gruppo Collegato di Udine, Sezione di Trieste, Udine; ^(b) ICTP, Trieste; ^(c) Dipartimento Politecnico di Ingegneria e Architettura, Università di Udine, Udine; Italy
⁶⁹ ^(a) INFN Sezione di Lecce; ^(b) Dipartimento di Matematica e Fisica, Università del Salento, Lecce; Italy
⁷⁰ ^(a) INFN Sezione di Milano; ^(b) Dipartimento di Fisica, Università di Milano, Milano; Italy
⁷¹ ^(a) INFN Sezione di Napoli; ^(b) Dipartimento di Fisica, Università di Napoli, Napoli; Italy
⁷² ^(a) INFN Sezione di Pavia; ^(b) Dipartimento di Fisica, Università di Pavia, Pavia; Italy
⁷³ ^(a) INFN Sezione di Pisa; ^(b) Dipartimento di Fisica E. Fermi, Università di Pisa, Pisa; Italy
⁷⁴ ^(a) INFN Sezione di Roma; ^(b) Dipartimento di Fisica, Sapienza Università di Roma, Roma; Italy
⁷⁵ ^(a) INFN Sezione di Roma Tor Vergata; ^(b) Dipartimento di Fisica, Università di Roma Tor Vergata, Roma; Italy
⁷⁶ ^(a) INFN Sezione di Roma Tre; ^(b) Dipartimento di Matematica e Fisica, Università Roma Tre, Roma; Italy
⁷⁷ ^(a) INFN-TIFPA; ^(b) Università degli Studi di Trento, Trento; Italy
⁷⁸ Universität Innsbruck, Department of Astro and Particle Physics, Innsbruck; Austria
⁷⁹ University of Iowa, Iowa City IA; United States of America
⁸⁰ Department of Physics and Astronomy, Iowa State University, Ames IA; United States of America
⁸¹ ^(a) Departamento de Engenharia Elétrica, Universidade Federal de Juiz de Fora (UFJF), Juiz de Fora; ^(b) Universidade Federal do Rio De Janeiro COPPE/EE/IF, Rio de Janeiro; ^(c) Instituto de Física, Universidade de São Paulo, São Paulo; ^(d) Rio de Janeiro State University, Rio de Janeiro; Brazil
⁸² KEK, High Energy Accelerator Research Organization, Tsukuba; Japan
⁸³ Graduate School of Science, Kobe University, Kobe; Japan
⁸⁴ ^(a) AGH University of Science and Technology, Faculty of Physics and Applied Computer Science, Krakow; ^(b) Marian Smoluchowski Institute of Physics, Jagiellonian University, Krakow; Poland
⁸⁵ Institute of Nuclear Physics Polish Academy of Sciences, Krakow; Poland
⁸⁶ Faculty of Science, Kyoto University, Kyoto; Japan
⁸⁷ Kyoto University of Education, Kyoto; Japan
⁸⁸ Research Center for Advanced Particle Physics and Department of Physics, Kyushu University, Fukuoka ; Japan
⁸⁹ Instituto de Física La Plata, Universidad Nacional de La Plata and CONICET, La Plata; Argentina
⁹⁰ Physics Department, Lancaster University, Lancaster; United Kingdom
⁹¹ Oliver Lodge Laboratory, University of Liverpool, Liverpool; United Kingdom
⁹² Department of Experimental Particle Physics, Jožef Stefan Institute and Department of Physics, University of Ljubljana, Ljubljana; Slovenia
⁹³ School of Physics and Astronomy, Queen Mary University of London, London; United Kingdom
⁹⁴ Department of Physics, Royal Holloway University of London, Egham; United Kingdom
⁹⁵ Department of Physics and Astronomy, University College London, London; United Kingdom
⁹⁶ Louisiana Tech University, Ruston LA; United States of America
⁹⁷ Fysiska institutionen, Lunds universitet, Lund; Sweden
⁹⁸ Departamento de Física Teorica C-15 and CIAFF, Universidad Autónoma de Madrid, Madrid; Spain
⁹⁹ Institut für Physik, Universität Mainz, Mainz; Germany
¹⁰⁰ School of Physics and Astronomy, University of Manchester, Manchester; United Kingdom
¹⁰¹ CPPM, Aix-Marseille Université, CNRS/IN2P3, Marseille; France
¹⁰² Department of Physics, University of Massachusetts, Amherst MA; United States of America
¹⁰³ Department of Physics, McGill University, Montreal QC; Canada
¹⁰⁴ School of Physics, University of Melbourne, Victoria; Australia
¹⁰⁵ Department of Physics, University of Michigan, Ann Arbor MI; United States of America
¹⁰⁶ Department of Physics and Astronomy, Michigan State University, East Lansing MI; United States of America
¹⁰⁷ Group of Particle Physics, University of Montreal, Montreal QC; Canada
¹⁰⁸ Fakultät für Physik, Ludwig-Maximilians-Universität München, München; Germany
¹⁰⁹ Max-Planck-Institut für Physik (Werner-Heisenberg-Institut), München; Germany
¹¹⁰ Graduate School of Science and Kobayashi-Maskawa Institute, Nagoya University, Nagoya; Japan
¹¹¹ Department of Physics and Astronomy, University of New Mexico, Albuquerque NM; United States of America
¹¹² Institute for Mathematics, Astrophysics and Particle Physics, Radboud University/Nikhef, Nijmegen; Netherlands
¹¹³ Nikhef National Institute for Subatomic Physics and University of Amsterdam, Amsterdam; Netherlands
¹¹⁴ Department of Physics, Northern Illinois University, DeKalb IL; United States of America
¹¹⁵ ^(a) New York University Abu Dhabi, Abu Dhabi; ^(b) University of Sharjah, Sharjah; United Arab Emirates
¹¹⁶ Department of Physics, New York University, New York NY; United States of America
¹¹⁷ Ochanomizu University, Otsuka, Bunkyo-ku, Tokyo; Japan
¹¹⁸ Ohio State University, Columbus OH; United States of America
¹¹⁹ Homer L. Dodge Department of Physics and Astronomy, University of Oklahoma, Norman OK; United States of America
¹²⁰ Department of Physics, Oklahoma State University, Stillwater OK; United States of America
¹²¹ Palacký University, Joint Laboratory of Optics, Olomouc; Czech Republic
¹²² Institute for Fundamental Science, University of Oregon, Eugene, OR; United States of America
¹²³ Graduate School of Science, Osaka University, Osaka; Japan
¹²⁴ Department of Physics, University of Oslo, Oslo; Norway
¹²⁵ Department of Physics, Oxford University, Oxford; United Kingdom
¹²⁶ LPNHE, Sorbonne Université, Université Paris Cité, CNRS/IN2P3, Paris; France
¹²⁷ Department of Physics, University of Pennsylvania, Philadelphia PA; United States of America
¹²⁸ Department of Physics and Astronomy, University of Pittsburgh, Pittsburgh PA; United States of America
¹²⁹ ^(a) Laboratório de Instrumentação e Física Experimental de Partículas – LIP, Lisboa; ^(b) Departamento de Física, Faculdade de Ciências, Universidade de Lisboa, Lisboa; ^(c) Departamento de Física, Universidade de Coimbra, Coimbra; ^(d) Centro de Física Nuclear da Universidade de Lisboa, Lisboa; ^(e) Departamento de Física, Universidade do Minho, Braga; ^(f) Departamento de Física Teórica y del Cosmos, Universidad de Granada, Granada (Spain); ^(g) Departamento de Física, Instituto Superior Técnico, Universidade de Lisboa, Lisboa; Portugal
¹³⁰ Institute of Physics of the Czech Academy of Sciences, Prague; Czech Republic
¹³¹ Czech Technical University in Prague, Prague; Czech Republic
¹³² Charles University, Faculty of Mathematics and Physics, Prague; Czech Republic
¹³³ Particle Physics Department, Rutherford Appleton Laboratory, Didcot; United Kingdom
¹³⁴ IRFU, CEA, Université Paris-Saclay, Gif-sur-Yvette; France
¹³⁵ Santa Cruz Institute for Particle Physics, University of California Santa Cruz, Santa Cruz CA; United States of America
¹³⁶ ^(a) Departamento de Física, Pontificia Universidad Católica de Chile, Santiago; ^(b) Millennium Institute for Subatomic physics at high energy frontier (SAPHIR), Santiago; ^(c) Instituto de Investigación Multidisciplinaria en Ciencia y Tecnología, y Departamento de Física, Universidad de La Serena; ^(d) Universidad Andres Bello, Department of Physics, Santiago; ^(e) Instituto de Alta Investigación, Universidad de Tarapacá, Arica; ^(f) Departamento de Física, Universidad Técnica Federico Santa María, Valparaíso; Chile
¹³⁷ Department of Physics, University of Washington, Seattle WA; United States of America
¹³⁸ Department of Physics and Astronomy, University of Sheffield, Sheffield; United Kingdom

- ¹³⁹ Department of Physics, Shinshu University, Nagano; Japan
¹⁴⁰ Department Physik, Universität Siegen, Siegen; Germany
¹⁴¹ Department of Physics, Simon Fraser University, Burnaby BC; Canada
¹⁴² SLAC National Accelerator Laboratory, Stanford CA; United States of America
¹⁴³ Department of Physics, Royal Institute of Technology, Stockholm; Sweden
¹⁴⁴ Departments of Physics and Astronomy, Stony Brook University, Stony Brook NY; United States of America
¹⁴⁵ Department of Physics and Astronomy, University of Sussex, Brighton; United Kingdom
¹⁴⁶ School of Physics, University of Sydney, Sydney; Australia
¹⁴⁷ Institute of Physics, Academia Sinica, Taipei; Taiwan
¹⁴⁸ ^(a) E. Andronikashvili Institute of Physics, Iv. Javakhishvili Tbilisi State University, Tbilisi; ^(b) High Energy Physics Institute, Tbilisi State University, Tbilisi; ^(c) University of Georgia, Tbilisi; Georgia
¹⁴⁹ Department of Physics, Technion, Israel Institute of Technology, Haifa; Israel
¹⁵⁰ Raymond and Beverly Sackler School of Physics and Astronomy, Tel Aviv University, Tel Aviv; Israel
¹⁵¹ Department of Physics, Aristotle University of Thessaloniki, Thessaloniki; Greece
¹⁵² International Center for Elementary Particle Physics and Department of Physics, University of Tokyo, Tokyo; Japan
¹⁵³ Department of Physics, Tokyo Institute of Technology, Tokyo; Japan
¹⁵⁴ Department of Physics, University of Toronto, Toronto ON; Canada
¹⁵⁵ ^(a) TRIUMF, Vancouver BC; ^(b) Department of Physics and Astronomy, York University, Toronto ON; Canada
¹⁵⁶ Division of Physics and Tomonaga Center for the History of the Universe, Faculty of Pure and Applied Sciences, University of Tsukuba, Tsukuba; Japan
¹⁵⁷ Department of Physics and Astronomy, Tufts University, Medford MA; United States of America
¹⁵⁸ United Arab Emirates University, Al Ain; United Arab Emirates
¹⁵⁹ Department of Physics and Astronomy, University of California Irvine, Irvine CA; United States of America
¹⁶⁰ Department of Physics and Astronomy, University of Uppsala, Uppsala; Sweden
¹⁶¹ Department of Physics, University of Illinois, Urbana IL; United States of America
¹⁶² Instituto de Física Corpuscular (IFIC), Centro Mixto Universidad de Valencia – CSIC, Valencia; Spain
¹⁶³ Department of Physics, University of British Columbia, Vancouver BC; Canada
¹⁶⁴ Department of Physics and Astronomy, University of Victoria, Victoria BC; Canada
¹⁶⁵ Fakultät für Physik und Astronomie, Julius-Maximilians-Universität Würzburg, Würzburg; Germany
¹⁶⁶ Department of Physics, University of Warwick, Coventry; United Kingdom
¹⁶⁷ Waseda University, Tokyo; Japan
¹⁶⁸ Department of Particle Physics and Astrophysics, Weizmann Institute of Science, Rehovot; Israel
¹⁶⁹ Department of Physics, University of Wisconsin, Madison WI; United States of America
¹⁷⁰ Fakultät für Mathematik und Naturwissenschaften, Fachgruppe Physik, Bergische Universität Wuppertal, Wuppertal; Germany
¹⁷¹ Department of Physics, Yale University, New Haven CT; United States of America

^a Also Affiliated with an institute covered by a cooperation agreement with CERN.

^b Also at Borough of Manhattan Community College, City University of New York, New York NY; United States of America.

^c Also at Bruno Kessler Foundation, Trento; Italy.

^d Also at Center for High Energy Physics, Peking University; China.

^e Also at Centro Studi e Ricerche Enrico Fermi; Italy.

^f Also at CERN, Geneva; Switzerland.

^g Also at Département de Physique Nucléaire et Corpusculaire, Université de Genève, Genève; Switzerland.

^h Also at Departament de Fisica de la Universitat Autònoma de Barcelona, Barcelona; Spain.

ⁱ Also at Department of Financial and Management Engineering, University of the Aegean, Chios; Greece.

^j Also at Department of Physics and Astronomy, Michigan State University, East Lansing MI; United States of America.

^k Also at Department of Physics and Astronomy, University of Louisville, Louisville, KY; United States of America.

^l Also at Department of Physics, Ben Gurion University of the Negev, Beer Sheva; Israel.

^m Also at Department of Physics, California State University, East Bay; United States of America.

ⁿ Also at Department of Physics, California State University, Sacramento; United States of America.

^o Also at Department of Physics, King's College London, London; United Kingdom.

^p Also at Department of Physics, University of Fribourg, Fribourg; Switzerland.

^q Also at Department of Physics, University of Thessaly; Greece.

^r Also at Department of Physics, Westmont College, Santa Barbara; United States of America.

^s Also at Hellenic Open University, Patras; Greece.

^t Also at Institutio Catalana de Recerca i Estudis Avancats, ICREA, Barcelona; Spain.

^u Also at Institut für Experimentalphysik, Universität Hamburg, Hamburg; Germany.

^v Also at Institute of Particle Physics (IPP); Canada.

^w Also at Institute of Physics, Azerbaijan Academy of Sciences, Baku; Azerbaijan.

^x Also at Institute of Theoretical Physics, Ilia State University, Tbilisi; Georgia.

^y Also at Lawrence Livermore National Laboratory, Livermore; United States of America.

^z Also at Physics Department, An-Najah National University, Nablus; Palestine.

^{aa} Also at Physikalisch-es Institut, Albert-Ludwigs-Universität Freiburg, Freiburg; Germany.

^{ab} Also at The City College of New York, New York NY; United States of America.

^{ac} Also at The Collaborative Innovation Center of Quantum Matter (CICQM), Beijing; China.

^{ad} Also at TRIUMF, Vancouver BC; Canada.

^{ae} Also at Università di Napoli Parthenope, Napoli; Italy.

^{af} Also at University of Chinese Academy of Sciences (UCAS), Beijing; China.

^{ag} Also at University of Colorado Boulder, Department of Physics, Colorado; United States of America.

^{ah} Also at Yeditepe University, Physics Department, Istanbul; Türkiye.

^{ai} Also at RWTH Aachen University, III. Physikalisches Institut A, Aachen; Germany.

* Deceased.